NETWORK-WIDE CHARGING INFRASTRUCTURE PLANNING AND MARKET SHARE ANALYSIS FOR ELECTRIC VEHICLES

By

Mohammadreza Kavianipour

A DISSERTATION

Submitted to
Michigan State University
in partial fulfillment of the requirements
for the degree of

Civil Engineering—Doctor of Philosophy

2022

ABSTRACT

NETWORK-WIDE CHARGING INFRASTRUCTURE PLANNING AND MARKET SHARE ANALYSIS FOR ELECTRIC VEHICLES

By

Mohammadreza Kavianipour

Electric vehicles (EVs) are widely considered a sustainable substitution to conventional vehicles to mitigate fossil fuel dependence and reduce tail-pipe emissions. However, limited ranges, long charging times, and lack of charging infrastructure have hindered EV's market acceptance. This calls for more investments in building charging stations and advancing battery and charging technologies to obviate issues associated with EVs and increase their market share and improve sustainability. This study introduces modeling frameworks to optimize fast-charging infrastructure locations at the network level to address the challenges associated with EVs. Furthermore, it investigates the required charging investments for the current and future EV market shares, technology advancements, and seasonal demand variations.

First, this study seeks an optimal configuration for plug-in electric vehicle charging infrastructure that supports their long-distance intercity trips at the network level. A mathematical optimization model is proposed which minimizes the total system cost and considers the range anxiety, multiple refueling, maximum capacity, charging delay, and detour time. This study considers the impacts of charging station locations on the traffic assignment problem with a mixed fleet of electric and conventional vehicles considering a user equilibrium framework. This study fills existing gaps in the literature by capturing realistic patterns of travel demand and considering flow-dependent charging delays at charging stations in intercity networks.

Then, the study focuses on Michigan and its future needs to support the intercity trips of EVs across the state in two target years of 2020 and 2030, considering monthly traffic demand and battery performance variations, as well as different battery sizes and charger technologies, the main contributing factors in defining the infrastructure needs of EV users, particularly in states with adverse weather conditions. This study incorporates the developed intercity model to suggest the optimal locations of EV fast chargers to be implemented in Michigan.

Next, this study introduces an integrated framework for urban fast-charging infrastructure to address the range anxiety issue in urban networks. Unlike intercity trips that start with fully charged batteries, urban trips might start with any state of charge because of home/work chargers' unavailability, being part of a trip chain, and forgetting to charge overnight. A mesoscopic simulation tool is incorporated to generate trip trajectories, and a state-of-the-art tool is developed to simulate charging behavior based on various trip attributes for these trajectories. The resulting temporal charging demand is the key element in finding the optimum charging infrastructure. The solution quality and significant superiority in the computational efficiency of the decomposition approach are confirmed in comparison with the implicit enumeration approach.

Finally, this study generates forecasting models to estimate the number of chargers and charging stations to support the EV charging demand for urban areas. These models provide macro-level estimates of the required infrastructure investment in urban areas, which can be easily implemented by policy-makers and city planners. This study incorporates data obtained from applying a disaggregate optimization-based charger placement model, for multiple case studies to generate the required data to calibrate the macro-level models, in the state of Michigan.

To my beloved wife, Selda, and my parents for their unconditional love and support.

ACKNOWLEDGMENTS

I would like to express my deepest gratitude to my advisor, Dr. Ali Zockaie, for his endless support, patience, and guidance during my Ph.D. Program. Not only he taught me the way of research, but also, he set an example of how to be a better person. I would also like to thank Dr. Mehrnaz Ghamami, for being so supportive and helping me whenever I had any problem. I am also indebted to my other dissertation committee members, Dr. Peter Savolainen, Dr. Timothy Gates, and Dr. Joydeep Mitra for their time, support, and guidance over the last five years.

My sincerest gratitude goes to my dear peers and friend in the Sustainable Mobility Group, especially to Fatemeh and Harprinderjot for sharing ideas and supporting me throughout this process. My special thanks go to my dear wife and best friend, Selda Abbasian, who has always supported me and made sacrifices to help me get to this point. Last, but not least, I am truly grateful to my dear parents, parents-in-law, and lovely siblings for their constant love, support, and encouragement.

TABLE OF CONTENTS

LIST OF TABLES

LIST OF FIGURES

Chapter 1 - Introduction

1-1- Overview and Objectives

In the U.S., transportation mostly hinges on gasoline and diesel fuels which contribute to energy insecurity and environmental issues. In 2019, transportation was responsible for 37% of the total energy used in the U.S., of which 70% is from burning petrolium in conventional vehicles (CVs) (U.S. Energy Information Administration, 2019). Furthermore, around 28 percent of Green House Gas (GHG) emissions in the U.S. were caused by transportation in 2018 (United States Environmental Protection Agency, 2018). The concerns about vehicle emissions and crude oil price fluctuations have pushed the car industry towards investment in electric vehicles (EV) production (Dong et al., 2014; He et al., 2013). EVs remove on-road emissions and can mitigate air pollution significantly if accompanied by green energy production. However, limited driving range and insufficient supporting infrastructure, as well as long charging times, have hindered the acceptance of EVs in the market (He et al., 2013; Nie and Ghamami, 2013). Although some current EV models can exceed 300 miles per charge, the range is still lower than that of similar conventional vehicles (CV). Also, unlike CVs, EVs' performance decreases further in cold weather (Krisher, 2019). Therefore, customers are concerned about being stranded along their way by running out of charge and not having access to charging stations, which is known as range anxiety (Tate et al., 2008). Providing adequate charging infrastructure mitigates some of the challenges associated with EVs and is known to be among the main factors to increase their market share (Nie et al., 2016).

In the U.S., the government has promoted EVs' adoption by contributing to the expansion of charging infrastructure (Deb et al., 2018). There have been numerous initiatives to favor EV charging stations across the U.S. For instance, in an attempt to provide long-distance travels for

Tesla vehicles, this company has installed a national network of 357 DCFC stations that underpin 2,478 fast chargers within the past five years (U.S Department of Energy, 2017). In addition, Electrify America is committed to a $2 billion investment in zero-emission vehicle initiative over the next decade (Electrify America, 2017; Green Car Reports, 2017). Electrify America plans to establish a vast community-based network of EV chargers and about 300 DCFC stations along corridors carrying high traffic volumes and linking metropolitan areas in 39 states. Recently, the U.S. Department of Transportation (USDOT) has specified a number of highways as alternative fuel corridors to promote an increased uptake of AFVs (U.S. Department of Transportation, 2017). To meet the aims of these initiatives, researchers should investigate the EV charging infrastructure needs in different states in order to take actions on building the required infrastructure that meets the potential EV demands.

Many technologies have been introduced to provide the charging infrastructure required for EVs. Battery swapping stations, dynamic chargers, and fast-charging stations are among the most well-known technologies. Battery swapping stations store different types of fully charged batteries and can exchange the EVs depleted batteries very fast. However, the problems regarding the storage of multiple types of batteries as well as the battery ownership dilemma have made this business model struggling (Mirchandani et al., 2014). Another technology is dynamic charging stations, a relatively new technology, which recharges the vehicles while they are traveling (Riemann et al., 2015). These chargers seem to be profitable for electric vehicles that have fixed routes e.g., buses and taxis. The next technology is associated with incorporating fast chargers, which are stationary and EVs need to be plugged into them to get charged. Although there are three levels of chargers, only the Level 3 chargers can provide a reasonable level of service and feasibility for network applications (Nie and Ghamami, 2013).

The charging problem needs to be addressed for urban and intercity trips separately. Intercity trips are often considered to be stand-alone trips, in which EVs are highly likely to have fully charged batteries due to their preplanned nature. However, even a fully charged battery may not be enough for EVs to reach their destination. Therefore, the objective of intercity studies is to provide feasibility across the network or maximize the coverage while maintaining a limited budget. Urban trips, however, are part of chain of trips, in which EVs might have any state of charge (depending on the availability of chargers and dwell time for recharging at the trip origin). Therefore, the charging incidence in one trip may depend on its sequential trips as well, i.e., the vehicle might recharge during a feasible trip to prevent charging in a subsequent infeasible one (Usman et al., 2020). To capture the differences in users' behavior, this study proposes different modeling frameworks for each case.

The purpose of this study is fivefold. First, it provides a framework for the optimization of charging station infrastructures for intercity networks considering range anxiety, charging and queuing delay, detour time, and network-wide trip feasibility. This study guarantees that all EV trips are fulfilled while minimizing the total system cost. Second, it sets out to incorporate monthly demand and battery performance variations at different months in the intercity network model in two target years of 2020 and 2030. The battery performance and traffic demand fluctuations in different months are expected to be extremely significant for the state of Michigan, because of the frequent severe weather conditions, as well as the tourism attractions in the state. Thirdly, this study investigates the charging requirements of EVs for intercity trips in Michigan, considering a variety of charging and vehicle technologies. Fourthly, the study introduces an integrated framework for urban fast-charging infrastructure to address the range anxiety issue. It guarantees the feasibility for all trips while minimizing the total system cost. Finally, this study introduces forecasting models to estimate the required charging infrastructure for small urban areas.

1-2- Knowledge Gap and Research Motivation

Despite the extensive research conducted on the charging station planning problem, there is still a further need to develop approaches to realistically capture the users' behavior in determining the optimal charging infrastructure configuration. More specifically, the trade-off between the infrastructure cost, which includes the charging station cost and charger cost, and users' delay cost, which includes charging time, queuing time, and detour time, need to be captured realistically. In intercity networks, the feasibility of routes for EVs might depend on the availability of charging stations along them. As more EVs would traverse routes with charging stations, the traffic on the network links would be affected by the availability of charging stations as well. Thus, assigned routes and charging station allocation need to be determined jointly in an integrated model. As a result, a user equilibrium framework needs to be embedded into a system optimal framework to capture the route and recharging choices of users.

The other factors affecting the users' behavior are battery performance reduction in cold seasons and monthly demand variations. These factors are expected to be extremely significant for the state of Michigan, because of the frequent severe weather conditions during the winter season, as well as tourism attractions in the state during warmer seasons. Although the effects of EV demand seasonality on power consumption of EVs are investigated in a few studies (Bikcora et al., 2015; Donadee et al., 2014; Murakami et al., 2014; Shortt and O'Malley, 2014), there is a lack of studies in the literature that account for realistic traffic demands of the mixed fleet of conventional and electric vehicles in different months in the charging placement problem.

Thirdly, as a part of strategic charging planning, there is a need to investigate the optimal charging infrastructure configuration in the light of future technological advancements. High-end batteries and chargers can decrease the charging demand and charging time, respectively, and increase the EVs' market share. This study captures the impact of technological advancements through sensitivity analysis on the optimal charging infrastructure and finds out the required investments to address the EV charging demand in two target years of 2020 and 2030.

Fourthly, unlike intercity trips, which are often considered as stand-alone trips and are highly likely to have fully charged batteries due to their preplanned nature, urban trips are part of chain of trips, in which EVs might start with any state of charge (depending on the availability of chargers and dwell time for recharging at the trip origin). Therefore, the charging incidence in one trip may depend on its sequential trip as well, i.e., the vehicle might recharge during a feasible trip to prevent charging in a subsequent infeasible one (Usman et al., 2020). Therefore, there is a need to introduce a framework for urban fast-charging infrastructure to address the range anxiety issue while considering the chain of trips and state of charge variations at the start of each trip.

Finally, estimating charging demand, modeling the problem, adopting integer programming, and efficiently solving the problem, make the urban charging infrastructure planning a demanding task in terms of input requirements and computational complexity. Thus, finding the optimal solution might not be practical or cost-efficient in all urban areas. A macro-level model can yield estimation to the required charging infrastructure, which provides insights to urban areas for planning purposes and high-level decision-making on policies and budget allocation.

1-3- Research Significance and Contributions

The main objective of this study is to provide mathematical frameworks to realistically capture the charging behavior of EVs, estimate their charging demand, and locate charging infrastructure to address this demand in large-scale intercity and urban networks. This study captures the realistic behavior of users and considers the demand/supply variations to address some of the existing gaps in the literature of the facility location problem in large-scale networks. The main contributions of this study are as follows:

- Suggesting a configuration for plug-in electric vehicle charging infrastructure to support long-distance intercity trips of electric vehicles at the network level.
- Capturing realistic patterns of travel demand and considering flow-dependent charging delays at charging stations.
- Considering monthly demand and battery performance variations, which are two contributing factors in defining the infrastructure needs of EV users, particularly in states with adverse weather conditions.
- Investigating the impact of different battery and charger technologies on the configuration of charging infrastructures.
- Developing a framework for urban fast-charging infrastructure to address the range anxiety issue.
- Presenting a framework to simulate EVs charging behavior and charging demand in urban areas using a trip-based model.
- Developing macroscopic models to forecast the future required charging infrastructure in small urban areas

1-4- Research Methods and Dissertation Outline

This dissertation is organized in seven chapters. The first two chapters provide the description of the concept and objectives of the study as well as a comprehensive background review on the dissertation topic. Chapter 3 presents a facility location problem to find the optimum charging infrastructure in intercity networks considering route choice and travel time delay for a mixed fleet of electric and conventional vehicles at the network level. At the network level, the impacts of charging station locations on the traffic assignment problem with a mixed fleet of electric and conventional vehicles need to be considered. To this end, a traffic assignment module is integrated with a simulated annealing algorithm. This problem is formulated as a mixed-integer program with nonlinear constraints, which is known to be NP-hard, including possible local optimal solutions. Therefore, an SA algorithm is used to solve the proposed model in the intercity network of Michigan.

Chapter 4 extends the intercity charging infrastructure model presented in Chapter 3 by considering monthly traffic patterns and battery performance variations. These two factors can affect the optimum charging infrastructure, particularly in states with adverse weather conditions. While the cold weather decreases the travel demand, the battery performance drops as well. On the other hand, the increased travel demand in warm seasons is associated with a higher battery performance. This chapter aims to propose a modified and robust framework to capture the impact of seasonality and provide a solution which is optimal throughout the year.

Chapter 5 investigates the impacts of technological advancements on the charging infrastructure configuration. The battery capacity and charging power determine the range of EV and charging rate, respectively. Higher capacity batteries alleviate the charging demand while high-charging-power stations increase the service rate. On the other hand, these technologies dictate a higher price to the network. This chapter studies the impact of these factors on the optimum charging infrastructure configuration.

Chapter 6 introduces an integrated framework for urban fast-charging infrastructure to address the range anxiety issue. A mesoscopic simulation tool is developed to generate trip trajectories and simulate charging behavior based on various trip attributes. The resulted charging demand is the key input to a mixed-integer nonlinear program that seeks charging station configuration. The model minimizes the total system cost including charging station and charger installation costs, and charging, queuing, and detouring delays. The problem is solved using a decomposition technique where one sub-problem finds the location of charging stations and the second sub-problem determines the number of required chargers within the charging station. The first sub-problem is solved by incorporating a commercial solver for small networks, and a heuristic algorithm for large-scale networks. The second sub-problem is solved using the Golden Section method.

Chapter 7 generates regression models to estimate the number of chargers and charging stations to support the EV charging demand for urban areas. These models provide macro-level estimates of the required infrastructure investment in urban areas, which can be easily implemented by policy-makers and city planners. This chapter incorporates data obtained from applying the disaggregate optimization-based charger placement model, developed in chapter 6, for multiple case studies to generate the required data to calibrate the macro-level models, in the state of Michigan. This simulated data set includes the number of charging stations and chargers for each market share, technology advancement scenario, and the transportation network topology. Finally, chapter 8 provides future research directions and a summary of the concluding remarks of this study.

Chapter 2 - State of the Art Review

2-1- Overview

A comprehensive review of the previous studies on the facility location problem is presented in this chapter. Then, the refueling charging infrastructure for alternative fuel vehicles, especially EV charging infrastructure, is studied. Then, the literature of EVs charging infrastructure is reviewed for both urban and intercity areas thoroughly. Finally, the external factors affecting the optimal location of charging stations are investigated.

2-2- Facility Location Problem

Private and public firms usually face the problem of where to locate their facility at least once in their history (Daskin, 1995). The quality of service and the transportation costs of an agency depends on its location. Many facility location models have been introduced to help private and public decision-makers with addressing this concern. These models are categorized into set covering models, center problems, median problems, and fixed charge facility location problems (Daskin, 1995).

Set covering models locate the minimum number of facilities while ensuring a given level of service, e.g., locating the required charging stations to provide service to a city in less than 5 minutes. On the other hand, center problems locate a given number of facilities to provide a service for customers within the tightest possible standard. In case of interest to locate a given number of facilities which can find the least average distance between the facilities and customers, median problems are usually implemented. In all these cases, the implicit assumption is a uniform facility cost that favors no location over others. However, infrastructure cost of a facility might depend on the location as well, e.g., building a charging station in downtown can provide greater access for the public. However, more expensive land would result in a higher infrastructure cost. Fixed charged location problems can make a balance between the different costs in the network. The models presented in this study consider the different costs in the system where a set of candidate locations are selected to minimize the total system cost.

Facility location problems are integer programming problems. Some of the preliminary models in this category have exact solutions. However, for the more complicated ones, and the ones with nonlinear constraints, there are no exact solutions, as they are np-hard problems. Therefore, heuristic algorithms are usually implemented to solve them, which might not yield to the optimum solution. In this study, the focus is to formulate the problems correctly and consider all the influential components in each model and solve it through proposed frameworks. Formulating the problem correctly and considering all important components is known to be the most important part of the problem, whether obtaining the optimal or suboptimal solution to it (Mirchandani and Francis, 1990).

2-3- Refueling Station Planning Problem

The refueling station location model is a part of facility location model where the location of refueling stations and their allocated demand are determined simultaneously. This problem is studied extensively in the literature for alternative fuel vehicles (AFVs) including vehicles driving on biodiesel, ethanol, propane, hydrogen, liquid natural gas (Erdoğan and Miller-Hooks, 2012; Kuby and Lim, 2007, 2005; Shukla et al., 2011; Upchurch et al., 2009), and electricity (Mirchandani et al., 2014; Nie and Ghamami, 2013).

EVs are considered new technology and their charging infrastructure have been studied in the past 15 years. At the start of employing EVs, plug-in hybrid electric vehicles (PHEVs) were more common. PHEVs have limited electric range and thus, numerous studies aim to maximize the distance traveled on electricity (Dashora et al., 2010; Dong and Lin, 2012; Eberhard and Tarpenning, 2006; He et al., 2013). With the advancement of battery and charging technology, higher capacity batteries become available while chargers provide more power, which reduces the charging time and induces a different charging pattern than the slow charging at home. Therefore, the next generation of EVs only have battery storage and are called battery electric vehicles (BEVs), or as referred to for the remainder of this study, EVs. The studies focusing on EVs charging station locations mainly distinguish between intercity trips (Kuby and Lim, 2007; Lim and Kuby, 2010) and urban trips (Chen et al., 2013; Dong et al., 2014; Frade et al., 2011; Ghamami et al., 2016b; Sweda and Klabjan, 2011) due to behavioral differences between these two types of trips. Similarly, these trips are studied separately in this study as well.

2-4- EVs Charging Infrastructure at Intercity Networks

Since the main deficiency of current BEVs , is their limited range, long distance intercity trips are the major concern for these vehicles. The optimization of charging locations for EV intercity trips is studied extensively in the literature (Ghamami et al., 2016b; He et al., 2015, 2018; Jing et al., 2017; Nie and Ghamami, 2013; Riemann et al., 2015). Some of the early studies used flow capturing location modes (FCLMs) to maximize the captured flow by providing the charging stations on the intersecting roads with the maximum flow (Berman et al., 1992; Hodgson, 1990). However, FCLM cannot address the multiple required refueling stops along paths exceeding the vehicle range. To address this issue, the flow refueling location model (FRLM) has been introduced, in which round trips are considered and vehicles can be refueled more than once on their path (Kuby and Lim, 2005; Mirhassani and Ebrazi, 2013; Nourbakhsh and Ouyang, 2010; Xie et al., 2016). An optimization model explores EVs travel along a long corridor, and captures the tradeoff between investing in charging stations or batteries to provide a certain level of service for travelers (Nie and Ghamami, 2013). The results suggest that for intercity travel, only fast-charging stations can provide an acceptable level of service. The model is then extended to minimize the total system cost, including infrastructure investment, battery cost, and users' time cost including queuing delay (Ghamami et al., 2016b). This model considers multiple origin-destination (OD) pairs for a single type of EV and one corridor of travel. Other studies have also considered queuing delay as an element of routing (Chen et al., 2020; Jung et al., 2014). However, there is a need to find the best allocation of EV charging stations throughout an intercity network, where parallel and intersecting corridors exist.

Path flow assignment and optimum location of facilities interact with each other, since the placement of facilities can affect traffic flow patterns. It is reasonable to assume that for long-distance trips, locations of charging facilities may affect the route choice of the EV users as well as other travelers. In other words, due to the technological advancement and ubiquitous presence of internet and routing apps, users are aware of the traffic on roads and behave selfishly and noncooperatively just to minimize their own travel time and costs. Wardrop defines this concept as the user equilibrium traffic assignment problem for intra-city transportation networks (Wardrop, 1952). This concept is implemented in intercity networks by many studies (Bai et al., 2011; Hajibabai et al., 2014; He et al., 2015). In user equilibrium for EVs, the limited range of EVs is also another element of the routing problem. Some studies have considered these factors to model the behavior of EVs and find the optimum location for charging stations (He et al., 2014; Jing et al., 2017; Zhang et al., 2018). However, these studies have not considered the queuing delay experienced by EVs.

There are numerous studies on the location of chargers for EVs, and each of these models has some underlying assumptions. One of the most recent studies on charger placement considers both users and investors by assuming queuing and charger cost. However, this study assumes charging after a fixed driving distance and only one facility is allowed on each link (Chen et al., 2020). In another study, a network-level analysis is proposed for the location of DC fast chargers. This study assumes that EVs follow the fixed shortest path between different OD pairs (He et al., 2019) and aims to solve the model based on this limiting assumption by proposing a comprehensive optimization framework.

2-5- EVs Charging Infrastructure at Urban Networks

Unlike intercity trips, which are often considered as preplanned and stand-alone trips and EVs are highly likely to depart from their origin fully charged, urban trips are part of a chain of trips, in which EVs might start with any state of charge (depending on the availability of chargers and dwell time for recharging at the trip origin). Therefore, the charging incidence in one trip may depend on its sequential trip as well, i.e., the vehicle might recharge during a feasible trip to prevent charging in a subsequent infeasible one (Usman et al., 2020).

One common approach is to incorporate data-driven models developed from travel surveys considering endpoint, distance, purpose, departure time, and arrival time of each trip to find the charging demand. The charging demand is then used to select charging stations from a set of candidate locations to minimize unfulfilled trips. In addition to travel survey data, exploiting trip trajectory travel data is another common approach to find the charging demand. The taxis' trip trajectory data has been used in numerous studies; e.g., to identify the locations with longest dwell times as the candidate points (Cai et al., 2014), adopt an optimization-based approach to find the hotspots maximizing the vehicles-miles-traveled (VMT) on electricity (Shahraki et al., 2015), and minimize the infrastructure cost considering congestion at charging stations (Yang et al., 2017). The models using taxi trajectories can be applied for taxis or buses but are not suitable for private

EVs due to the limited availability of GPS data. Therefore, an alternative approach to capture travel data is to use traffic simulation for the origin-destination demand tables. In this regard, some studies consider the fixed-route choice and travel patterns (Berman et al., 1992; Hodgson, 1990; Kuby and Lim, 2007, 2005; Lim and Kuby, 2010; Nourbakhsh and Ouyang, 2010; Upchurch et al., 2009; Xie et al., 2016; Zockaie et al., 2016), while others capture the interactions between service facility locations and the traffic assignment problem (Bai et al., 2011; Ghamami et al., 2020a; Hajibabai et al., 2014; He et al., 2013, 2018; Riemann et al., 2015). Capturing these interactions makes the problem computationally cumbersome in large scale networks. This study relies on traffic simulation to generate vehicle trajectories. It captures the interaction between charging station locations and vehicles' assignment and introduces a heuristic technique to reduce the problem complexity.

Due to the lack of real-world data on details of EVs' trip trajectories and their state of charge along their trips, simulations were implemented to generate this data. Some studies locate charging stations using a simulation-optimization model minimizing investment cost for different types of chargers and/or the number of trajectories that are unable to reach their destination due to the lack of infrastructure (Dong et al., 2014; Xi et al., 2013). Another approach adopts real-time taxi trajectories and uses a time-series simulation model for traveling and charging behavior of plug-in hybrid electric vehicles to provide insights on optimal charging station development plans (Li et al., 2017). This study addresses charging and trip trajectory data unavailability by developing a state of charge simulator within a simulation-optimization framework.

2-6- Impact of Queuing on Charging Infrastructure

The queuing delay is usually considered to determine the number of chargers as a bi-level or separate problem (Jung et al., 2014; Wang et al., 2019; Xie et al., 2018). Xie et al. 2018 defined one feasible path for each OD and provided enough chargers to certify a certain level of service (Xie et al., 2018). Jung et al. 2014 located the charging stations for electric taxis introducing a stochastic dynamic itinerary-interception refueling location model considering the queuing delay (Jung et al., 2014). They considered that users have information on the expected queuing delay in each charging station through a bi-level setting. The lower level incorporates an activity-based simulation framework to simulate the behavior of EVs based on the charging stations and chargers found in the upper-level program. Wang et al. 2019 defined different charging scenarios and embedded the expected waiting time into link travel times underlying the assumption that EVs have access to the expected waiting time information (Wang et al., 2019). In another approach, the nonlinear queuing constraints within the optimization models are linearized with logarithmic transformation and solved using commercial solvers (Yang et al., 2017). The impact of queuing on the assignment of vehicles to charging stations has been studied for locating chargers and charging stations that support the intercity trips of EVs. Some studies capture the exact deterministic and non-deterministic queuing delay, as well as range anxiety and detour time, in bi-level or single-level optimization frameworks (Chen et al., 2020; Ghamami et al., 2020a; Zhang et al., 2018). The intercity studies generally assume a fully charged battery at the start of trips, which makes them inapplicable to urban networks since almost all urban trip distances are in the range of current EVs.

2-7- Seasonal Variations

Two important contributing factors in defining the infrastructure needs of EV users are battery performance and traffic demand fluctuations in different months (Hao et al., 2020). These factors are expected to be extremely significant for networks experiencing frequent severe weather conditions due to the reduction of battery performance in adverse weather and increased travel demand in favorable weather conditions. Therefore, traffic demand variations across different months are accounted for in this study to capture multi-view perspectives and better equip the study network as part of the desired more electrified U.S. transportation system. Although the effects of EV demand seasonality on power consumption of EVs are investigated in a few studies (Bikcora et al., 2015; Donadee et al., 2014; Murakami et al., 2014; Shortt and O'Malley, 2014), there is a lack of studies in the literature that account for realistic traffic demands of the mixed fleet of conventional and electric vehicles in different months in the charging placement problem. In addition to travel demand fluctuations, this study differentiates between battery performances in favorable and extreme (or cold) weather conditions.

2-8- Technology Advancements

Although there are many studies on charging station planning, a few studies explore the future required charging infrastructure considering EV technologies advancements. A study investigates the entire U.S. network for EV charger placement needs considering 2010 long-distance travel data and maximizes the long-distance trips completions (He et al., 2019). The designed scenarios in this study consider discrete charging powers from 50 kW to 250 kW and EV ranges from 60 mi to 250 mi. Another study investigates charging powers of 50 kW, 100 kW, and 150 kW, and driving ranges of 62.5 mi, 125 mi, and 187.5 mi using an aggregate model and simulation of EV drivers' charging behavior (Gnann et al., 2018). A recent research explores the long-term DCFC charging planning in the U.S., which considers a 15-year horizon starting in 2015 (Xie et al., 2018). In this study, a multi-period framework is proposed and solved using a genetic algorithm (GA) to determine the location and timing of station openings, as well as the number of required chargers at each location. Several battery types and fuel efficiencies, leading to different vehicle driving ranges (from 75 mi to 300 mi), are considered. However, planning for the future requires more in-depth and detailed analyses, which cannot be captured correctly by aggregate models. Also, as infrastructure advancements and expansions are required to increase market acceptance of EVs, user convenience should also be considered when building a network of charging stations.

2-9- Forecasting Models

Estimating charging demand, modeling the problem, adopting integer programming, and efficiently solving the problem, make the charging infrastructure planning a demanding task in terms of input requirements and computational complexity (Singh et al., 2022). Thus, finding the optimal solution might not be practical or cost-efficient in all urban areas. A macro-level model can yield estimation to the required charging infrastructure, which provides insights to urban areas for planning purposes and high-level decision-making on policies and budget allocation. The variation in the exact location of charging stations would not cause significant variation in detours in small urban areas. The current urban charging infrastructure planning tools, e.g., EVI-Pro (Wood et al., 2017) and BEAM (Sheppard et al., 2017), simulate the activities of EVs, which can be used in optimization models. EVI-Pro provides two different modules for intercity and urban networks. The EVI-Pro intercity module locates charging stations and chargers along intercity corridors. This module considers traffic volume and determines the number of chargers per station as a function of charging time, EV adoption level, peak traffic volume, and station spacing. On the other hand, the urban module tracks the EV state of charge for a sample of available trajectories provided by GPS devices. This module finds the feasible charging scenarios for each agent by ensuring a minimum threshold of available charge. Then, it finds the infrastructure required to satisfy the charging demand depending on the spatial/temporal charging incidence. This module assumes that charging events occur only during dwell times and does not consider the day-to-day charging demand variations. M.J. Bradley & Associates (“M.J. Bradley & Associates,” 2021) developed a regression-based planning tool to estimate the required infrastructure for intercity travels. However, to the authors' best knowledge, there is no ready-to-use regression model designed for urban areas to be adopted by municipalities.

Chapter 3 - Charging infrastructure planning in intercity networks

3-1- Overview

Despite the extensive research conducted on the charging station planning problem, there is still a further need to develop approaches to realistically capture the users' behavior in order to determine the optimal charging infrastructure configuration. More specifically, the trade-off between the infrastructure cost and users delay cost need to be captured realistically. In this chapter, the problem of EV charging infrastructure to support long-distance intercity trips of electric vehicles at the network level is formulated. The problem of interest is to find the optimal infrastructure investment to support the intercity trips for electric vehicles in such networks. The decision variables are where to build charging stations in the network and how many chargers must be provided within them. The main constraints are the travel feasibility for electric vehicles between all OD-pairs with positive demand and ensuring a certain level of service in terms of total travel delay for electric vehicle users. A feasible network provides at least one feasible path for each OD pair for all classes of vehicles. A path is feasible for a class of vehicle if it can be traveled by those vehicles without getting stranded along the way, whether they need refueling or not. Therefore, by providing travel feasibility, it is ensured that all vehicles can fulfill their trips and reach their destinations.

This problem is solved for a single corridor with multiple OD-pairs located along that corridor (Ghamami et al., 2016b). However, in this study, we focus on an intercity network of corridors. The element of the earlier corridor model that tracks the state of fuel in (Ghamami et al., 2016b) cannot be directly applied to the intercity networks since there is no directionality of traffic flow. In addition to tracking the state of fuel, the integration of a routing problem for refueling with the charging station locating problem adds to the complexity of the network-wide model.

Considering travel time on corridors as a function of flow relates routing of different electric vehicle classes and conventional vehicles and calls for a new equilibrium state in the network that considers the refueling for electric vehicles. It should be noted that the location of charging stations affects the route choice of EV users, which affects the traffic flow pattern in the network, the energy consumption, and the optimum location of charging stations as a result. Thus, routes and locations need to be determined simultaneously in an integrated model.

In this problem, the objective is to minimize the total system cost, including the investment in charging stations and the extra travel delay (detour delay, queue waiting delay, and recharging delay) due to recharging for all EV users. However, in the route choice problem, all users including the EV users are seeking to minimize their own travel time regardless of other travelers. Therefore, a user equilibrium problem needs to be embedded into a system optimal problem in the proposed model. This problem finds the optimal location of charging stations in a network, where users with various classes of vehicles try to minimize their travel times (including recharging delays for EV users), subject to change by travel flows along the routes. The level of service constraint is considered in the system optimal objective function by multiplying the value of time by the total delay for all the electric vehicles (including charging time, waiting time, and refueling detour travel time).

3-2- Modeling framework

This section first provides definitions of all variables and parameters used in the modeling framework. Then, the assumptions used to simplify the problem without losing the generality are presented. Then, modeling framework for the queuing procedure is presented and the desired equations are extracted. Finally, the bi-level mixed-integer program with non-linear constraints is presented, followed by brief discussions for each constraint.

In this study, the following notation in Table 3-1 is used.

Table 3-1 Nomenclature

Parameters	Definitions
$G(I, E)$	Road network
$e \in E$	Set of links
$i \in I$	Set of nodes
$m \in M$	Set of user classes
M'	Set of user classes except conventional vehicles
N_1^m	Set of current refueling stations
N_2^m	Set of candidate refueling stations
N'^m_1	Set of dummy nodes for current refueling stations
N'^m_2	Set of dummy nodes for candidate refueling stations
I'	Entire set of nodes, including nodes and dummy nodes, $I' = I \cup N'^m_1 \cup N'^m_2$
$\omega \in \Omega$	Set of OD-pair
$r \in R_m^\omega$	Set of routes for users in class m between OD-pair ω
R'^ω_m	Set of feasible routes for users in class m between OD-pair ω
$k = 1, 2, \dots, K_r$	Set of consecutive nodes in which K_r is the total number of nodes visited in route r
a_k^r	Tracks the sequences of nodes of the network in route r ($a_k^r = i, k = 1, 2, \dots, K_r$)
S_k^r	State of fuel after visiting each node (k) in route r
$h^m_{(a_k^r, a_{k-1}^r)}$	Required energy to travel between nodes a_k^r and a_{k-1}^r by vehicles in class m
F^m	Maximum amount of energy a vehicle in class m can take
x_i^m	Binary variable, which equals 1 if there is a station in node i for vehicles in class m and 0 otherwise
δ_i^r	Binary parameter, which equals 1 if node $i \in I'$ belongs to route r and 0 otherwise
Δ_e^r	Binary parameter, which equals 1 if link $e \in E$ belongs to route r and 0 otherwise
b_i^r	Sequence of node i (k^{th} node) in route r
f_r	Total flow on route r
y_i^m	Total flow visiting the dummy station i from vehicles in class m
v_i^m	Total refueling demand from vehicles in class m visiting charging/refueling station i
f_e	Total flow for link e
TT_d	Total detour travel time required for refueling, defined as the additional time electric vehicle users spend on the road to reach a recharging station
T_{elec}	Entire electric vehicle travel time if, hypothetically, no charging is needed at all
M'	All classes of vehicles except conventional ones
t_e	Travel time on link e
σ_e	Capacity of link e
A_1	Congestion factor in BPR function, which is considered 4 in this study
A_2	BPR function parameter, which equals 0.15 in this study
B_k^r	Binary parameter, which equals 1 if route r in node k is feasible based on the state of fuel
C_P^m	Fixed cost of building refueling/charging stations for vehicles in class m

Table 3-1 (cont'd)

C_s^m	Cost per charger for class m vehicles
γ	Value of time
π_i	Total delay for all users at each station i, consisting of refueling time and waiting time in queue for an available pump or charger
α	Charging efficiency of batteries
z_i^m	Number of chargers for vehicles in class m at node i
P	Charging power of chargers
t_i^m	Refueling time in node i for class m
$t_i'^m$	Queuing time occurring due to excess demand in a charging station
μ_i^m	Service rate, which is the average number of users each charger can serve in a station per hour
λ_i^m	Arrival rate, which is the average number of users visiting each charger in a station per hour
T_0	Design period
q_ω^m	Travel demand for OD-pair ω for vehicles in class m
L	An arbitrary big number
CT_r	Travel time in the set of routes r
CT_r^{min}	The minimum travel time for the set of routes r
α_n	Step size in method of successive averages
f_r^n	Path flow for route r in the n^{th} iteration in method of successive averages

Following assumptions have been made in this study:

I. Each vehicle has access to charging station to fully charge the battery before starting its intercity trip.

II. The energy consumption of vehicles is a function of traveled distance.

III. The vehicles assigned to charging stations (based on the traffic assignment module) have a uniform temporal arrival distribution.

The network G considered here includes a set of links ($e \in E$), and a set of nodes ($i \in I$), which has two main subsets: the set of current refueling stations ($N_1^m \subset I$), and the set of candidate points for building refueling stations ($N_2^m \subset I$). Notation $m \in M$ denotes different classes of vehicles in the network such as conventional vehicles and EVs with certain battery sizes. Any node belonging to the set of current refueling stations or candidate refueling stations may be visited by users for two reasons: refueling or as a midpoint along their route. These reasons need to be differentiated as a result of their impacts on the state of fuel. To this end, two sets of dummy nodes are introduced. The first dummy set is a duplicate of the current refueling stations set, which represents the set of current refueling stations visited for refueling purpose $\left(N'^{m}_{1}\right)$. The second dummy set is a duplicate of the candidate refueling stations set, which represents the set of candidate refueling stations that may be visited for refueling purpose $\left(N'^{m}_{2}\right)$. Thus, the entire set of nodes in the network is $I' = I \cup N'^{m}_{1} \cup N'^{m}_{2}$. The dummy nodes of the network are connected to the original nodes using dummy links with zero travel times and zero fuel consumption. The model considers multiple sets of OD-pairs ($\omega \in \Omega$) in a network. There is a known set of routes for each class of users between each origin and destination ($r \in R^{\omega}_{m}$). Each route consists of a set of consecutive nodes $k = 1, 2, \ldots, K_r$, in which K_r is the total number of nodes visited by route r. Also, a^r_k tracks the sequences of nodes of the network in route r ($a^r_k = i, k = 1, 2, \ldots, K_r$).

The refueling and queuing waiting time can be extracted based on assumption III as follows.

Refueling time for all vehicles in class *m* using station *i* for refueling is defined as:

$$t^m_i = \alpha \, \frac{\mathrm{v}^{\mathrm{m}}_{\mathrm{i}}}{P} \qquad \forall m \in M, i \in N'^{m}_{1} \cup \, N'^{m}_{2}, \tag{3.1}$$

In which $\alpha > 1$ represents battery's charging efficiency and *P* is the charging power of each charger (Nie and Ghamami, 2013). The average refueling time, $\tilde{t}^m_i$ (h), for each vehicle in class *m* can be calculated by dividing t^m_i by the total number of vehicles visiting station i.

$$\tilde{t}^m_i = \frac{t^m_i}{y^m_i} \qquad \forall m \in M, i \in N'^{m}_{1} \cup \, N'^{m}_{2}, \tag{3.2}$$

Then, the service rate can be defined as follows:

$$\mu^m_i = \frac{1}{\tilde{t}^m_i} \qquad \forall m \in M, i \in N'^{m}_{1} \cup \, N'^{m}_{2}, \tag{3.3}$$

In which, μ_i^m is the service rate for vehicles in class m at station i (vehicle per hour). This value defines the number of vehicles that can be served in one hour. The arrival rate of customers $\lambda_{\mathrm{i}}^{\mathrm{m}}$, which is the average number of users per hour visiting each charger or fuel dispenser in a station, is defined as follows:

$$\lambda_{\mathrm{i}}^{\mathrm{m}} = \frac{y_i^m}{T_0 z_i^m} \qquad \forall m \in M, i \in {N'}_1^m \cup {N'}_2^m, \tag{3.4}$$

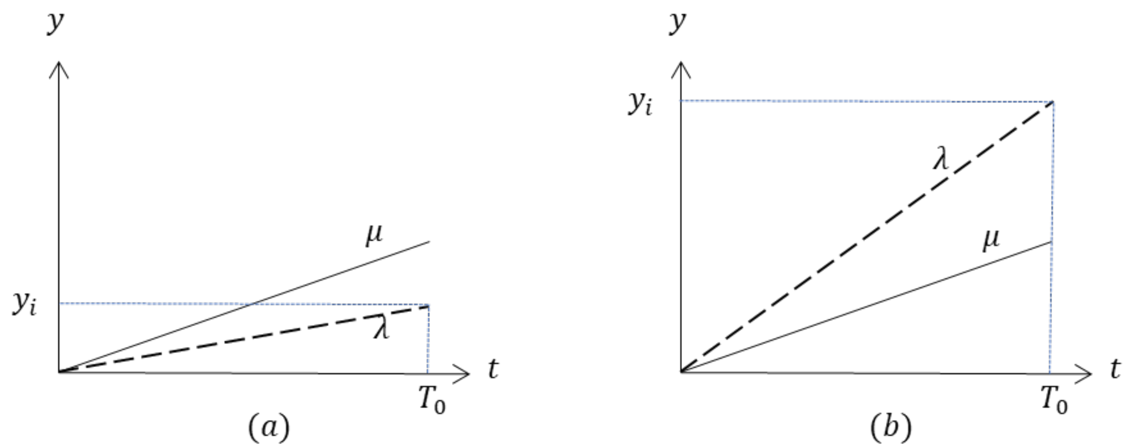

Figure 3-1 (a) Arrival rate lower than service rate (b) arrival rate greater than service rate resulting in queue

Where T_0 is the design period in hours. Assuming a uniform arrival rate (assumption III), deterministic queuing is considered in this study (Zukerman, 2013). Therefore, no queue forms when the service rate is greater than the arrival rate (Figure 3-1(a)). Otherwise, the queuing happens in a charging station if the number of users visiting each charger per hour (arrival rate of customers) is higher than the available service rate (Figure 3-1(b)). When the hourly visiting flow for a charger is higher than the number of vehicles that can be served by that charger per hour, the extra vehicles have to wait in line for the chargers to become available. The total queuing delay for each station in each class is the summation of all queuing delays for all vehicles in that class visiting that station. Assuming a right triangle waiting time function, the first vehicle visiting the station has no queuing delay while the last person experiences the longest one, assuming the queue would be recovered at the end of the day. Considering a constant flow, the total queuing time must be the area of the triangle. One side of the triangle is the number of users and the other side is the last person waiting time. Last person waiting time is the average charging time multiplied by the difference between the arrival rate and the service rate. Therefore, the total queuing time is defined as:

$$t_i'^m = 0.5T_0\, \tilde{t}_i^m y_i^m\, (\lambda_i^m - \mu_i^m), \qquad \forall m \in M, i \in N'^m_1 \cup N'^m_2, \tag{3.5}$$

With all the above definitions, we can formulate the proposed model as follows:

$$\min_{x_i^m, z_i^m} \sum_{m \in M} \sum_{i \in N'^m_2} (C_P^m x_i^m + z_i^m\, C_S^m) + \gamma\Big(\sum_{i \in N'^m_1 \cup N'^m_2} \pi_i + TT_d \Big) \tag{3.6}$$

Subject to:

$$x_i^m \in \{0,1\}, \qquad \forall m \in M, i \in N'^m_2 \tag{3.7}$$

$$z_i^m \in Z, \qquad \forall m \in M, i \in N'^m_2 \tag{3.8}$$

$$z_i^m \leq x_i^m L, \qquad \forall m \in M, i \in N'^m_2 \tag{3.9}$$

$$S_k^r = S_{k-1}^r - h^m_{(a_k^r, a_{k-1}^r)}, \qquad \forall\, \omega \in \Omega, m \in M, r \in R_m^\omega, k = 1, 2, \dots, K_r, a_k^r \in I \tag{3.10}$$

$$S_k^r = F^m, \qquad \forall\, \omega \in \Omega, m \in M, r \in R_m^\omega, k = 1, 2, \dots, K_r, a_k^r \in N'^m_1 \tag{3.11}$$

$$\begin{aligned} S_k^r = F^m x^m_{a_k^r} + S_{k-1}^r \left(1 - x^m_{a_k^r}\right), \qquad &\forall\, \omega \in \Omega, m \in M, r \in R_m^\omega, k \\ &= 1, 2, \dots, K_r, a_k^r \in N'^m_2 \end{aligned} \tag{3.12}$$

$$S_k^r \leq B_k^r L, \qquad \forall\, \omega \in \Omega, m \in M, r \in R_m^\omega, k = 1, 2, \dots, K_r \tag{3.13}$$

$$S_k^r \geq (B_k^r - 1)L, \qquad \forall\, \omega \in \Omega, m \in M, r \in R_m^\omega, k = 1, 2, \dots, K_r \tag{3.14}$$

$$B_k^r \in \{0,1\}, \qquad \forall \omega \in \Omega, m \in M, r \in R_m^\omega, k = 1, 2, \dots, K_r \tag{3.15}$$

$$TT_d, \pi_i \epsilon \operatorname*{argmin}_{f_r} \sum_{m \in M} \sum_{\omega \in \Omega} \sum_{r \in R'^{\omega}_m} f_r * (CT_r - CT_r^{min}) \tag{3.16}$$

Subject to

$$f_r \leq B_k^r L, \qquad \forall\, \omega \in \Omega, m \in M, r \in R_m^{\omega}, k = 1, 2, \dots, K_r \tag{3.17}$$

$$\sum_{r \in R_m^{\omega}} f_r = q_{\omega}^m, \qquad \forall\, \omega \in \Omega, m \in M \tag{3.18}$$

$$\sum_{\omega \in \Omega} \sum_{r \in R_m^{\omega}} f_r\, \delta_i^r \leq x_i^m L, \qquad \forall m \in M, i \in N'^{m}_2 \tag{3.19}$$

$$f_e = \sum_{m \in M} \sum_{\omega \in \Omega} \sum_{r \in R_m^{\omega}} f_r\, \Delta_e^r, \qquad \forall e \in E \tag{3.20}$$

$$t_e = t_{0_e} \left(1 + A_2 \left(\frac{f_e}{\sigma_e} \right)^{A_1} \right), \qquad \forall e \in E \tag{3.21}$$

$$TT_d = \Big(\sum_{m \in M'} \sum_{\omega \in \Omega} \sum_{r \in R_m^{\omega}} \sum_{e \in E} f_r \Delta_e^r\, t_e \Big) - T_{elec} \tag{3.22}$$

$$y_i^m = \sum_{\omega \in \Omega} \sum_{r \in R_m^{\omega}} f_r\, \delta_i^r, \qquad \forall\, m \in M, i \in N'^{m}_1 \cup N'^{m}_2 \tag{3.23}$$

$$v_i^m = \sum_{\omega \in \Omega} \sum_{r \in R_m^{\omega}} f_r\, \delta_i^r \left(F^m - S^r_{(b_i^r - 1)} \right), \qquad \forall i \in N'^{m}_1 \cup N'^{m}_2, \forall\, m \in M \tag{3.24}$$

$$t_i^m = \alpha\, \frac{\mathrm{v}_\mathrm{i}^\mathrm{m}}{P} \qquad \forall m \in M, i \in N'^{m}_1 \cup\ N'^{m}_2 \tag{3.25}$$

$$\lambda_\mathrm{i}^\mathrm{m} = \frac{y_i^m}{T_0 z_i^m} \qquad \forall m \in M, i \in N'^{m}_1 \cup\ N'^{m}_2, \tag{3.26}$$

$$t_i'^m = 0.5 T_0\, \tilde{t}_i^m y_i^m\, (\lambda_\mathrm{i}^\mathrm{m} - \mu_i^m), \qquad \forall m \in M, i \in N'^{m}_1 \cup\ N'^{m}_2, \tag{3.27}$$

$$\sum_{m \in M} (t_i^m + t_i'^m) \leq \pi_i, \qquad \forall\, i \in N'^{m}_1 \cup\ N'^{m}_2 \tag{3.28}$$

$$\sum_{m \in M} t_i^m \leq \pi_i, \qquad \forall\, i \in {N'}_1^m \cup {N'}_2^m \tag{3.29}$$

$$CT_r = \sum_{i \in {N'}_1^m \cup {N'}_2^m} \delta_i^r \frac{\pi_i}{\sum_{m \in M} y_i^m} + \sum_{e \in E} t_e \Delta_e^r \qquad \forall \omega \in \Omega, m \in M, r \in R_m^\omega \tag{3.30}$$

$$CT_r^{min} \leq CT_r, \qquad \forall \omega \in \Omega, m \in M, r \in R_m^\omega \tag{3.31}$$

$$\pi_i \geq 0, \qquad \forall m \in M, i \in {N'}_1^m \cup {N'}_2^m \tag{3.32}$$

$$f_r \geq 0, \qquad \forall \omega \in \Omega, m \in M, r \in R_m^\omega \tag{3.33}$$

$$f_e \geq 0, \qquad \forall e \in E \tag{3.34}$$

The objective function (3.6) consists of two main terms. The first term represents infrastructure investment cost, which includes the fixed cost of building a charging station at any location and the variable cost of chargers. For charging station cost, the number of charging stations is multiplied by C_P^m (measured in \$ per day per station), which is the cost of a charging station for a vehicle in class m. In order to calculate the charger cost, the number of chargers is multiplied by C_s^m (measured in \$ per day per spot), which is the cost to provide one charger for the vehicles in class m. The second term represents the monetary value of the total time spent on refueling and waiting in queue and required detour times to access charging stations. The total time is multiplied by γ, which is the value of time (\$ per hour).

Constraint (3.7) states that the problem is an integer programming and stations are built $(x = 1)$ or not $(x = 0)$ at any location. Constraint (3.8) indicates that the number of spots in charging stations must be selected from a given set. Constraint (3.9) is a feasibility constraint that ensures there is no allocated charger $(z = 0)$ at a location that is not selected to have a charging station $(x = 0)$. Constraints (3.10-12) monitor the state of fuel over the routes and different classes of vehicles to ensure the feasibility of travel along each route by each class of vehicles. Constraint (3.10) reduces the state of fuel along the route due to the energy consumption on each link of the route. Constraint (3.11) changes the state of fuel status to the full capacity once the dummy node associated with an existing charging station is visited along a route. Constraint (3.12) changes the state of fuel status to the full capacity once the dummy node associated with a candidate charging station is traveled along a route if the candidate node is selected in the solution. Otherwise, it does not change the status of the fuel. Constraints (3.13-15) are feasibility constraints. Constraint (3.13) ensures that when the state of fuel is positive along a route, then it is feasible. Constraint (3.14) states that when the state of fuel becomes negative along a route, this route becomes infeasible at that certain point. Constraint (3.15) states that each route is either feasible or infeasible.

Objective function (3.16) implies that travelers' behavior for the route choice and selecting charging stations along their routes is based on the user equilibrium concept. According to this concept, as mentioned earlier, users behave selfishly to minimize their own travel time. Therefore, the travel times on all used routes for each OD pair are equal and lower than unused routes.

Constraint (3.17) enforces the flow to be zero for any path that includes at least a node with a negative state of fuel (infeasible case). Once the required fuel to travel between any two consecutive charging stations exceeds the fuel capacity of the vehicle, we would have a negative state of fuel, which is an infeasible solution. Constraint (3.18) is the flow conservation equation. It denotes that the total flow from all routes for each class of vehicles between an OD-pair forms the given travel demand between that OD-pair for that class of vehicles. Constraint (3.19) states that if a candidate node is not selected as a charging facility, then the path flow must be zero for all paths that include the dummy node associated with that candidate node. Constraint (3.20) finds the flow on each link and Constraint (3.21) finds travel time on each link of the network using BPR function. Constraint (3.22) defines the difference between the total link travel time for any feasible solution excluding the required time for refueling and the total link travel time when no vehicle changes its path for the refueling purpose. Therefore, it is the total detour time.

Constraint (3.23) calculates the total incoming flows to a refueling station node by summing up all flows from different OD-pairs for a specific vehicle class. Constraint (3.24) calculates the charging demand at each charging station assuming the state of fuel for each vehicle crossing the dummy node of this station needs to be changed to the full capacity from the state of fuel right before entering the dummy link. In intercity travels, users typically try to minimize their number of stops; thus, it is reasonable to assume a full recharge at each stop. However, this assumption can be modified to consider different charging behaviors in the proposed framework of this study, without loss of generality. Constraint (3.25) calculate the total required charging time for all travelers at a certain station. Constraint (3.26) finds the arrival rate which is the average number of users visiting each charger per hour. Constraint (3.27) calculates the total queuing delay in each station for each class. If the average number of visits per hour for chargers in a station is higher than the inverse of the average charging time in the same station, then queuing would take place. The total delay consists of the terms calculated in Constraints (3.25) and (3.27) is reported in Constraint (3.28). Constraint (3.29) assures that when the provided supply is larger than the demand (resulting in negative average waiting time in queue), the delay would be only equal to the total refueling time and would not be reduced due to the negative waiting time. Constraint (3.30) defines the travel time along each route, including two terms: the first term is the delay in charging stations for waiting in the queue and recharging time, and the second term captures the travel time along with the links of each route. In the first term, the total delay in each station is divided by the total number of travelers using that station to calculate the average delay. Then, for the route of interest, these delays are summed up over the stations located along the route. In the second term, link travel times, a function of link flows, are summed up over the links located along the route. Constraint (3.31) implies that the minimum path travel time for each OD-pair and vehicle class is smaller or equal to the other path travel times for that specific OD-pair and class of vehicles. Finally, Constraints (3.32-34) are feasibility conditions for different variables.

3-3- Solution Methodology

The formulated model is a mixed-integer problem with non-linear constraints, which is known to be NP-hard. Due to the complexity of the problem, current commercial solvers like CPLEX and Knitro are either slow or unable to solve the problem especially when the problem size grows. This often calls for a metaheuristic algorithm to find a good solution with a proper approximation and in a reasonable time. In this study, a metaheuristic algorithm based on Simulated Annealing (SA) is implemented to solve the problem (Metropolis et al., 1953). Recent papers (Ghamami et al., 2016a; Zockaie et al., 2016) show that the SA algorithm can solve flow-capturing mixed integer programs (MIPs) efficiently. Figure 3-2 provides the framework of the proposed solution algorithm, which is discussed in detail in the following.

3-3-1- Simulated Annealing

The metaheuristic solution method proposed in this study includes two iterative procedures. In the first iterative procedure, a new solution (selected locations to be equipped with charging stations with a certain number of spots at each station) is generated by perturbing the solution in the previous iteration, which is then called neighbor solution. Then, the objective function needs to be evaluated for the neighbor solution. To this end, travelers' behavior needs to be determined in terms of route choice and selecting charging stations for refueling among the existing options in the current solution. As the decision of each traveler being affected by other travelers' decision through congestion, an equilibrium state needs to be found by solving a traffic assignment problem specifying routing and charging station selection for refueling simultaneously for all travelers. Users select routes to minimize their total delays including the travel time, charging time, and waiting time in queue. Thus, a second iterative procedure is proposed to find such an equilibrium state. Once the equilibrium state is reached, then the objective function can be evaluated for the neighbor solution. This new objective function for the neighbor solution needs to be compared with the objective function of the current solution as part of the simulated annealing algorithm. In this algorithm, the neighbor solution would be accepted deterministically as the new current solution, if it improves the objective function. It would be also probabilistically accepted, based on the difference between the objective function values even if it does not improve the objective function. This ensures that the algorithm avoids getting trapped in local optimum solutions. Once the neighbor solution is accepted as the new current solution or rejected (thus no change in the current solution), another neighbor solution would be generated randomly based on the current solution in the next iteration. The process would continue for a certain number of iterations to find the best solution in terms of the objective function. The probability of accepting a worse neighbor solution (in terms of the objective function) as the new current solution decreases in higher iterations to ensure the optimality of the best-found solution.

To apply the general SA algorithm framework to solve the proposed model, certain assumptions and definitions are needed to generate feasible initial and neighbor solutions. The solution framework based on the SA algorithm is provided in Figure 3-2 followed by the assumptions and definitions used to enhance the performance of the solution framework.

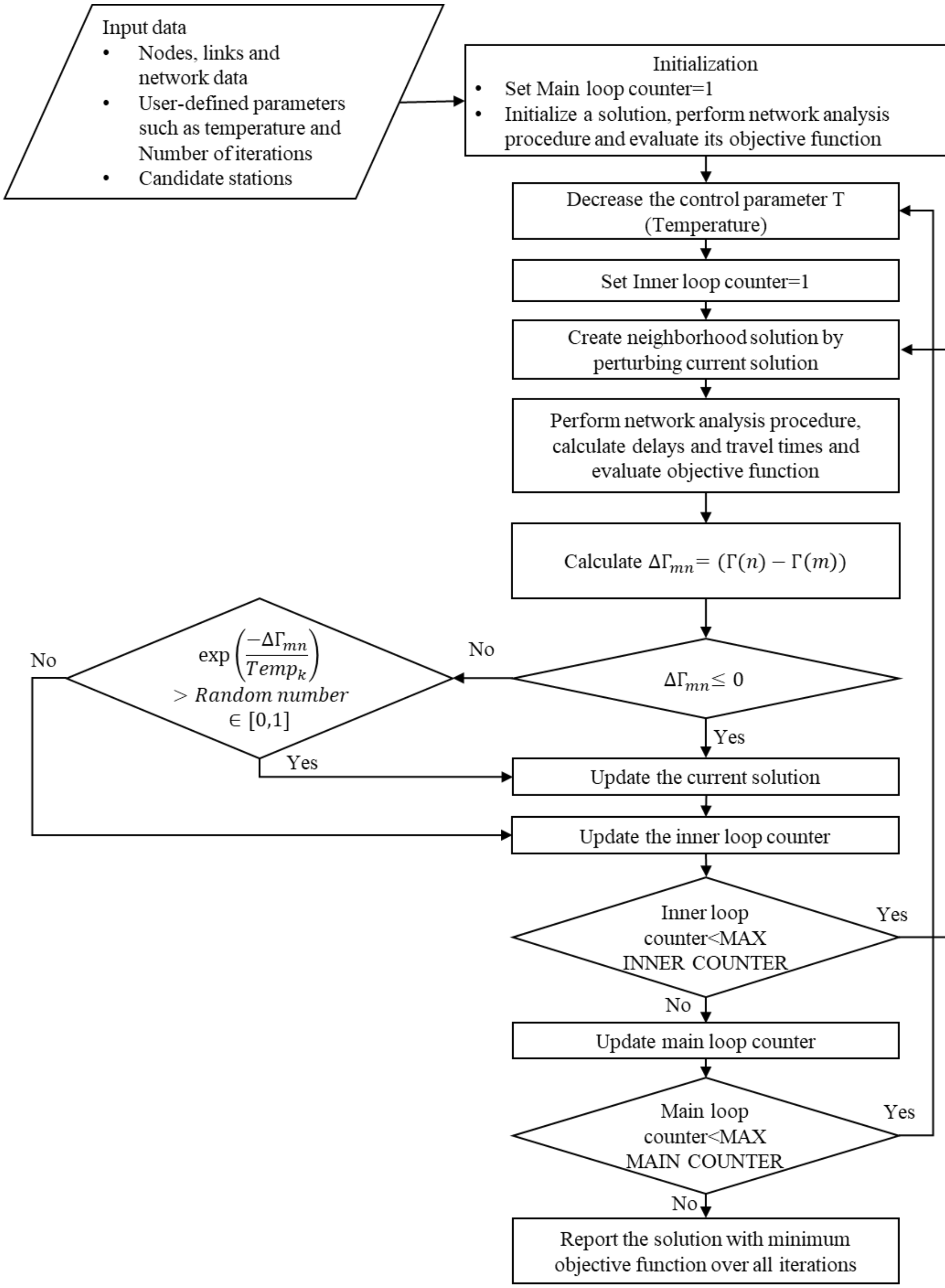

Figure 3-2 The proposed solution framework based on the simulated annealing algorithm

First, we need to modify the variables associated with the number of spots. Considering these variables as integer variables results in an infinite set of possible values and generation of various feasible solutions. Therefore, instead of a continuous integer variable for the number of spots in each candidate station, we define five levels for the number of spots (very low, low, medium, high, and very high, which are respectively considered as 2,3,5,10, and 15 chargers). Each candidate station selected as a part of any feasible solution must have one of these levels as its number of chargers.

To obtain an initial solution, instead of a random initial solution, we set x=1 for all the candidate nodes to ensure the feasibility of the initial solution. This assumption assures that there is at least one feasible path for all vehicle classes and all OD-pairs in the network. For the number of spots, we assume the medium level for all candidate charging stations in the initial solution.

To move from a current solution to a neighbor solution, we propose to use a weighted random approach to improve the efficiency of the algorithm. There are multiple possible perturbations such as adding or removing a candidate station or increasing or decreasing the level of number of spots for a candidate station in the current solution. According to the type of perturbation, each location is associated with a weight factor (e.g., total flows, total delays). Then, the location is picked based on a weighted random selection. More specifically, we define:

$$\Phi(N) = \sum_{i=1}^{N} \phi_i \tag{3.35}$$

where ϕ_i is the weight factor for station i , $\Phi(N)$ is the cumulative weight factor, and N is the number of stations. Then, the location l is selected if it satisfies the following:

$$\frac{\Phi(l-1)}{\Phi(N)} \leq \rho \leq \frac{\Phi(l)}{\Phi(N)} \tag{3.36}$$

where ρ is a random number drawn from a uniform distribution between 0 and 1, written as $\rho = \text{u}[0,1]$. In addition, the following rules are used to guide the perturbation process. At each iteration, one of these rules is selected randomly to perturb the current solution. If there is no feasible option available for a certain rule, the random number is regenerated to select another rule.

Rule 1: When a new station is to be added, each location $i \in N_2^m$, not being in the current solution, is weighted based on the total crossing flow at that node, i.e. $\phi_i = \sum_{\omega \in \Omega} \sum_{r \in R_m^\omega} f_r \, \delta_i^r$. This means that locations with higher flows are prioritized to be selected. The medium level of number of spots is considered for the new station.

Rule 2: When a new station is to be removed, each station $i \in N_2^m$, being in the current solution, is weighted based on the inverse of total crossing flow at that node, i.e. $\phi_i = 1 / \sum_{\omega \in \Omega} \sum_{r \in R_m^\omega} f_r \, \delta_i^r$. This implies that locations with lower flows are prioritized to be selected. However, if removing the selected station makes an OD infeasible for any classes of vehicles, then the perturbation process would be repeated to keep the neighbor solution feasible. In this case, weight factors are calculated based on a new set, which includes all the previous stations excluding the aforementioned one.

Rule 3: When new chargers are to be added to a station, each location $i \in N_2^m$, being in the current solution with the spot level at very low, low, medium, and high is weighted based on the queuing delay at that station, i.e. $\phi_i = \pi_i$. This means that stations with higher queuing delays are prioritized to be selected.

Rule 4: When chargers are to be removed from a station, each location $i \in N_2^m$, being in the current solution with the spot level at low, medium, high, and very high is weighted based on the inverse of total queuing delay at that station, i.e. $\phi_i = 1/\pi_i$. This implies that the stations with lower queuing delays are prioritized to be selected.

3-3-2- Network Analysis Procedure

In this section, the users' behavior for selecting their routes and charging stations is discussed. Due to congestion on links and charging stations, travelers cannot choose their route independently. Therefore, an equilibrium framework is needed to solve this problem. First, we discuss the enumeration and generation of a feasible set for the routes between each OD-pair as the main element of the assignment problem. Then, we propose a route-based formulation for the equilibrium problem. Finally, a solution algorithm is proposed to solve this problem. The assignment algorithm finds the user equilibrium state by switching travelers' routes iteratively. Note that a route is defined by the sequence of nodes to be traveled from the origin to the destination. This list of nodes might include dummy nodes in which recharging occurs. Solving the assignment problem to define travelers' route choice is required at each iteration of the main heuristic algorithm to evaluate the objective function for each neighbor solution.

The set of all feasible and practical paths is the main input for the assignment subproblem. In urban networks, where the enumeration of all feasible paths is impossible, a column generation approach can be applied, which incorporates the shortest path algorithm to augment the set of used paths by travelers. However, in this problem, due to the range anxiety, the existence of multi-classes of vehicles, and tracking the state of fuel along the routes, incorporating a shortest path algorithm is not straightforward. Furthermore, unlike the classic routing problem, where no path can include any loop, the routing sub-problem in this study might need to consider loops to arrange visiting charging stations. Thus, in the intercity networks, enumerating all feasible paths might be a better approach. However, in large networks (such as the intercity network of Michigan) this enumeration itself could be computationally demanding. Therefore, two assumptions are used to reduce the computational efforts as follows:

1) It is assumed that no vehicle can visit a node twice unless it is visiting the node for refueling, i.e. loops are allowed just for refueling purposes and only one time for each station. (This assumption is consistent with minimization of travel time in a static network)
2) It is assumed that for each OD-pair, instead of all feasible paths, at least five paths with minimum distance and without refueling (not crossing dummy nodes) must be provided.

As each route is a set of consecutive nodes, considering different options for the refueling purpose, i.e. visiting dummy nodes, would increase the total number of paths depending on the number of available charging stations along the initial path set for each OD-pair. For each OD pair, the Euclidian distance between each origin and destination is calculated. While enumerating all feasible paths via the branch and bound method, the distance between the origin and the last node in the branch is calculated. If the branch length, which is the sum of all link lengths to that point, is larger than a prespecified distance limit factor multiplied by the Euclidian distance, the branch is not considered for the path enumeration anymore. The distance limit factor is set to 1.2 in this study. After enumerating all available paths with these conditions for each OD-pair, if there are at least five paths (a reasonable number of existing paths in the intercity networks), enumeration for the OD-pair would stop. Otherwise, the enumeration is repeated while the distance limit factor is increased by 10%. This process continues until at least five paths, not including any dummy node, are available for each OD-pair. Once there are five paths for each OD-pair, these paths would be augmented to routes considering the dummy nodes along these paths for refueling, i.e., each refueling path represents a specific refueling pattern with its specific assigned flow. Tracking the state of fuel along these routes, a set of feasible routes considering refueling would be available for each OD-pair. At this point, the original problem is reduced to assigning all OD flows to the constructed feasible routes.

As the focus of this study is to find the required number of chargers and their locations in an inter-city network, a path-based approach along with some simplistic assumptions are incorporated to support inter-city trips. However, for urban networks, some efficient models can consider the limited range of EVs for a link-based traffic assignment model ensuring computational feasibility. Nonetheless, these efficient algorithms do not consider multiple recharging or the required amount of charge, since they deal with short-range trips. Thus, these approaches are not applicable to our study.

In the assignment problem, it is assumed that users try to minimize their travel times and they cannot decrease their travel time by changing their routes. Thus, the travel time for every used route should be equal to the least travel time associated with its OD-pair. In the assignment problem, which is the lower level problem, the variables of the upper-level problem, i.e. x and z, are known and used to generate the set of feasible routes. The only decision variable in the lower level problem is f_r, which is the path flow for each vehicle class m along with the route r. To solve the assignment problem, a gap function is defined along with an algorithm that reduces the gap through an iterative process. This algorithm solves the user equilibrium problem once the gap function is close to zero (Lu et al., 2009). By defining R'^{ω}_{m} as the set of feasible routes for vehicles in class $m \in M$ and OD-pair $\omega \in \Omega$, we can formulate the assignment problem as follows:

$$Gap(r, \min\{CT_r\}) = \sum_{m \in M} \sum_{\omega \in \Omega} \sum_{r \in R'^{\omega}_{m}} f_r * (CT_r - CT_r^{min}) \tag{3.37}$$

$$\sum_{r \in R'^{\omega}_{m}} f_r = q^m_\omega, \qquad \forall\, \omega \in \Omega, m \in M \tag{3.38}$$

$$CT_r^{min} \leq CT_r\,, \qquad \forall \omega \in \Omega, m \in M, r \in R'^{\omega}_{m} \tag{3.39}$$

$$f_r \geq 0, \qquad \forall \omega \in \Omega, m \in M, r \in R'^{\omega}_{m} \tag{3.40}$$

In this formulation, *CT* is the route travel cost including link travel times and the average waiting times at charging stations. We incorporate a decent direction method combined with the method of successive averages (MSA) to find the equilibrium state through a certain number of iterations (Lu et al., 2009; Peeta and Mahmassani, 1995). For the decent direction, we use the minimum cost of each feasible route set considering the current traffic assignment in each iteration. For the MSA, the step size ($\alpha_n = \frac{2}{2+n}$) is used at each iteration *n*. The stopping criterion in this method is set to be 100 iterations, as it provides a reasonable convergence and gap for the case study that is considered here. We begin with an initial solution for the route flow assignment and update the route flows in the n^th iteration according to the following equations:

$$argmin(CT_r) = r^*, \qquad \forall \omega \in \Omega, m \in M, r \in R'^{\omega}_{m} \tag{3.41}$$

$$f_r^n = f_r^{n-1} + \alpha_n * f_r^{n-1} * \frac{CT_r^{min} - CT_r}{CT_r}, \qquad \forall \omega \in \Omega, m \in M, r \in R'^{\omega}_{m} - \{r^*\} \tag{3.42}$$

$$f_r^n = f_r^{n-1} + \sum_{r \in R'^{\omega}_{m} - \{r^*\}} \alpha_n * f_r^{n-1} \frac{CT_r^{min} - CT_r}{CT_r} \qquad r = r^* \tag{3.43}$$

Average gap for all vehicle classes in the network is considered as a measure of effectiveness (Lu et al., 2009):

$$AGap(r) = \frac{\sum_{m \in M} \sum_{\omega \in \Omega} \sum_{r \in R'^{\omega}_{m}} f_r * (CT_r - CT_r^{min})}{\sum_{r \in R'^{\omega}_{m}} f_r} \tag{3.44}$$

As the average gap is independent of the problem size, it is a useful criterion to monitor the convergence pattern of a decent direction method.

3-4- Numerical Results

This section first presents the intercity network considered for the case study. The case study description is followed by presenting the numerical results to (1) evaluate the performance of the proposed metaheuristic algorithm, (2) present the optimal solution for the base case (considering current battery size and EV market share), and (3) assess the sensitivity of the optimal solution to the critical input for future hypothetical EV market shares and battery sizes. Afterwards, the performance of the proposed algorithm is compared with a benchmark for a small case study. The SA algorithm is implemented in MATLAB with an Intel(R) Core (TM) i5-2400 CPU and 16 GB RAM. The default values for the parameters used in the model are listed in Table 3-2, which are mainly adopted from the basic and general corridor model (Ghamami et al., 2016b; Nie and Ghamami, 2013). For simplicity, all parameters are assumed not to vary with location or OD-pairs, even though the model can capture such variations. We note that all capital costs (charging facility) are later amortized based on the life cycle of the facility.

Table 3-2 Base case parameter values

Parameters	Description	unit	Value
C_s	Fixed construction cost of charging stations	k$	520
C_p	Per spot construction cost of recharging outlet	$\frac{\$}{kW}$	500
β	Battery performance	$\frac{mile}{kW\ h}$	2.5
θ	Range tolerance (confident range)	-	0.8
α	Energy efficiency (converting energy/power ratio to charging time)	-	1.3
T_0	Time period	h	12
γ	Value of time	$\frac{\$}{h}$	18
C_e	Battery cost	$\frac{\$}{kW\ h}$	205
A_1	Congestion factor in BPR function	-	4
A_2	Coefficient in BPR function	-	0.15

3-4-1- Case Study

The purpose of the case study is twofold:

I. Implementing the proposed model on a real-world network to assess its performance and viability.

II. Studying the sensitivity of the optimal solutions to the inputs. We are especially interested in two types of parameters: those related to the demand, such as the current and future EV market share, and those related to technology, such as the battery size.

The sketch network of the Lower Peninsula of the State of Michigan is considered as the case study. The travel distance between some of the major cities in Michigan is beyond the range of current electric vehicles. Also, there are often multiple travel corridors between most of the OD-pairs. The network used in this study consists of 26 nodes, 96 links, and 272 OD-pairs with almost 3 million daily trips. The network is simplified in terms of links and demand zones from the state-wide network of Michigan provided by the planning division of the Michigan Department of Transportation (MDOT). The demand matrix is almost symmetrical. The size of each circle in Figure 3-3 represents the amount of demand generated/attracted to that node.

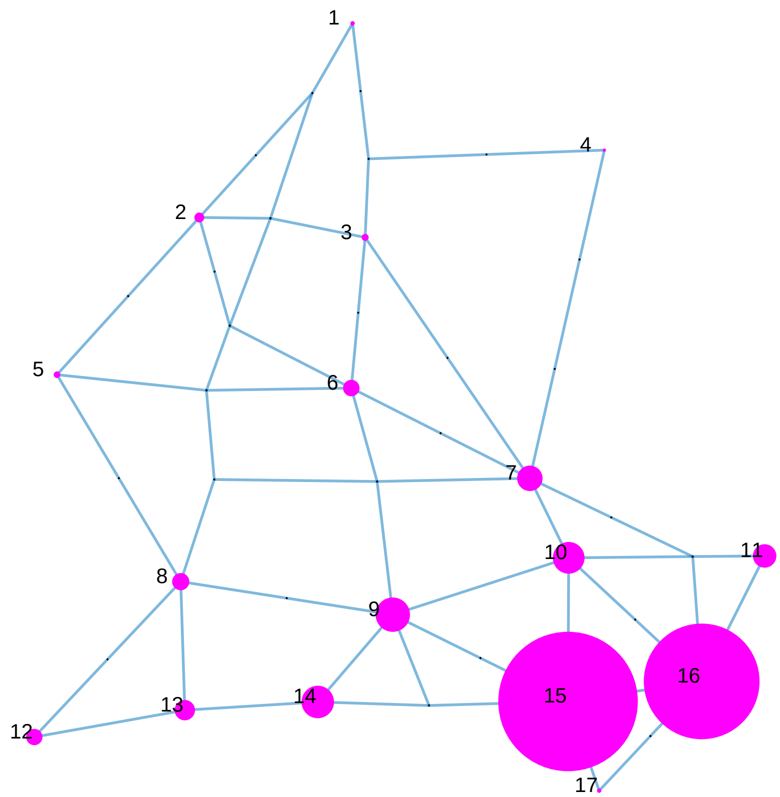

Figure 3-3 Sketch network of the State of Michigan with demand generation/attraction points.

The model is able to consider various classes of vehicles, e.g. CVs, plug-in hybrid electric vehicles, EVs, hydrogen fuel vehicles, etc. However, the focus of this study is on CVs and EVs. CVs affect the lower level traffic assignment as link flows include both EVs and CVs. Herein, it is assumed that there is no detouring for CVs to reach gas stations due to manifold gas stations along the roads. A recent study confirms that a reasonable level of service could only be achieved with Type III (fast) chargers (Nie and Ghamami, 2013). Therefore, it is assumed that all installed chargers have a power of 50 kW, a typical value for Type III chargers. Also, 67 percent of EVs are assumed to have a 40-kWh battery with an average range of 100 miles, while 33 percent are assumed to have a 100-kWh battery with a range of 250 miles. Furthermore, it is assumed that there is no fast charger currently available because there is almost no DC fast charger available to the public in the state of Michigan. Finally, two different sets of nodes are considered as candidate points:

1. Every node that represents an intersection or demand generation/attraction in the network

   Points along the links to prevent the distances longer than 50 miles between any two consecutive nodes in the network.

The 50-mile threshold is selected as it can provide feasibility across the network, while maintaining the efficiency of the solution algorithm in terms of computation time. In Figure 3-4, the second set of the candidate points are located in the middle of links 1-19, 2-5, 2-18, 2-21, 3-6, 3-7, 4-19, 5-8, 6-7, 7-25, 8-9, 8-12, 9-15, 10-16 and 16-17. As the length of link 4-7 is longer than 100 miles, there are two candidate points along with it. Unless otherwise specified, the parameter values mentioned above are used throughout the numerical results section.

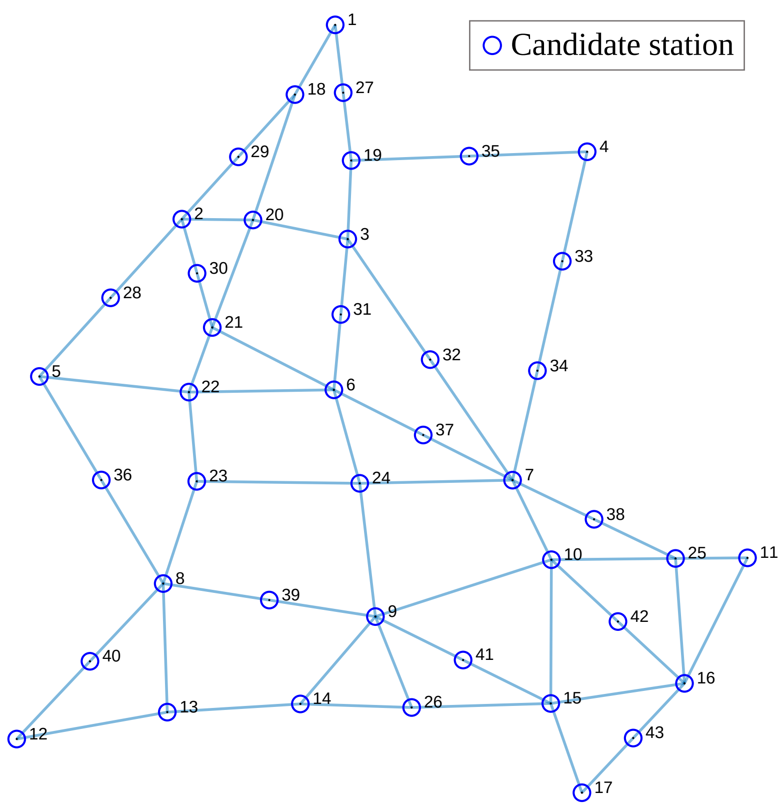

Figure 3-4 Candidate stations in the sketch network of Michigan Lower Peninsula

3-4-2- Model Calibration

Metaheuristic algorithms typically require calibration of some parameters to be adjusted to a specific problem. Iteration numbers and temperature changes are among these parameters for the proposed SA-based algorithm. The initial temperature is set to 0.05 with a decreasing factor of 0.85 for each temperature change (Kavianipour et al., 2019; Zockaie et al., 2018). As the number of required iterations at each temperature and the number of temperature changes depend on the feasible set, sensitivity analyses are performed to find a proper setting for these parameters. Finally, in this study, an iterative process is used to solve the lower level problem that assigns travelers to different routes and charging stations. The number of iterations in this process is another parameter that needs to be set.

3-4-2-1- Number of iterations (inner and main) for SA algorithm

The proper numbers of main and inner iterations for the SA algorithm are selected through testing different values. The combination that provides the minimum objective function (closer to optimal) with the minimum required number of total iterations is selected for the rest of the analyses. Table 3-3 shows the objective functions measured through the application of the proposed solution algorithm. Each row represents a certain number of temperature changes (number of main iterations), and each column represents a certain number of iterations at each temperature (number of inner iterations). According to Table 3-3, increasing the number of iterations (inner or main) results in a decreasing pattern for the measured objective function. However, after a certain point increasing the number of iterations does not provide any reduction in the objective function value. Thus, the number of main and inner iterations are set to 25 for the rest of this study.

Table 3-3 Optimum objective function ($/day) values for different numbers of main and inner iterations in the SA algorithm

Main iterations	Inner iterations					
	5	10	15	20	25	30
5	12882.59	11859.09	10916.87	10236.86	9753.54	9644.55
10	11859.09	10236.86	9644.55	9243.83	9175.34	9141.09
15	10916.87	9644.55	9223.28	9141.09	9134.24	9134.24
20	10236.86	9243.83	9141.09	9134.24	9134.24	9134.24
25	9753.54	9175.34	9134.24	9134.24	9134.24	9134.24
30	9644.55	9141.09	9134.24	9134.24	9134.24	9134.24

3-4-2-2- Number of iterations for the Assignment Problem

As mentioned earlier, the travelers' route choice behavior is assumed to follow a user equilibrium model. To test the effectiveness of the proposed assignment algorithm, the average gap values are plotted versus the assignment iteration numbers for a given inner iteration of the main algorithm. The plot is provided in Figure 3-5.

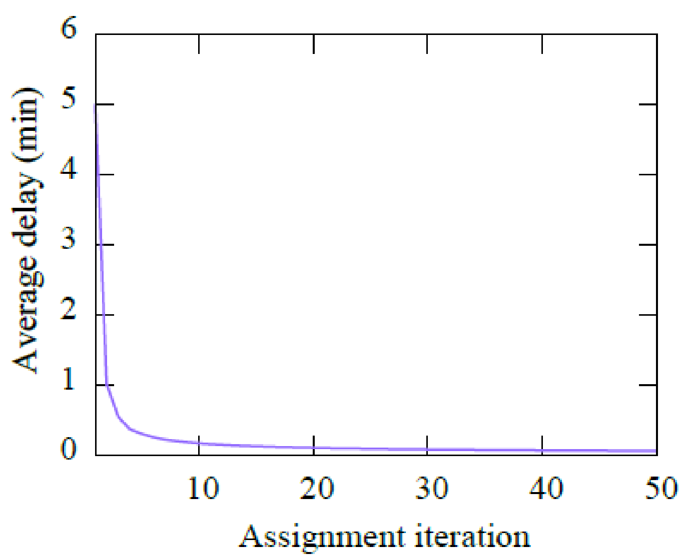

Figure 3-5 The average gap for different iterations in the path and charging station assignment sub-problem

A significant decreasing pattern can be observed in the early iterations. However, after a certain number of iterations, the changes in the average gap become minimal. The total number of assignment iterations for this study is set to 100, which provides less than a minute average gap values (acceptable for inter-city networks) in a reasonable computation time.

3-4-2-3- Enumeration versus SA

To evaluate the performance of the SA, we incorporate an enumeration approach as a benchmark. Enumerating all the possible combinations of charging station locations and number of chargers and is not practical for the proposed case study, since it requires evaluating the objective function for each of 6^{43} possible combinations. Therefore, we limit the search space by considering only a subset of candidate points for building charging stations. To this end, the number of candidate points need to be larger than the number of optimal charging stations. Thus, the following scenario is defined for the evaluation purpose. Assuming a 1% market share and a battery capacity of 100 kWh, the SA approach finds an optimum solution with four charging stations and a maximum of two chargers at a station. Therefore, we select a random subset of eight nodes, i.e., {2,5,7,9,15,20,29,35}, as candidate locations and consider three levels of chargers as {1,2,3} for each selected charging station, which makes the total number of facility combinations equal to 4^8 =65,536. The optimal objective function value found by the enumeration approach for this simplified network (i.e., only allowing the charging stations at candidate points) is 1,766 $/day, where nodes 7, 9 and 20 are selected with 3, 1 and 3 chargers, respectively. The SA approach reports the same solution as the best solution. However, it takes almost 33,000 seconds to find the optimum solution using the enumeration approach versus 75 seconds for the SA approach. These results strongly suggest computational efficiency of the proposed solution approach in terms of the objective function quality and computational performance.

3-5- Results

3-5-1- Base case

In this section, the convergence of the SA algorithm is demonstrated for the selected number of main and inner iterations (K_0 and K_1) in the previous section. After a certain number of main and inner iterations, there is no clear indication that a higher number of iterations would help reduce the objective function value, as one might expect. On the other hand, the computational time increases with the number of iterations. Figure 3-6 presents the convergence of the objective function values as the number of iterations increases. In Figure 3-6(a), the objective function values are plotted continuously for different main and inner iterations. Figure 3-6(b) reports the changes in the objective function value plotted for each outer or main iteration. After 17 main iterations, the objective function value does not improve any more. To account for different analyses in this study, the numbers of main and inner iterations are both set to 25 to ensure the optimality of the final solution.

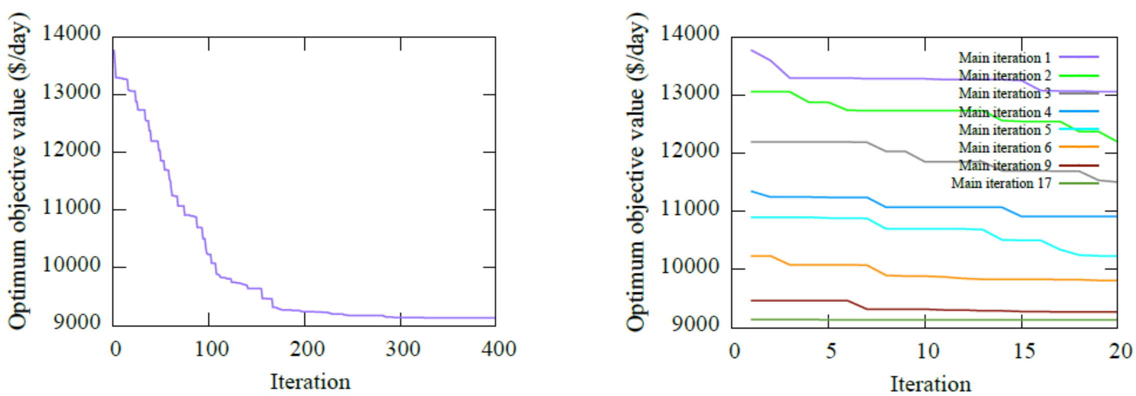

(a) (b)

Figure 3-6 Metaheuristic algorithm convergence (a) General trend of the objective function for different iterations and (b) Changes in objective function value for different main and inner iterations

Figure 3-7 shows the optimal configuration of the charging stations for the State of Michigan sketch network in the Lower Peninsula with the current demand level for electric vehicles (0.38 percent of EV market share). The optimal solution chooses 18 charging stations among the candidate nodes of the network in the Michigan Lower Peninsula. It suggests one high-level station (with 10 chargers), one medium-level station (5 chargers), four low-level charging stations (3 chargers) and 12 very low-level charging stations (2 chargers). In the plot, each circle represents a charging station and the size of the circle visualizes the spot (charger) level in that station. The total objective function for this case is 9,134 ($/day) which consists of 2,913 ($/day) investment cost and 6,221 ($) delay cost. The optimum solution for the base case causes 20,736 (min) of total delay including the charging time, waiting time, and detour for charging. Note that the existing charging stations do not support intercity trips in the studied network.

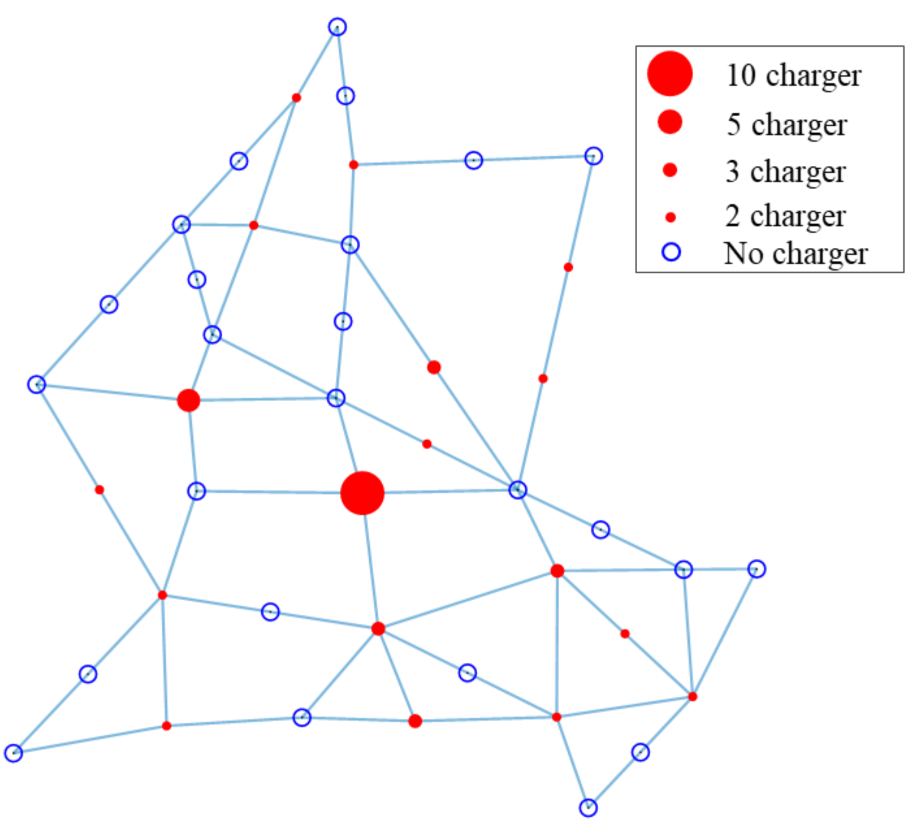

Figure 3-7 Optimal configuration (size and location) of selected candidate charging stations

3-5-2- Sensitivity analysis

In the previous section, the optimal solution is presented for the base case including the current market share and a 40 kWh battery size assuming a fixed value of time and investment cost for acquiring charging stations and chargers. In this section, through multiple sensitivity analyses, each of these parameters is set to different possible values, while the other ones are assumed to be the same as the base case. These analyses provide insights regarding the impacts of technology development on EVs in the future.

3-5-2-1- Battery Size

Battery size is one of the factors that car companies invest in to overcome the range anxiety issue for EV users. Considering the unit battery cost of 205 ($/kWh) (Union of Concerned Scientists, 2018), increasing the battery size for the entire population of EVs requires certain investments as shown in Figure 3-8(a). Increasing the battery size reduces the number of required charging times, the total waiting time, and charging station investment cost (see Figure 3-8(b) and (c)). However, increasing the battery size beyond 70 kWh does not reduce waiting time and infrastructure cost significantly. Thus, a proper investment seems to be increasing the EVs' battery size to 70 kWh. It is noteworthy to mention that this result is based on the assumption that the cost of the battery size is an increasing linear function of its size.

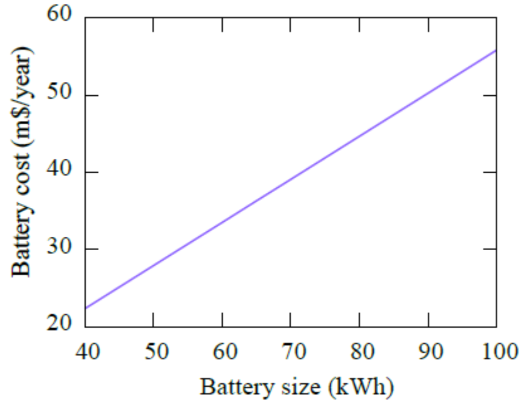

(a)

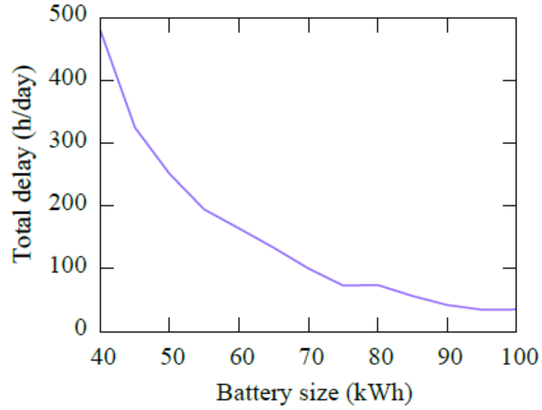

(b)

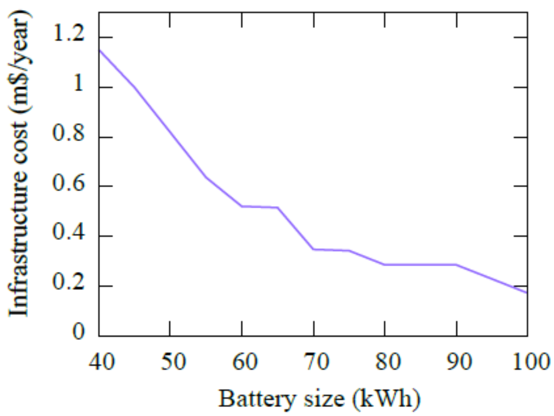

(c)

Figure 3-8 (a) Effects of the battery size on the battery investment cost (b) Effects of the battery size on the waiting time (c) Effects of the battery size on the infrastructure investment costs

By comparing these figures, some insightful findings can be extracted. The average per year cost of increasing the battery size from 40 kWh to 70 kWh for the current market share is \$16.74M:

$$\begin{aligned}&\text{Battery size increase} * \text{price per kW} * \text{market share} * \text{number of cars in Michigan}\\&* \left(\frac{1}{\text{lifetime}}\right) = (70 - 40\text{kWh}) * 205\,\frac{\$}{\text{kWh}} * 0.0038 * 7164651 * 0.1\\&= \$16.74\text{M}\end{aligned} \tag{3.45}$$

However, the total saving in the investment cost is just about \$0.8M per year (Figure 3-8(c)). It means that providing batteries with higher capacities can reduce delays by more than 90 percent, however, it needs significant investments. It is noteworthy to mention that the saving due to reduced delay is almost $2.5M per year.

3-5-2-2- Market share

Due to the environmental benefits of EVs, certain incentives have been provided to increase the market share for EVs to maximize their benefits. Increasing the market share results into increase of the optimum objective function and total delay. To decrease the total delay, more chargers are needed in charging stations. Therefore, the initial setting of five different charger levels, with 2, 3, 5, 10 and 15 capacities can not support the demand in the future. Thus, in this section, we use various five-level sets, where the number of spots for each level is set based on the demand in each scenario. It should be noted that the number of spots should be deemed as the total number of chargers in a small region in an aggregate model. This assumption brings in some approximations, but it is pivotal for the sake of computational time. The sensitivity analysis on the market share is shown in Figure 3-9. Figure 3-9(a) plots the objective function (k$) for different EVs' market share. This figure shows that the objective function increases when EVs' market share increases. Figure 3-9(b) shows the total delay (h/day) increases almost linearly as the market share increases, which means that the average delay is almost constant for different EVs' market shares. It is noteworthy that although the total delay consists of refueling delay, queuing delay and detouring delay, the queuing delay is almost zero in all scenarios. The assumed value of time and per unit charger cost justify adding chargers to the station to remove the queuing. Figure 3-9(c) plots the number of required spots for different EVs' market shares. Increasing the market share increases the number of required spots, which explains the increased investment cost and constant average delays.

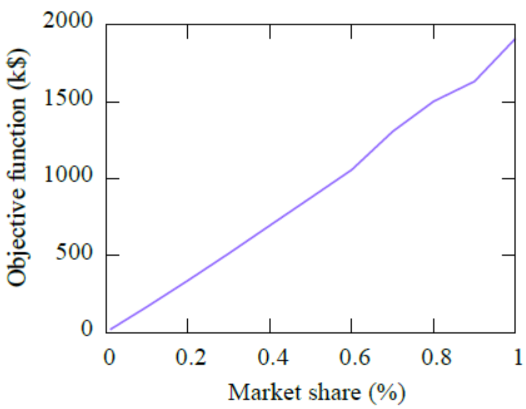

(a)

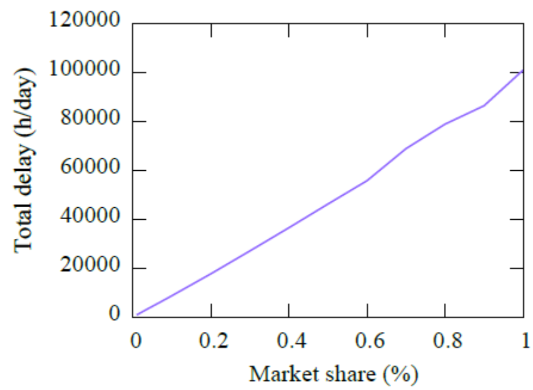

(b)

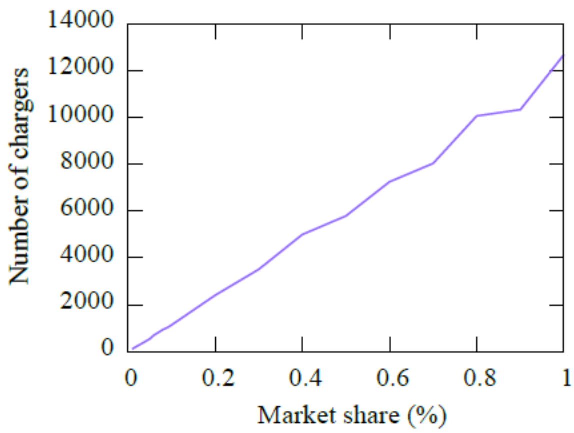

(c)

Figure 3-9 (a) Effects of the market share on the objective function value (b) Effects of the market share on the total delay (c) Effects of the market share on the total number of spots

3-5-2-3- Value of time

Figure 3-10(a) shows the relation between the optimum objective function (k$/day) for different value of times, γ ($/h). As the value of time increases, the optimum objective function increases, which is consistent with the equation (12). Figure 3-10(b) shows the relation between the total delay (h/day) and the value of time ($/h). As the value of time increases, the model compensates its effects on the objective function by decreasing the total delay. However, after a certain value of time, the total delay cannot be reduced any further and remains almost constant. The reason is that the total delay is the summation of detour time, queuing time and charging time. By increasing the value of time, model builds more charging stations and chargers to decrease detour time and queuing time respectively. But after some point, there is no more queuing time and the detour time cannot be decreased any more, while the charging time remains constant. Figure 3-10(c) plots the total number of spots for different values of γ ($/h). By increasing the value of time, the number of spots increases to decrease the total delay. After some point, when there is no queuing delay and all candidate stations are selected to be equipped with chargers, increasing the value of time has no impact on the number of spots.

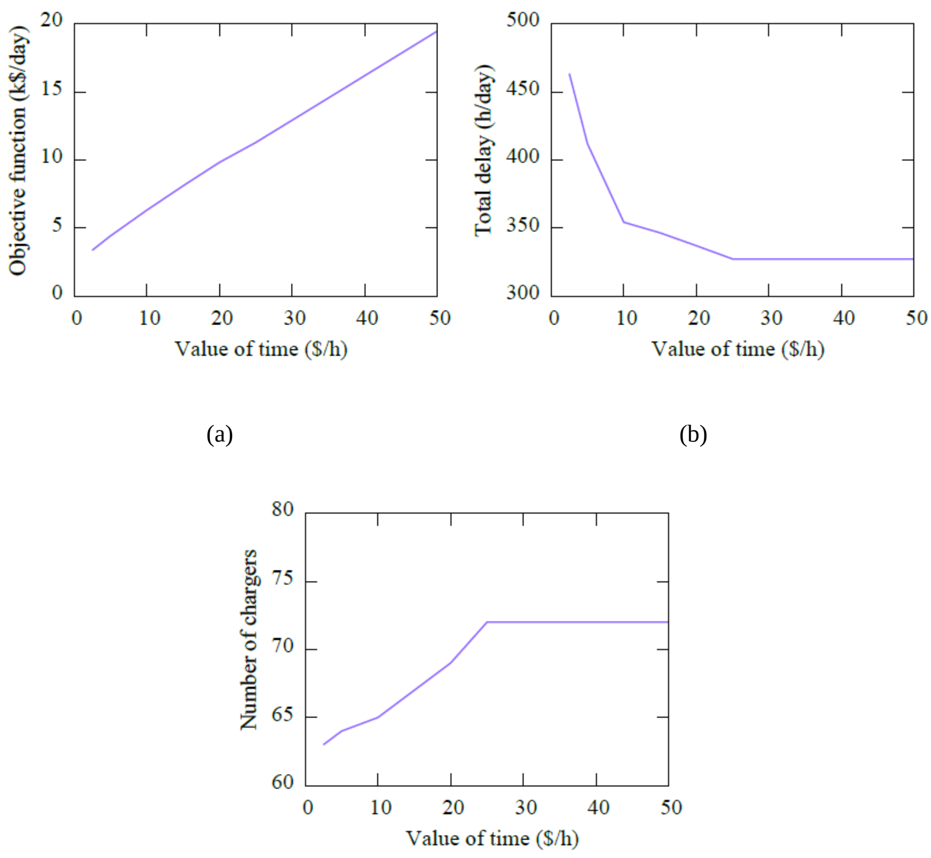

(a) (b)

(c)

Figure 3-10 (a) Effects of the value of time on the objective function (b) Effects of the value of time on the total delay (c) Effects of the value of time on the number of spots

3-5-2-4- Battery Size and EV Market Share

Battery size and market share of EVs are two of the main factors affecting the charging needs of EVs. Figure 3-11(a) plots the number of spots for different EV market shares up to 20 percent for different battery sizes (kW).

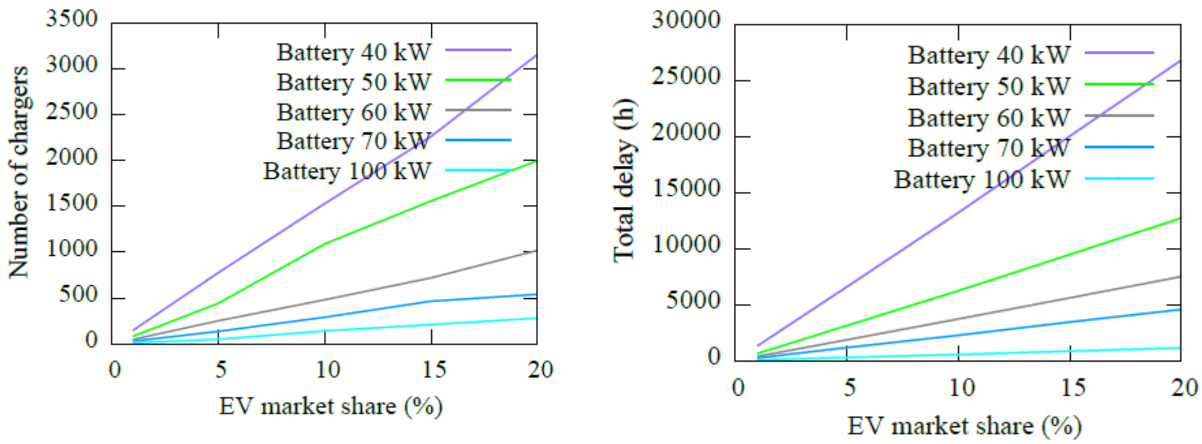

(a) (b)

Figure 3-11 (a) The effect of EV market share on number of spots for different battery size (b) The effect of EV market share on total daily delay for different battery size

By increasing the market share for each battery type, the number of charging stations and chargers increases as well. For a fixed market share, increasing the battery size leads to less chargers. By increasing the battery size from 40 kW to 70 kW, the number of spots decreases by almost 80 percent. Figure 3-11(b) shows the relation between the total delay (h/day) and EVs' market share for different battery sizes (kW). By increasing the market share for a certain battery size, the total delay increases as the number of EVs increases. For each market share, increasing the battery size decreases the total delay due to a lower charging demand. This means that EVs would be able to travel longer distances without the need for charging. However, increasing the battery size beyond the 70 kWh does not result in a significant decrease in the total delay. This is due to the fact that the 70 kWh battery, providing a range of 175 miles, is enough to get to a close city or the next charging station. Thus, the number of in-trip charging decreases and the total delay remains almost constant up to 20 percent market share. However, for smaller battery sizes, there is a significant charging delay that increases with the increase in the market share. Although larger battery size results into less total delay, there is a significant cost associated with it. This cost increases linearly when the market share increases.

Battery size and market share of EVs affect the configuration of charging stations in addition to the number of charging stations and chargers, which are discussed in the above sections. Figure 3-12 illustrates the impact of battery size and market share on the configuration of charging stations. In the first three scenarios, the market share is kept constant while the battery capacity increases. With higher capacity batteries, the need for charging decreases. Therefore, the required number of chargers drop from 19 in scenario 1 to 6 in scenario 2 (Also reflected in Table 3-4 and Table 3-5). The number of charging stations also drops to 3 when the battery capacity is increased to 100 kWh. In scenario 4-6, the battery capacity is 40 kWh while the market share of EVs increases from 1 percent in scenario 4 to 5 percent in scenario 5 and to 10 percent in scenario 6. While the number of stations and their configuration is not affected significantly by the increased market share, the required chargers have increased from 150 in scenario 4 to 730 in scenario 5 and to 1,510 in scenario 6. Similarly, the market share increases in scenario 7 to 9 from 1 percent to 10 percent while the battery capacity is held at 70 kWh. As shown in Figure 3-12, the location of charging station has not changed significantly based on the market share while the number of chargers increased from 27 to 280. Based on these nine scenarios, the location of chargers is merely dictated by the battery capacity, while the number of chargers reflects the market penetration rate. Two other elements of this study, the congestion level and users' delay, are compared in Table 3-4 and Table 3-5, respectively. Comparing the first three scenarios in Table 3-4, the charging station visiting flow decreases when the battery capacity increases. However, the increased market share results in more congestion level as more vehicles need recharging, which is reflected in scenarios 4-6 and 7-9 in Table 3-4.

Table 3-4 Charging station, number of stations and chargers, and congestion level under nine different scenarios

Scenario	Battery	Market Share	Station Num.	Charger Num.	Congestion level (Veh/day)	
					Ave.	Max.
1	40	0.38%	19	64	72	253
2	70	0.38%	6	12	27	44
3	100	0.38%	3	6	13	19
4	40	1%	23	150	155	526
5	40	5%	24	730	747	2564
6	40	10%	26	1510	1385	5210
7	70	1%	7	27	60	113
8	70	5%	10	140	215	470
9	70	10%	10	280	430.7	939

Table 3-5 Charging station, number of stations and chargers, and users' delay under nine different scenarios

Scenario	Battery	Market Share	Station Num.	Charger Num.	Users delay (min)	
					Ave.	Max.
1	40	0.38%	19	64	21.9	43
2	70	0.38%	6	12	34.6	59.7
3	100	0.38%	3	6	28.9	45.5
4	40	1%	23	150	22.4	41.8
5	40	5%	24	730	23.4	42
6	40	10%	26	1510	23.8	42.7
7	70	1%	7	27	34.1	62.7
8	70	5%	10	140	31.6	50
9	70	10%	10	280	31.6	49

Table 3-5 compares the users delay under the mentioned scenarios. Comparing scenarios 1, 4, 5, and 6, the users' average delay is mainly influenced by the battery capacity. Similarly, scenarios 2, 7, 8, and 9 that share the same battery capacity have an almost the same average delay. Increasing the battery capacity changes the users' delay, which can be reflected by comparing scenarios 1, 4, 5, and 6 with scenarios 2 and 3. In these scenarios, EVs need to spend more time to get recharged. Although higher capacity batteries barely need recharging, but they require more power to be recharged. Therefore, an increase in users delay is expected, which is reflected Table 3-5. However, this increase is also a function of the network structure.

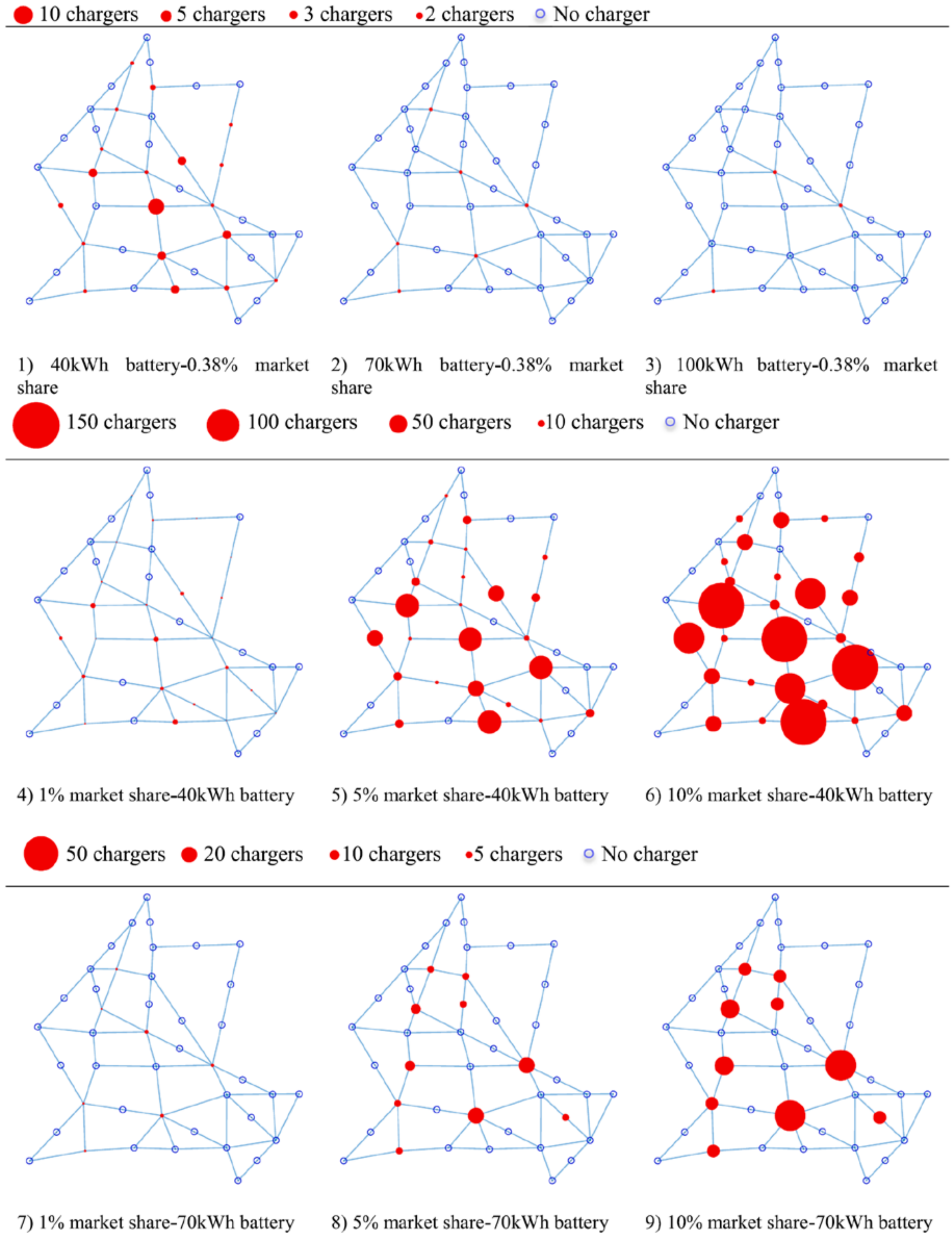

Figure 3-12 Visualized configuration and capacity of charging stations under different battery size and market shares

3-6- Summary

This study proposes a mixed integer program with non-linear constraints to formulate the infrastructure planning problem for EVs in the intercity networks considering the range anxiety issue. Dummy nodes and links are used to differentiate between visiting a node along a trip and visiting it for the refueling purpose. The objective function makes a trade-off between the investment of building charging stations with a certain number of chargers and EV users' total delay, including the charging time, waiting time, and required detour time to access a charging station. A metaheuristic solution approach is proposed based on the simulated annealing to solve this problem for the intercity network of Michigan with realistic daily travel demand and trip distances. The numerical experiments show a successful application of the solution methodology resulting in key findings as follows:

- Increasing the battery size beyond 70 kWh does not improve the delay or the investment cost significantly since the delay is within the minimum range.
- The current charging stations in Michigan do not support intercity trips. To support such trips for EVs, a substantial investment is required. Adding 18 charging stations consisting of 1 station with 10 chargers, 1 station with 5 chargers, 4 stations with 3 chargers and 12 stations with 2 chargers would facilitate the intercity trips for current EV users while maintaining an acceptable level of service.
- Increasing the market share by as much as 20 percent requires significant investment in either the charging infrastructure or the battery size.
- By increasing the battery size, the need to build more charging stations decreases. If we have a fleet of EVs with the highest battery technology available in the market, the required number of charging stations and spots decreases tremendously. However, a significant

battery investment cost is associated with this approach that scales up with the increase in the market share.

- Providing more charging stations and spots is the more economical approach to support EVs intercity trip feasibility compared to increasing battery's size.
- With the current chargers' cost and value of time, providing enough chargers to remove the queuing in charging stations is the cost-effective approach.
- The size of the battery determines the location of charging stations while the market share affect the charger count within charging stations.

Chapter 4 - Monthly Traffic Demand and Battery Performance Variations Impact on EV charging infrastructure

4-1- Overview

Monthly traffic patterns and battery performance variations are two main contributing factors in defining the infrastructure needs of EV users, particularly in states with adverse weather conditions. Knowing this, the current study focuses on Michigan and its future needs to support the intercity trips of EVs across the state in two target years of 2020 and 2030, considering monthly traffic demand and battery performance variations. This chapter incorporates a recently developed modeling framework to suggest the optimal locations of EV fast chargers to be implemented in Michigan. Considering demand and battery performance variations is the major contribution of the current study to the proposed modeling framework by the same authors in the literature. Furthermore, many stakeholders in Michigan are engaged to estimate the input parameters. Therefore, the research study can be used by authorities as an applied model for optimal allocation of resources to place EV fast chargers. This study suggests the optimum location and number of chargers to meet the growing EV demand. The results also show that the reduced battery performance in cold weather is a more critical factor than the increased demand in warm seasons in designing the EV infrastructure.

This chapter sets out to incorporate monthly demand and battery performance variations at different months in the intercity network model, developed in chapter 3, in two target years of 2020 and 2030, in such a way that the considered travel needs of BEV users for their intercity trips are satisfied in Michigan. Two important contributing factors in defining the infrastructure needs of BEV users are battery performance and traffic demand fluctuations in different months (Hao et al., 2020). These factors are expected to be extremely significant for the state of Michigan, because of the frequent severe weather conditions, as well as the tourism attractions in the state. Therefore, traffic demand variations across different months are accounted for in this study to capture multi-view perspectives and better equip Michigan as part of the desired more electrified U.S. transportation system. Although the effects of EV demand seasonality on power consumption of EVs are investigated in a few studies (Bikcora et al., 2015; Donadee et al., 2014; Murakami et al., 2014; Shortt and O'Malley, 2014), there is a lack of studies in the literature that account for realistic traffic demands of the mixed fleet of conventional and electric vehicles in different months in the charging placement problem. In addition to travel demand fluctuations, this study differentiates between battery performances in favorable and extreme (or cold) weather conditions. It is worth noting that the present study considers currently available battery and charging technologies. Stakeholders at numerous meetings throughout the "Electric Vehicle Charger Placement in Michigan", a project funded by Michigan Department of Environment, Great Lakes, and Energy (EGLE), provided the available battery and charging technologies' data for the present study. Therefore, the results of the current study can be used by authorities as an applied model for optimal allocation of resources to place BEV fast chargers in Michigan. The charging station counts and locations found in this study serve vehicles to reach their destination with 20% charge, assuming that they started their trip fully charged.

The structure for the remainder of this chapter is as follows. The second section states the problem of interest. The third section presents a modeling framework to minimize the total cost considering the variations in traffic demand and battery performance. The fourth section explains the data collection process. The fifth section delineates the solution algorithm to find the optimal charger placement by incorporating travel demand fluctuations in different months and battery performance reduction in cold weather. Finally, the sixth section contains the results and discussion following by the summary.

4-2- Problem Statement

In a state-wide roadway network, there are usually numerous parallel and intersecting corridors between different OD pairs. The integration of these corridors form a network, known as an intercity network. The problem of interest in this study is to find the optimal DC fast charging infrastructure investment to support the intercity trips of BEVs in the state of Michigan in light of the expected BEV demands over the years, the variations of electric and conventional vehicles' (CVs) traffic demands over different months, and battery performance reduction in cold weather. In this problem, the objective is to minimize the total system cost, including the investment on charging stations and the additional travel delay (detour delay, queuing delay, and charging delay) due to charging of all BEV users. However, in the route choice problem, all users including the EV drivers would like to minimize their own travel time regardless of other travelers. Therefore, in the proposed model, a user equilibrium problem needs to be embedded into a system optimal problem. This problem finds the optimal location of charging stations in a network, where users with various classes of vehicles try to minimize their own travel times (including charging delays for BEV users), subject to change by travel flows along the routes.

Therefore, realistic traffic demands of different OD pairs, which fluctuate over different months should be considered to find the infrastructure needs of BEV users throughout a year. However, the monthly OD demands were not available for Michigan. Thus, we propose to estimate traffic demand variations using the traffic counts available from the Michigan Department of Transportation (MDOT) loop detectors installed across Michigan roadways. In addition, the battery performance reduction of BEVs in cold weather is a significant factor that should be considered. Taking these two factors into account, one can find the optimal charging station location and charger counts that meet the BEV users' needs in all months and as a result, more reliable infrastructure would be provided for potential BEV users.

Table 4-1 Definitions of parameters and variables

Parameter	Definition
$e \in E$	Set of links
$i \in I$	Set of nodes
$N_1^k \subset I$	Set of current refueling/charging stations for vehicles in class *k*
$N_2^k \subset I$	Candidate points for building refueling/charging stations for vehicles in class *k*
$k \in K$	Different classes of vehicles in the network
$N'^k_1 \& N'^k_2$	Sets of dummy nodes for charging purposes
C^k ($ per station per lifetime)	The fixed cost of a charging station for a vehicle in class *k*
x_i^k	A binary variable taking the value of 1 when a charging station is located on candidate node *i* for a vehicle of class *k*
z_i^k	The number of chargers located on candidate node *i* for a vehicle of class *k*
S^k ($ per spot per lifetime)	The cost to provide one charger for vehicles in class *k*
γ ($ per hour)	Value of time
Y (yrs)	Lifetime of the charging stations and chargers
π_i^m (hr per month per yr)	Total queuing and charging time at charging station *i* during month *m*
T^{km} (hr per month per yr)	Detour time for vehicle class *k* during month *m*
$\hat{f}(e)$ (vehicles)	Estimated link flow for link $e \in E$
$f(e)$ (vehicles)	Actual link flow for link $e \in E$
$\hat{t}$ (trips per day)	Estimated OD demand matrix containing the number of trips per day for different OD pairs
$G(\hat{t})$	A function that finds link flow based on the user equilibrium process and OD demand matrix, $\hat{t}$
φ_e^m	An average value of the monthly factors for link *e* in month *m*
κ_{OD}	Set of all links with a positive share of demand for the OD pair
P_e^{OD}	The proportion of each OD demand that uses each link *e*
Φ_{OD}^m	Demand factor of month *m* for each OD pair
$\Gamma \& \Gamma_n$	Objective function value & the neighbor solution objective function value in the metaheuristic algorithm

4-3- Modeling Framework

The modeling framework used in this study captures link travel time variations by link flows along the routes, and tracks the state of fuel and electricity for groups of vehicles traveling between different OD pairs. In this framework, the objective function value, which is a summation of the total investment costs and the monetary value of detour and queuing delays, is minimized over the year to capture the traffic demand and battery performance variations over different months of the year. The model considers BEVs with limited driving ranges, and ensures the feasibility of long-distance trips by providing the required infrastructure en-route, while minimizing investment cost as well as the total delay for all BEVs. Different locations along major roads are differentiated by their land acquisition costs and electric power availability.

In this study, the road network contains a set of links ($e \in E$), and a set of nodes ($i \in I$). The set of current refueling/charging stations and candidate points for building refueling/charging stations are defined by $N_1^k \subset I$ and $N_2^k \subset I$, respectively, where $k \in K$ denotes different classes of vehicles in the network. Note that CVs and PEVs with certain battery sizes are assumed as different classes of vehicles. Any node, belonging to the set of current or candidate refueling/charging stations, may be visited by users for refueling/charging purposes or as a midpoint along their route. Given the impacts of the visiting purpose on the state of fuel/charge, two sets of dummy nodes are introduced for charging purpose as ${N'}_1^k$ and ${N'}_2^k$. The objective function below, which is adopted from the function provided by (Ghamami et al., 2020a), aims to minimize the investment cost (charger, grid, construction, land, etc.) and also the users' refueling/charging, detouring and queuing time cost:

$$\min \sum_{k\in K}\left(\sum_{i\in {N'}_2^k}(C^k x_i^k + z_i^k S^k) + \gamma Y\left(\sum_m \sum_{i\in {N'}_1^k \cup {N'}_2^k}({\pi_i}^m + T^{km})\right)\right) \tag{4.1}$$

The objective function (4.1) consists of two main terms. The first term represents infrastructure investment cost, which includes the fixed cost of acquiring a charging station at any location and the variable cost of charging spots. For charging station cost, the number of charging stations is multiplied by C^k (measured in $ per station per lifetime), which is the fixed cost of building a charging station for a vehicle in class *k*. x_i^k is a binary variable taking the value of 1 when a charging station is located on candidate point *i* for a vehicle of class *k*. For the charging spot cost, the number of charging spots, z_i^k, is multiplied by S^k (measured in $ per spot), which is the fixed cost to provide one charging spot for vehicles in class *k*. The second term of the objective function represents the monetary value of time spent waiting and charging in the stations, and required detours to access charging stations. The total time for waiting in queue, charging, and detour is multiplied by γ, which is the value of time ($ per hour). Therefore, π_i^m denotes the total queuing and charging time at charging station *i* during month *m*, while T^{km} is the detour time of vehicle in class k in month *m*. In (4.1), delays are summed over the lifetime of charging stations, *Y*. The decision variables of the study are the location and capacity of the charging stations (number of charging spots). The model ensures the feasibility of travel for BEVs traveling between different OD pairs considering their route choice options.

In order to find the optimal location and capacity of charging stations, the objective function defined in (4.1) is minimized, given the traffic demand and battery performance provided for different months. Therefore, traffic demand needs to be estimated for different months using the available information (i.e., the base OD demand matrix and traffic counts on a subset of links). Thus, the OD demand matrix that best matches the traffic volumes of the subset of links for each month should be found. The daily traffic demand is then expanded to monthly traffic demand, and the OD demand matrices of different months are used to find the optimum charging station location and capacity considering the traffic demand and battery performance variations over different months of a year. Note that the EV demand is considered to be 6 percent of the total traffic demand. The objective function of the sub-model used to generate the monthly OD demand matrices, which are the inputs of the main problem in (4.1), is as follows (Eisenman and List, 2004).

$$min \sum_{e \in E} |\hat{f_e} - f_e| \tag{4.2}$$

Subject to

$$\hat{f} = G(\hat{t}) \tag{4.3}$$

$$\hat{f} > 0, \hat{t} > 0 \tag{4.4}$$

where $\hat{f}$ is the vector of estimated flows for all links, $e \in E$, and f is the count observations for the same links. $\hat{t}$ is the estimated OD demand matrix while $G(\hat{t})$ is a function that estimates link flow based on the OD demand matrix. This function allocates users to different routes and charging stations for charging in a way that there is no other route or charging option to reduce their total travel time (including detour, waiting, and charging time). Note that the total travel time of each route depends on the number of assigned users to the routes and charging stations. The function finds the link flow vector, $\hat{f}$, for all links, $e \in E$, based on the user equilibrium process and the OD demand matrix.

4-3- Data Summary

Input variables reflecting the local information in Michigan are significantly important in finding the optimal charging facility locations and the associated number of chargers. Therefore, the required data to find the optimum charging facility in Michigan are collected through different stakeholder meetings and requests from relevant companies. Thus, in this section, data acquisition details are presented, which entail associated costs of each station and its chargers based on the station location, electricity provision costs, types of chargers, PEV specifications and market share, and travel demand information to capture the effects of seasonality in trip making. In this study, a value of time of $18/hour is considered to calculate the monetary value of experienced delay. The details of the other collected data and the sources are presented as follows.

4-3-1- Costs Data

In this chapter, the costs of site acquisition, utility upgrade, electrical panel and switch gear, engineering and design, permitting, and project management are incorporated as station costs. Station set-up costs, including project management, equipment, construction, and maintenance costs, were requested and provided by different charging station companies. The charging stations supporting 50 kW chargers have costs of $48,437. The 50 kW chargers also cost $33,750. Land acquisition cost for siting fast DC charging stations depends upon many factors. Several studies state that population density is the most visible and measurable basis that should be taken into account at macro-level assessment. Seo et al. (2018) estimated that a one percent increase in population density increases commercial land values by 3.5 percent when other factors are unchanged. This finding is supported by an earlier study by McDonald (Mc Donald, 1993), who found elasticity measures between 3.05 and 3.21. Another contributing factor in the site acquisition cost is the commercial property values of the neighborhood, which also depend on various factors. The population density in this study is extracted from the U.S. Census (U.S. Census Bureau, 2010) data, which provides the population counts and density values at the zip code level in the 2010 decennial census. The population densities of Michigan for different zip codes are illustrated in Figure 4-1. The modeling nodes for route placement of charging stations are overlaid with Figure 4-1, and land costs are calculated to develop comparative land costs that are combined with other costs in modeling optimal EV charger placement. Statistics on land costs are provided in Table 4-2.

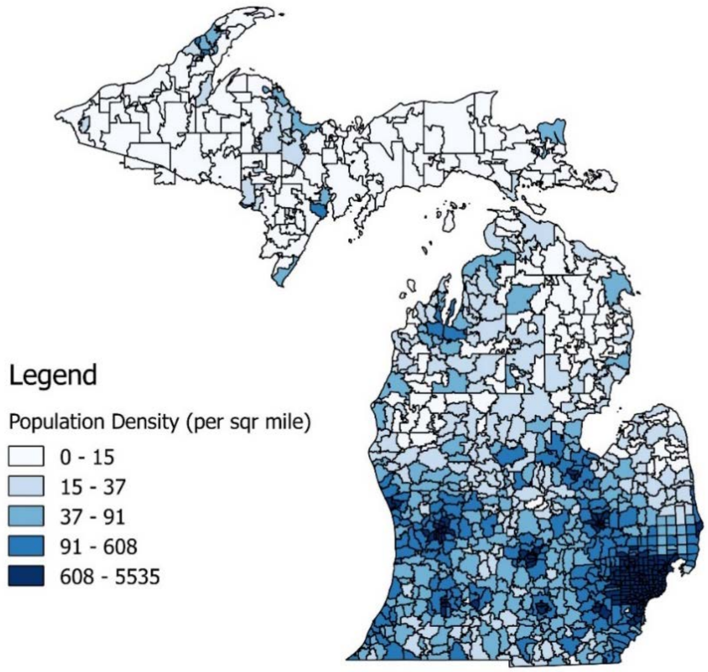

Figure 4-1 Population density of Michigan at the zip code level (U.S. Census Bureau, 2010)

Power availability is another contributing factor in BEV charging facility placement. In this study, the utility coverage at each candidate location across the state is checked through the Michigan Public Service Commission website ("MPSC - MI Public Service Commission," 2019). Subsequently, the coordinates of each candidate location are provided to the related responsible utility company to obtain the electricity provision costs. These costs include but are not limited to: conduit from the transformer to the meter enclosure, meter enclosure, protective equipment, and conduit and conductor from the meter enclosure to the charging station. Considering the fact that electricity provision costs could vary substantially in even matters of meters, the provided costs at each location are the average values within the area. Also, for candidate locations under jurisdiction of multiple utility companies, the average cost is used as an input to the proposed modeling framework. Statistics on electricity provision costs are also provided in Table 4-2.

Table 4-2 Estimated land cost and electricity provision cost at candidate points

	Minimum	Average	Maximum	Standard Deviation
Land Cost ($)	162,410	171,095	250,175	16,638
Electricity Provision Cost ($)	12,230	69,539	275,000	55,924

4-3-2- PEV Specifications and Market Share

In order to reflect the needs of the current and projected future PEV demand, PEV market share at present and into the future is accounted for in this study. In addition, current battery size and performances in different weather conditions are considered as other vehicle specific characteristics in this study. Auto companies' representatives at various stakeholder meetings associated with this study, recommended using a 70 kWh EV battery size for the model. In terms of charging power, this study considers 50 kW DC fast chargers. The battery efficiency in this study is considered to be 3.5 mi/kWh in favorable weather conditions based on the suggestion of vehicle manufacturers and other stakeholders (i.e. in summer and fall) (Ghamami et al., 2019b). This value is called the nominal battery performance throughout the study. Various studies suggest that the battery performance declines by 25% to 30% in cold temperatures (which is assumed to occur on December, January, and February in this study) (Department of Energy, 2020). Battery performance variation highly depends on the model and type of the car. Therefore, the value suggested by vehicle manufacturers and Office of Energy Efficiency and Renewable Energy (Department of Energy, 2020) is used in this study. Given the mentioned PEV specifications, the present study focuses on developing a BEV DC fast charger optimized placement map for 2030. As such, projections for future EV market share in Michigan are also required. Based on the

Midcontinent Independent System Operator (MISO) predictions, a recent study in Michigan recommends the market shares of 1.49% in 2020 and 6.00% in 2030 (*Electric Vehicle Cost-Benefit Analysis Plug-in Electric Vehicle Cost-Benefit Analysis: Michigan*, 2017).

4-3-3- OD Travel Demand and Michigan Road Network

Michigan road network configuration and OD travel demand, which is associated with a typical fall weekday traffic demand, were provided by MDOT. The network physical structure was designed in TransCAD® (Figure 4-2(a)) and simplified (Figure 4-2(b)) for the purpose of this study to avoid the computational challenges and roadway details which are unnecessary for the intercity network evaluation. The base OD demand values were obtained from state travel surveys and were transferred to an OD demand matrix using the planning travel models of the state DOT. This demand table is estimated for about 2,300 traffic analysis zones (TAZs) for a weekday in fall season with normal weather conditions. First, the 2,300 TAZs are aggregated to 24 nodes representing large cities throughout Michigan with populations higher than 50,000. Moreover, the aggregated demand table (base demand) is modified to capture monthly variations in demand as a result of different factors, such as tourism or weather conditions. The monthly variations are calculated based on the continuous counting station data provided by MDOT. The modifications applied to consider demand at border points of Michigan and monthly variations of demand are elaborated in the following.

4-3-3-1- State of Charge

The modeling framework presented in this study is designed to support intercity trips within Michigan. The network level problem considered in this study is solved considering all BEVs begin their trips fully charged (assuming that intercity trips are well-planned with available chargers at trip origins). Our model also ensures that BEVs arrive at their destinations with at least

20 percent battery charge level (Nie and Ghamami, 2013). To this end, BEV users might need to charge their battery depending on their trip length to ensure this minimum battery charge at the destination. In case of multiple required charges along the BEV trips, the battery would be charged up to 80 percent of the battery capacity (due to exponential increase in charging time in the last 20 percent of the battery capacity) except for the last required charging before reaching the destination. For the last required charging along the BEV trip, the model assumes the battery would be charged only up to a level that can ensure the minimum available charge at the destination. This study assumes that a charger is available at both ends of a trip, unlike the common FRLM studies that ensure completion of a symmetrical round trip with a single charge.

4-3-3-2- Demand Estimation at Border Points

In this chapter, the border points or boundary nodes, which are nodes connecting Michigan to the neighbor states and Canada, are also considered as origin or destination nodes. These trips are supported by providing charging stations to fully charge the vehicles that are leaving the state. For BEV trips with out-of-state origins or destinations, the model considers only the portion of these trips that occur in Michigan. This study refers to these trips as external demand. To enable external demand of BEVs, additional charging spots are required at the border nodes. In this study, based on the nationwide OD matrix, the external outgoing flows for each boundary node is estimated. Based on the intended charge level and the charging demand, the required number of charging spots at boundary nodes are determined.

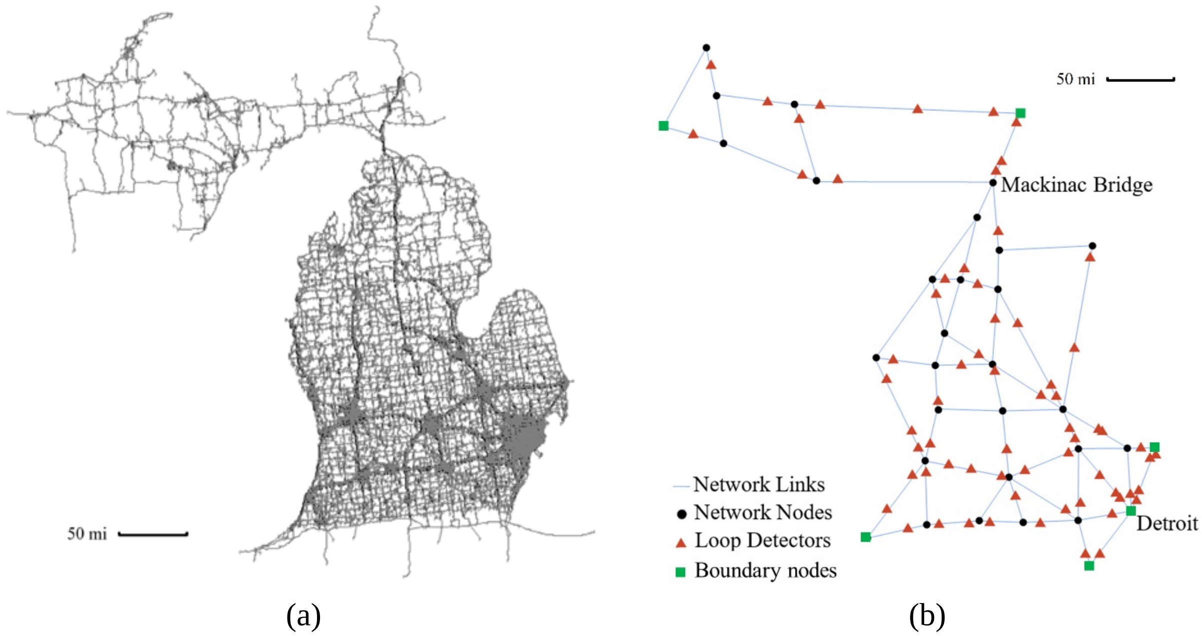

Figure 4-2 Michigan road networks (a) Original Michigan road network provided by MDOT (b) Simplified intercity road network along with the location of continuous counting stations

4-3-3-3- Monthly Demand Estimation

Monthly demand is estimated using the counting station data provided by MDOT. Given the fluctuating traffic patterns in different months of a year, monthly demands, which reflect the existing traffic patterns in the network, should be estimated for each OD pair. The resulting monthly demands can be used as inputs to the charger location model to ensure that the estimated charging station locations and number of spots are adequate. In this study, it is assumed that a proportional relationship exists between the traffic counts of the stations and the OD demands. Thus, the observations from count stations located on Michigan highways are used as a priori information. MDOT provided the counts of 122 continuous counting stations installed on Michigan highways from which 66 detectors are located on the current simplified network links. Having assigned detectors to their relevant links (both directions) in the Michigan network, 90 one-directional links out of 114 links have at least one count station. Note that the information of each individual detector is used for both directions of the corresponding link connecting two specific nodes.

Figure 4-3(a)-(c) demonstrate the variations of OD demands over different months for two specific locations across the state as well as the sum of all OD pairs. The variations of attracted traffic demand over different months for a candidate point located around Mackinac Bridge (as a tourist attraction location), connecting the Upper and Lower Peninsula, are demonstrated in Figure 4-3(a), while the variations of generated demand for a candidate location on the boundaries of Detroit are shown in Figure 4-3(b). As shown in these figures, traffic demands throughout a year are distributed differently for these two locations which indicates the importance of considering a specific demand matrix for each month and each OD pair. The sum of all estimated OD demands over different months for the state of Michigan is also demonstrated in Figure 4-3(c) as well as the average monthly demand over all months. The fluctuation of total demand in different months can be observed in this figure, with the least total demand in January and the highest total demand in July.

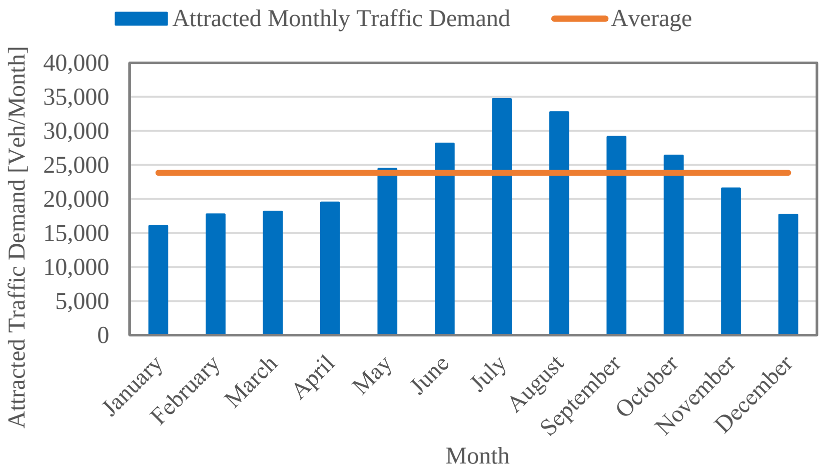

(a) Attracted traffic demand to a node located around Mackinac Bridge

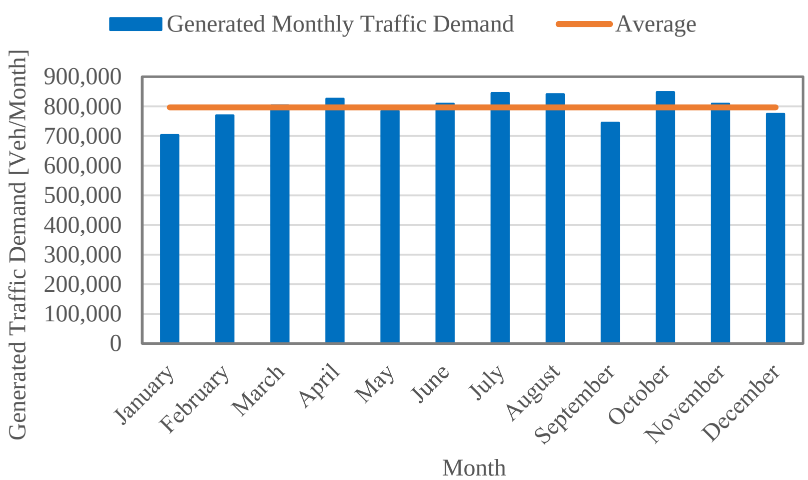

(b) Generated traffic demand from a node located on Detroit

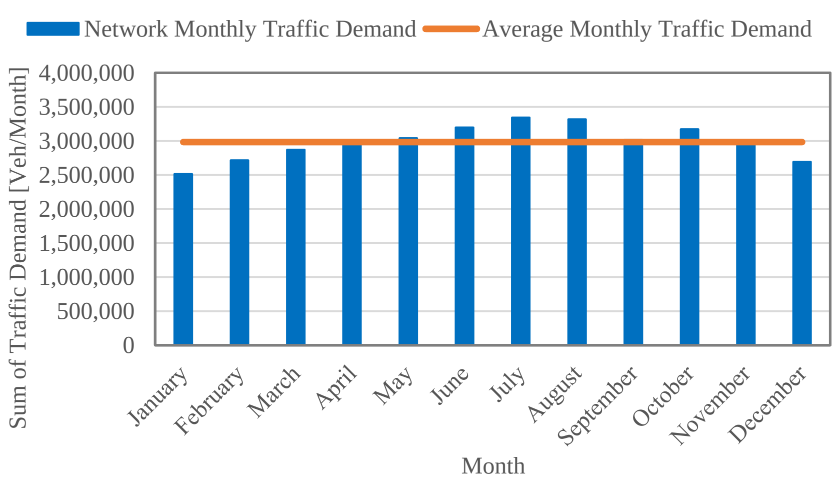

(c) Total monthly demand of the Michigan network in addition to the average monthly demand

Figure 4-3 Demand variations over different months of a year

4-4- Solution Algorithm

The optimization model used in this study to find the charging station counts and locations, which is adopted from chapter 3, is a mixed integer problem with non-linear constraints. As discussed in chapter 3, this problem is known to be NP-hard (refer to chapter 3 for more details about the problem and its constraints). The road network for the state of Michigan is considered a large-scale network. Solving such problems is computationally challenging or even impossible for the current commercial solvers in the market. Therefore, solving this problem requires a metaheuristic algorithm that is designed for this purpose. The metaheuristic algorithm used in this chapter to find the optimum charging station locations and capacity is a modification of the algorithm presented in chapter 3 based on the Simulated Annealing algorithm. The algorithm of the current study finds the optimum charging station locations and counts given the monthly traffic demands and battery performances. The following explains the procedure to estimate monthly OD demands and incorporating the variations in traffic demand and battery performance into the modeling framework. Afterward, the SA algorithm, which is the core of the modeling framework to find the optimum charging station locations and counts over the year, is explained.

4-4-1- Considering Monthly Variations of Demand in the Modeling Framework

Due to the cold weather in winter and scenic views in spring, summer, and fall, the traffic demand varies significantly in Michigan which leads to different travel patterns throughout the year. The travel pattern variations are accompanied by changes to the battery performance, as Li-Ion batteries do not fulfill their potential in cold temperatures. In order to capture the impact of these factors, the solutions are determined for each month considering weather influences on battery performance and monthly demands. It should be noted that these two factors are not positively correlated. In winter season, the performance of the battery is the worst, while the maximum demand occurs during summer season. Therefore, the optimal design for the BEV charging infrastructure network should be identified considering a trade-off between these two factors. Furthermore, the link performance functions are modified to capture the scenic routes' specifications (such as US-31, which runs along western lake shore of Michigan before ending south at Mackinaw City). A heuristic method is developed and used to estimate the monthly demands incorporating the information of 66 continuous counting stations across the roads of the intercity network of Michigan. The monthly demands are then used to find the optimal charger location and capacity throughout the year.

Monthly factors for each count station, representing the share of annual demand for each month, are utilized as main inputs of this method. The base OD demand estimated for a typical day in fall season, provided by MDOT, is also used as a reference value to be multiplied by estimated monthly factors for the OD pairs to result in monthly demands. The method developed to estimate monthly demands for each OD pair is an iterative approach consisting of multiple steps:

1- Finding an average factor for each month and each link with at least one detector (continuous count station)
2- Calculating shares of OD pairs' demands that are traveling on each link by executing a traffic assignment algorithm
3- Assigning adjacent count stations to OD pairs without any assigned continuous counting station

Estimating monthly factors for each OD pair in the network.

Since there might be multiple counting stations on each individual link in the network, an average value of the monthly factors (φ_i^m) should be estimated to represent the traffic pattern of link *i*, in month *m*. Note that no factor is assumed for the links without any detector. Furthermore, the share of base OD demand is found for each link using a traffic assignment module. To do so, the base OD demand is given initially as the input to the traffic assignment module and the proportion of each OD demand that uses each link are defined as p_i^{OD}, where i is the link number and *OD* is an origin and destination pair. In each iteration of the algorithm, the monthly OD demands of the previous iteration is given as the input to the traffic assignment module. Once the set of used paths for each OD pair is identified, it should be checked whether all OD pairs have at least one count station in their paths set to be used as an estimation factor. The count stations of the links reaching the origin or departing from the destination are used as an estimator for the OD pairs without any counting station. Finally, monthly factors for each OD pair, Φ_{OD}^m, are estimated using the share of each link from demand and the average factors of the links as below.

$$\Phi_{OD}^m = \frac{\sum_{i \in k_{OD}} \varphi_i^m P_i^{OD}}{\sum_{i \in k_{OD}} P_i^{OD}} \tag{4.4}$$

where k_{OD} is the set of all links with a positive share of demand for the OD pair, derived from the traffic assignment module. Using the monthly factor estimated by (4.4) and the base OD demand, monthly demands for all OD pairs are estimated and used as the input of traffic assignment for the next iteration. This iterative process needs to be repeated till there is a convergence in the monthly OD demands for two consecutive iterations. Figure 4-4 illustrates the algorithm to estimate monthly OD demands using loop detector data.

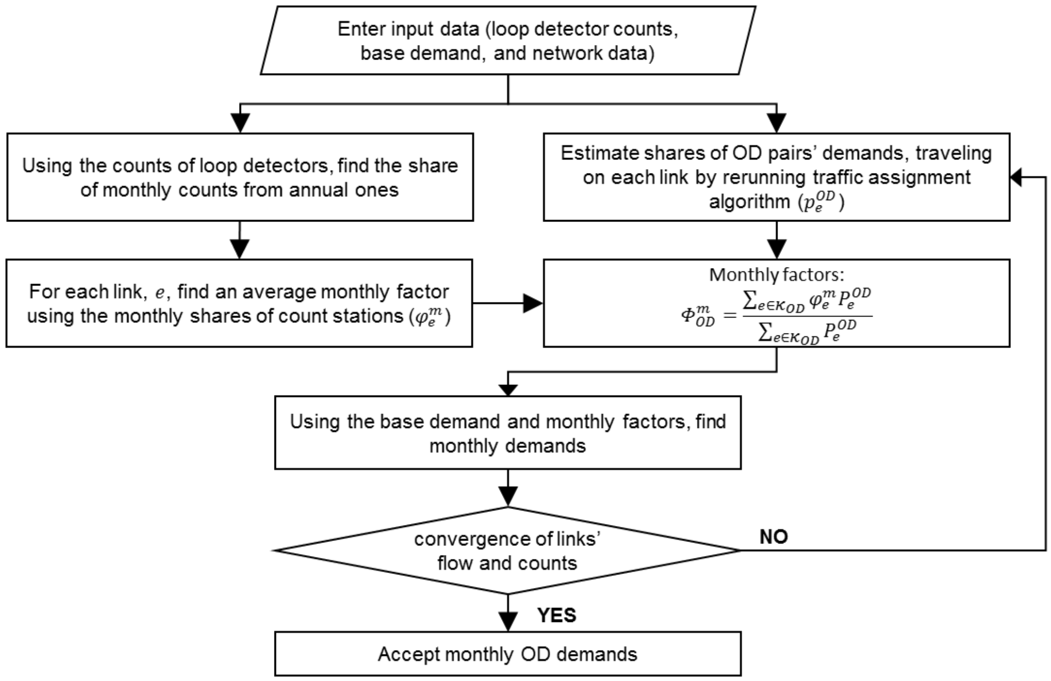

Figure 4-4 A brief illustration of the algorithm to estimate monthly demands for each OD pair

4-4-2- Metaheuristic algorithm to find the optimum solution

An SA algorithm is used to find the charging station counts and locations that serve the travel demand of BEVs throughout the year. Figure 4-5 illustrates the SA algorithm to find optimum charging locations and counts given the monthly OD demands and battery performance. Monthly OD demands, estimated in the previous subsection (Figure 4-4), and battery performance variations are the inputs to the algorithm. In this algorithm, different levels are defined for the number of chargers in each candidate station instead of a continuous integer variable: very low, low, medium, high, and very high. Each candidate station that is part of any solution has one of the five defined levels for the number of chargers. To ensure path feasibility for all vehicle classes and OD pairs, the decision variables for all candidate nodes are set to one in the initial solution. In addition, the number of chargers is set to the medium level for all charging stations. This initial solution, which guarantees feasibility, can be considered as the current solution. By perturbing the current solution, a neighbor solution can be generated by randomly changing one of the decision variables (adding/removing charging station or increasing/decreasing number of chargers level). The neighbor solution generation process is designed in a way to ensure feasibility in case of removing charging stations from any candidate nodes. The general procedure in the SA algorithm to find the optimal solution with the minimum objective function is as follows.

According to the type of perturbation, each location is associated with a weight factor (e.g., total flows and total delays), which is used to select the location based on a probabilistic greedy algorithm. To implement the probabilistic greedy algorithm, some rules are considered. Only one of these rules is used at each iteration of the algorithm. First, in order to add a new station, each location is weighted based on the total flow. The locations with higher crossing flow have priority in this rule. Second, to remove an existing station, each station is weighted based on the inverse of total flow. This rule implies that the locations with lower total flow get priority to be removed. Third, each location is weighted based on the total delay to add new chargers to a station. Finally, to remove chargers from a station, each location is weighted based on the inverse of total delay. These perturbation rules improve the convergence speed of the algorithm to the optimal solution. Perturbing the current solution according to these perturbation rules generates the neighbor solution and then a probabilistic decision is made to replace the current solution by the neighbor solution or not. If the neighbor solution improves the objective function relative to the current solution, it would be deterministically selected. However, even if it has a worse objective function, it might be selected probabilistically to avoid trapping in a local optimal solution. The process of generating neighbor solution and making a probabilistic decision on replacing the current solution would be repeated for many iterations to efficiently search the feasible area of the optimization problem and converge to the optimal solution. The probability of accepting a worse solution is reduced over the iterations to ensure convergence of the SA algorithm. A more detailed version of this discussion is provided in Ghamami et al. (Ghamami et al., 2020a). To find the objective function of each neighbor solution a network analysis procedure needs to be performed.

To consider users' route choice behavior in the algorithm, the network analysis procedure is embedded in the SA algorithm to find traffic flow for all feasible paths between each OD pair. The network analysis procedure is solved using the method of successive averages (MSA). For each solution, which consists of the available charging stations and the number of chargers within them, the vehicles are assigned to routes based on the user equilibrium concept. The MSA, which is used to assign vehicles to their optimum route, has a decreasing step size at each iteration. The process terminates when a defined gap value is lower than a small threshold. The average charging time is calculated based on the total required charge at each station. To address the queuing delay, a uniform arrival rate to stations is considered. Based on the arrival rate and the charging station service rate, which depends on the number of chargers, the queuing delay is calculated using a deterministic queuing approach. The charging, queuing, and detour delays affect the assignment of vehicles, as well as the objective function. A detailed explanation of this approach is provided in the study by Ghamami et al. (Ghamami et al., 2020a).

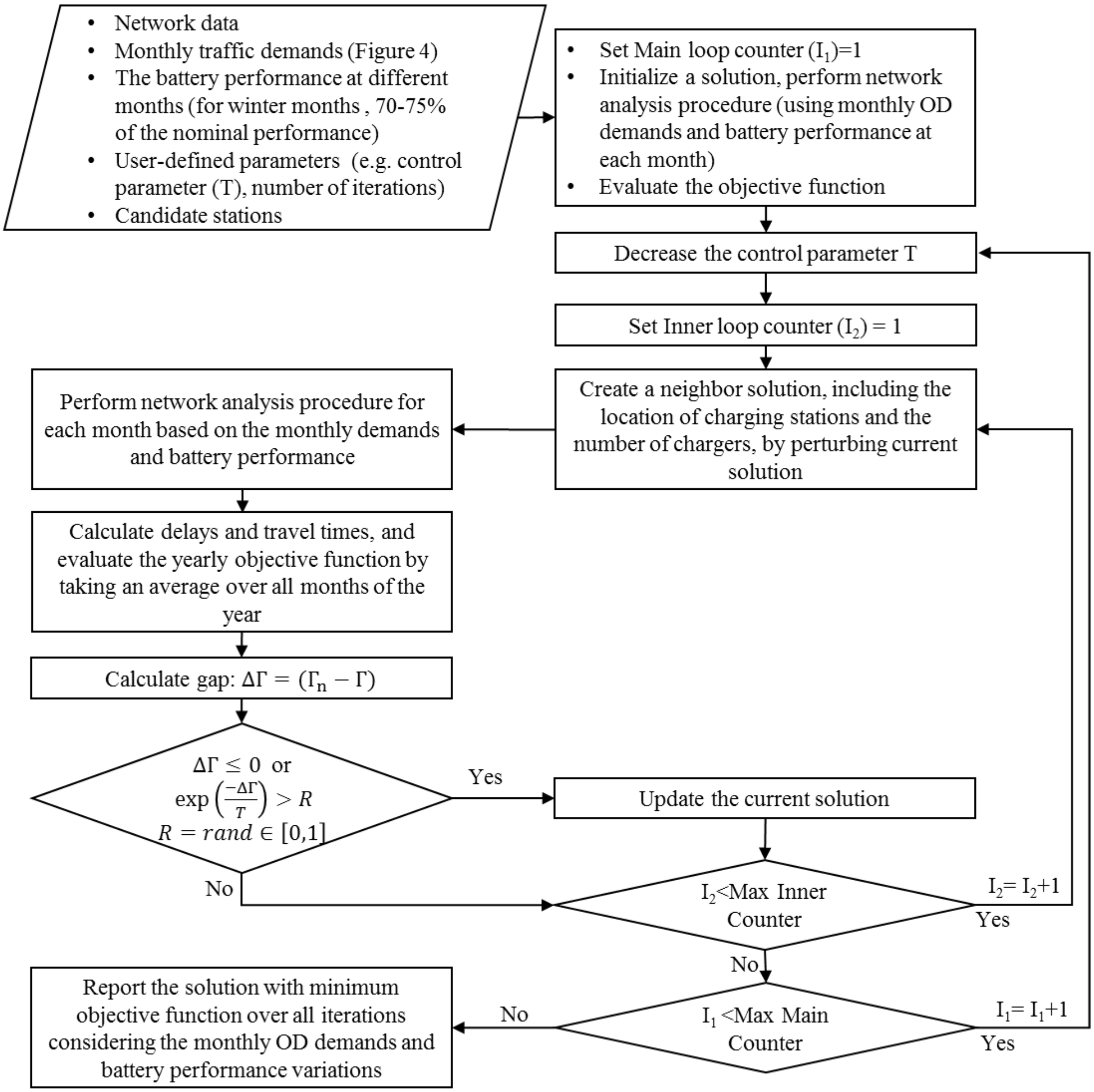

Figure 4-5 A schematic view of the SA algorithm to find the optimal charging station counts and locations given the varying battery performances and monthly OD demands over the year

4-5- Results and Discussion

In this study, future BEV infrastructure needs in Michigan are investigated in light of the recommended current battery size and charging power. The intention is to illuminate the charging demands accounting for future demands under the assumption of variable monthly traffic demands and battery performance. This study differentiates between battery performance in favorable and cold weather conditions. Conclusively, for each target year, BEV charging demands are first investigated for four different months to show the impacts of traffic demand and battery performance variations on the charging station configuration and counts. In addition, the optimum charging station locations and counts are presented with estimated traffic demands and assumed battery performances over the year. The lifetime of the chargers is assumed 10 years in this study.

The results of link performance modifications for scenic routes such as US-31 indicate that although scenic routes are more desirable, drivers mainly opt for major highways due to their reduced travel times. Therefore, considering scenic routes' effect on the link performance function does not affect the optimum charging station locations and spots. Thus, the effects of scenic routes are only considered through OD demand variations. Figure 4-6 and Figure 4-7 depict the optimized locations and capacities required across Michigan so that the related demands of different scenarios for January (the lowest battery performance), July (the highest traffic demand), February (a higher demand than January and lower battery performance than July), and October (a moderate demand) are satisfied. The scenarios reflect different demands, performances, and market shares of different months for the 2020 (Figure 4-6) and 2030 (Figure 4-7) target years. In all the figures of this section, solid circles are used to pinpoint charging station locations, the radii of which illustrate capacity. In this regard, Table 4-3 presents the number of required charging stations and chargers for different scenarios (months). Also, the investment costs of charging stations and chargers, and land costs are provided in this table. The sum of these costs forms the total cost of each scenario. Total charging time which is the summation of charging time and queuing time (waiting time in queue prior to charging) is also demonstrated in this table. Average charging delays in the system are also reported in minutes per charging vehicle in this table.

Comparing the results of Figure 4-6 and Figure 4-7 shows that, as we move onwards from 2020 to 2030, more charging stations and chargers are needed due to the increased BEV market share. Accordingly, as evident in Table 4-3, cost components and the total cost follow the same trend across the years. In terms of charging time, each month experiences a rising charging time as we move forward into the future. Note that total charging time reflects the time required for all BEVs in the network to charge including queuing time at the station.

As shown in Figure 4-6 and Figure 4-7, for each target year, January scenarios need larger charging infrastructure when compared to the other months. According to Figure 4-3c, total monthly demand of January falls below that of February, July, and October. However, as EV battery performance is lower in cold temperature by almost 30%, more chargers must be allocated to fulfill the EV demand. Accordingly, the results of Table 4-3 show that the January scenario in each target year evinces higher charging time, more required charging stations and chargers, and larger investment costs. It is noteworthy that the battery performance in July and October are considered identical due to comparable weather conditions. Considering the relatively close total traffic demands for July and October (Figure 4-3), these two scenarios in each target year share almost similar specifications. Although the average charging delays and investment costs are smaller for July and October scenarios, the charging station locations and counts of these scenarios cannot serve the EV demands of January and February scenarios with up to 30% battery performance reductions. However, it is observed that the required infrastructures for January and February scenarios fulfill the charging demands of BEVs in other scenarios, even though charging station locations may not overlap entirely.

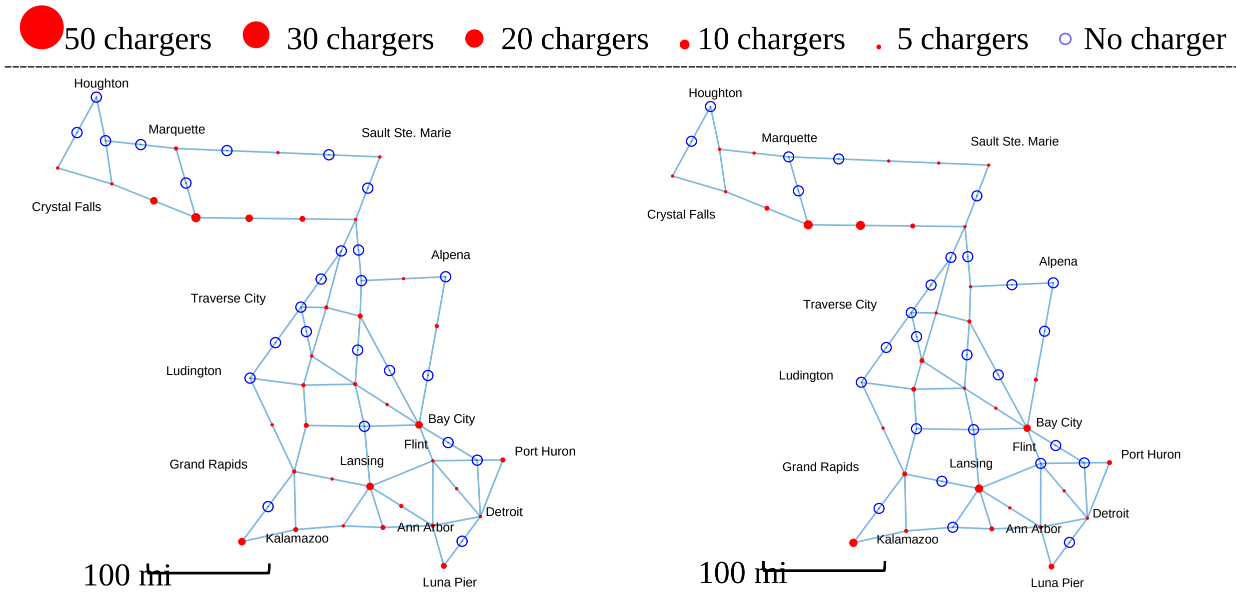

a) January with 70% battery performance of the nominal performance

b) February with 75% battery performance of the nominal performance

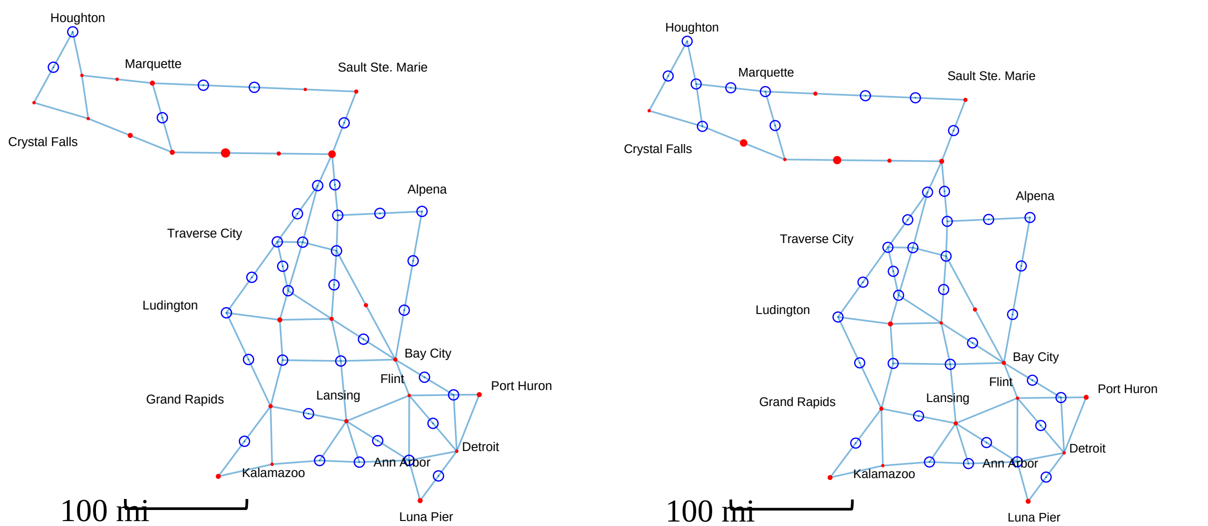

c) July with nominal battery performance

d) October with nominal battery performance

Figure 4-6 Visualized location and capacity of charging stations under different demand and battery performance scenarios with 2020 BEV market growth (1.49%)

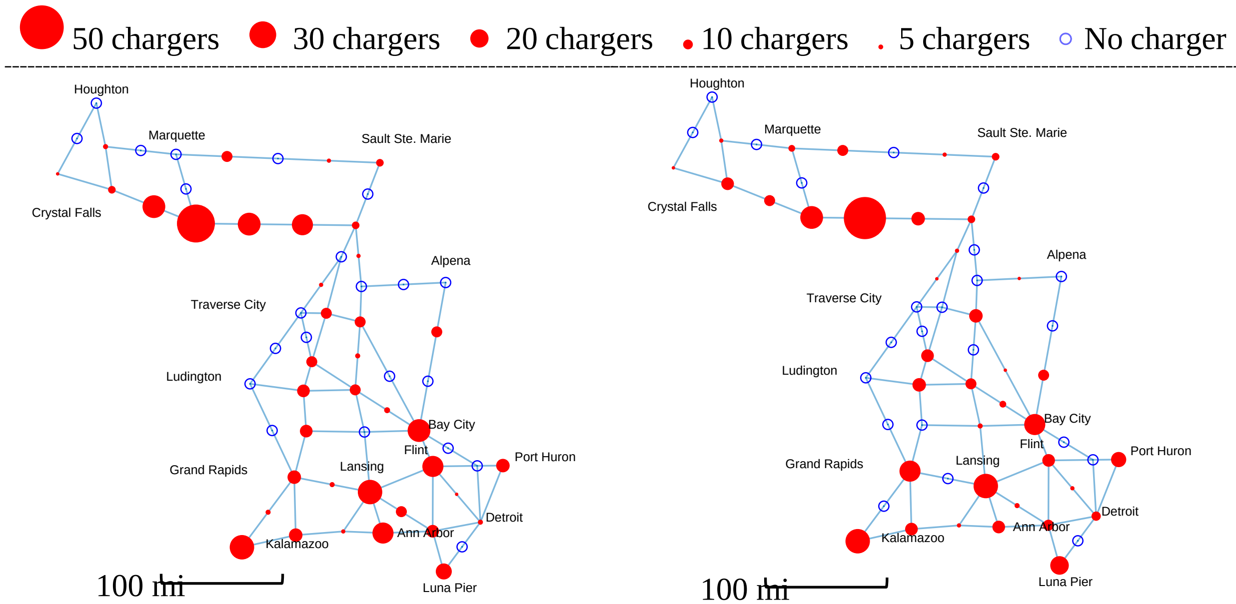

a) January with 70% battery performance of the nominal performance

b) February with 75% battery performance of the nominal performance

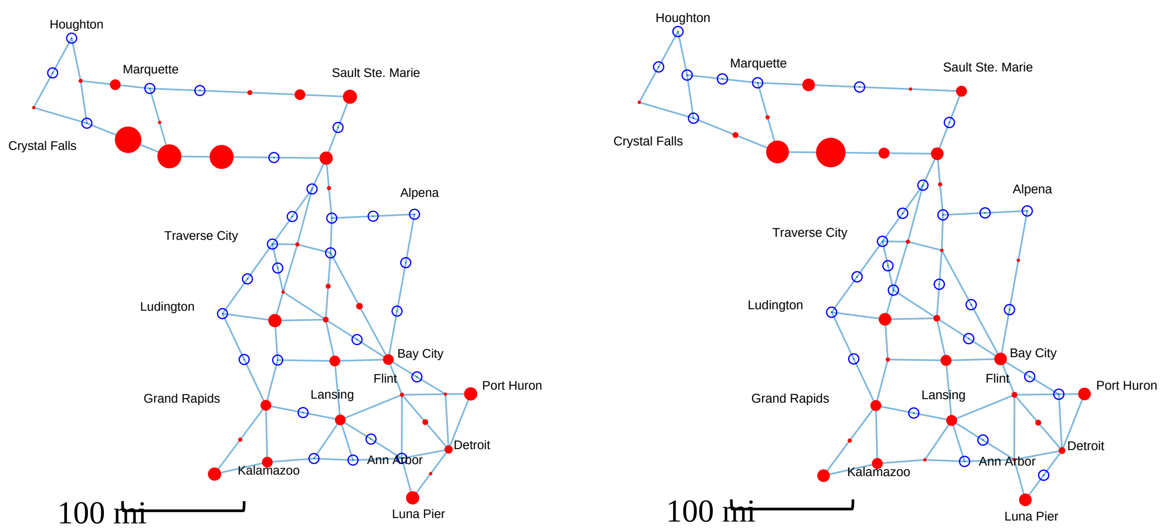

c) July with nominal battery performance

d) October with nominal battery performance

Figure 4-7 Visualized location and capacity of charging stations under different demand and battery performance scenarios with 2030 BEV market growth (6.00%)

Table 4-3 Summary of results for different month scenarios: charging stations counts and capacity, chargers, required investment, detour time, and charging time and delay

Variable\Scenario	January 2020	February 2020	July 2020	October 2020
Optimum Charging Infrastructure				
Number of charging stations	35	33	24	20
Number of chargers	126	118	81	68
Investment Cost				
Charging station cost (million $)	5.56	5.33	3.65	3.08
Land cost (million $)	0.24	0.22	0.15	0.13
Charger cost (million $)	4.25	3.98	2.73	2.30
Total cost (million $)	10.05	9.54	6.53	5.50
Delay Time				
Total charging time (hr)	901.72	796.78	526.55	420.06
Average charging delay (min)	31.54	30.90	29.74	29.83
Total detour time (hr)	7.72	21.56	30.21	18.49
	January 2030	February 2030	July 2030	October 2030
Optimum Charging Infrastructure				
Number of charging stations	38	37	32	31
Number of chargers	478	437	303	269
Investment Cost				
Charging station cost (million $)	6.04	5.76	5.05	4.84
Land cost (million $)	0.90	0.83	0.57	0.51
Charger cost (million $)	16.13	14.75	10.23	9.08
Total cost (million $)	23.07	21.33	15.84	14.43
Delay Time				
Total charging time (hr)	3642.09	3211.78	2135.40	1712.50
Average charging delay (min)	30.90	31.16	27.81	28.74
Total detour time (hr)	30.01	66.18	71.16	47.15

Although the required infrastructures for January and February scenarios fulfill the charging demands of BEVs in other scenarios, the charging station configuration and counts for these two scenarios are not the optimum for the entire year. Thus, using the algorithm presented in Figure 4-5, further analyses are performed to find the optimum charging station location and counts that serve the entire year demand with varying traffic demands and battery performances over the months. Figure 4-8 illustrates the visualized location and capacity of charging stations required across Michigan to satisfy the entire year demand with estimated 2020 and 2030 BEV market growths. Table 4-4 presents the number of required charging stations and chargers to serve the entire year demand as well as the investment costs of charging stations and chargers, land costs, detour time, and charging time and delay for the two target years. Similar to the results of monthly scenarios, more charging stations and chargers, and consequently a higher investment cost, are required to serve the BEV demand in 2030 relative to 2020. Although the total charging time of the system have significantly increased from 2020 to 2030, the average charging delay has slightly decreased. In addition, the investment costs and number of charging stations and chargers in Figure 4-8 and Table 4-4 are relatively close to the costs and counts of January scenario. Less number of charging stations are selected with more number of chargers in the entire year model relative to the January scenario. However, the average charging delays are lower for the entire year results, while total detour times are slightly higher. Another observation from Figure 4-8 is that charging station locations of 2020 and 2030 do not overlap at some candidate points. Thus, the optimal design may vary depending on the target year demand. The implementation of the stations resulted from 2030 scenarios is suggested in this study.

Overall, this study finds the optimum charging stations to support intercity trips in the state of Michigan, as well as to its neighbor states and Canada. These stations are proposed to support the trips started with a full battery to reach their destination with 20% battery. Different scenarios are considered for traffic demand and battery performance variations during different months of two target years (i.e. 2020, 2030). The results show the sensitivity of charging station configurations to traffic demand variation and battery performance reduction in winter months. The configuration of charging stations for winter demand supports the summer travel demand. In addition, the charging station locations and counts that satisfy the entire year demand are found considering battery performances and traffic demands in all months. The results for 2030 target year are suggested to be the main focus of implementation to ensure serving the future predicted demand. Even though the advancement in batteries are expected to happen by 2030, some older vehicles with smaller batteries or vehicles with degraded batteries are expected to still be on the roads in 2030. Thus, this study assumes a fast charging option with smaller batteries to ensure coverage and feasibility of trips for these vehicles. It is recommended to build charging stations for the 2030 scenario to ensure trip feasibility for all the vehicles in the market. Although the presented algorithm in this study can be applied to any other state, the resulting configurations and patterns among different months highly depend on the input data, which should be gathered for the state of interest.

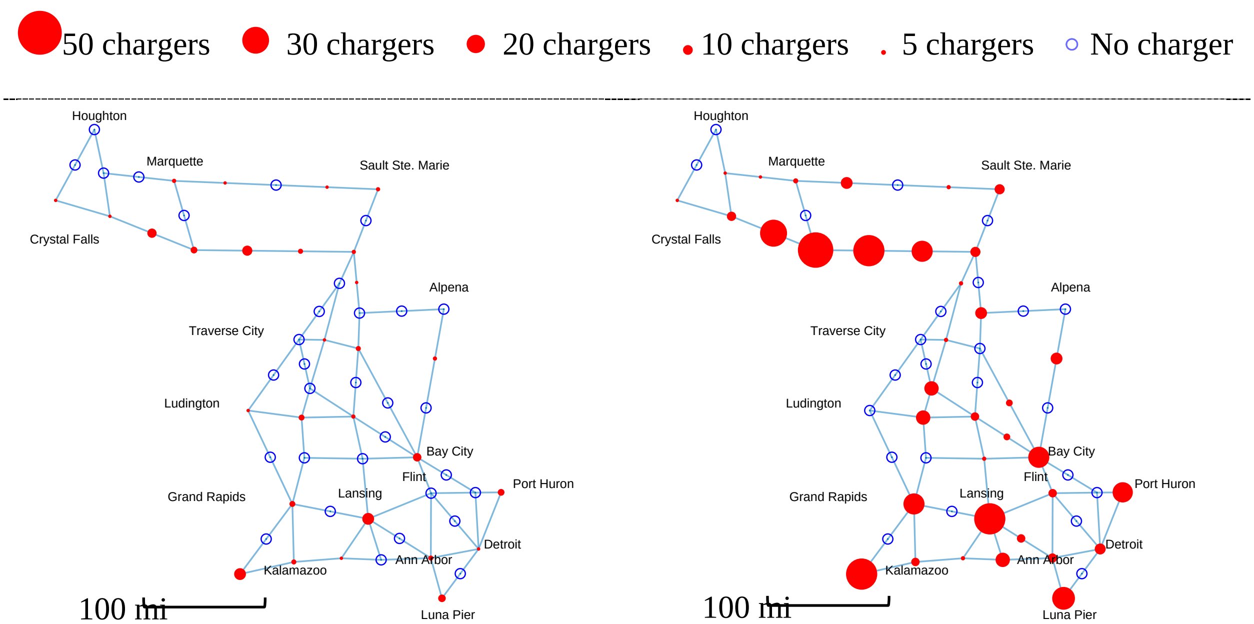

a) 2020 BEV market growth (1.49%) b) 2030 BEV market growth (6.00%)

Figure 4-8 Visualized location and capacity of charging stations optimized for the entire year demand and battery performance

Table 4-4 Summary of results optimized for the entire year demand: charging stations counts and capacity, chargers, required investment, and charging time and delay

Variable\Year	2020	2030
Optimum Charging Infrastructure		
Number of charging stations	28	36
Number of chargers	129	490
Investment Cost		
Charging station cost (million $)	4.34	5.62
Land cost (million $)	0.24	0.92
Charger cost (million $)	4.35	16.54
Total cost (million $)	8.94	23.08
Delay Time		
Total charging time (hr)	521.41	2097.32
Average charging delay (min)	28.85	28.57
Total detour time (hr)	20.5	79.81

4-6- Summary

Recent studies have shown that the lack of charging infrastructure is a key obstacle in the way of BEV adoption. Therefore, charger placement problems have attracted the attention of researchers to make charging stations accessible, and thus spur more potential BEV buyers to BEV ownership. The current study finds the optimum configuration of charging stations to support intercity trips within the state of Michigan as well as to its neighbor states and Canada. The study focuses on minimizing the investment cost and user delay, and compares the anticipated BEV demand scenarios in two target years (i.e., 2020, 2030). Due to weather conditions in Michigan as well as tourism attractions across the state, battery performance and traffic demand fluctuations in different months are accounted for to capture multi-view perspectives and better equip Michigan's electrified transportation system.

Based on the SA algorithm, a metaheuristic SA algorithm is utilized in this study to find the optimal charging station locations and capacity, considering the route choice behavior of BEV and CV users. Input variables reflecting the local information in Michigan are collected and requested via stakeholder meetings and relevant companies. Monthly OD demands are also estimated using a base OD demand for a typical weekday in fall, and the information of 66 continuous counting stations across Michigan roads provided by MDOT. In addition, the battery performance is considered between 70% and 75% of the nominal performance in cold weather. Given these inputs, the optimized charger placement for 2020 and 2030 are generated for the current battery technology (i.e., 70kWh), and 50kW DC fast charger. The analyses of this study lead to the following findings:

- Since the configuration of charging stations in 2020 does not overlap with the one resulted from 2030 scenarios, the results of 2030 scenarios should be the main focus of implementation to ensure serving the future predicted demand.
- The results of January scenario are closer to the optimum results for the entire year rather than scenarios of other months. In addition, the configuration and counts of charging stations and chargers vary significantly when the OD traffic demands change monthly. These findings show the importance of considering monthly OD demand variations and battery performance reduction in winter months.
- All system costs are relatively reasonable to build a network supporting BEV travel continuity in Michigan. Total estimated investment costs vary from 5.50 to 23.08 million dollars, depending on the desired scenario and the target year. If there is a funding model where multiple entities share the cost of implementation, the cost to build the system is reasonable and likely within means.

Chapter 5 - Impacts of Technology Advancements on Electric Vehicle Charging Infrastructure Configuration

5-1- Overview

High-end batteries and chargers can decrease the charging demand and charging time, respectively, and hence increase the EVs' market share. Based on a recently developed intercity model presented in chapter 3, this study investigates the impact of different battery and charger technologies on the configuration of charging infrastructure for the intercity network of Michigan in 2030. The major contributions of this study are considering the effects of a variety of technology advancements on infrastructure requirements, developing a realistic modeling framework considering the intercity network of Michigan, and using realistic assumptions and parameters calibrated through multiple stakeholders' meetings. Therefore, the parameters and findings of this study can be used for future studies requiring realistic data. This study finds that the location of charging stations merely depends on the battery capacity while the charging power dictates the number of required chargers. Furthermore, high-tech charging infrastructures showed to be the cheaper option compared to low-tech ones.

This chapter aims to bridge the gap in the current literature by investigating the charging requirements of EVs for intercity trips in Michigan, considering a variety of charging and vehicle technologies, using a modeling framework proposed in chapter 3. The solution algorithm is adjusted through various strategies such as refining the discrete set of chargers based on the local factors. A supplemental aggregate framework is proposed to capture and serve the out of state travel demand. The remainder of this study is structured as follows. The next section is the Modeling Framework followed by the Solution Approach section. Then the Data collection, Numerical Results, and Discussions are presented. The last section provides Conclusions and insights for future work.

5-2- Modeling Framework

This study aims to investigate the impacts of different charging technologies and batteries on the optimal configuration of infrastructure supporting the intercity trips of EVs in the state of Michigan. To this end, this project draws on the proposed methodology in chapter 3 to answer the following questions:

- Where to deploy charging stations?
- How many chargers are required at each station?
- What are the impacts and costs of each technology?

Thus, the objectives are 1) providing enabling infrastructure to support intercity trips of EV users while maintaining an acceptable level of service, and 2) evaluating the impacts of different technologies on the required investment cost and experienced delay. Thus, a modeling framework is proposed to find the optimal location and number of chargers at each charging facility in an intercity network, considering the impacts of charging station locations and the route choice of EV users on one another. Then, the effects of different charging and battery technologies on the charging location problem are investigated. A framework is proposed in this study to capture the impacts of "Technology Advancements" on the configuration of charging stations (Figure 5-1). The technology advancements include battery type and its maximum energy capacity, charging power, and charging infrastructure cost. Then, the charging infrastructure size and location is optimized for the desired technology. The other inputs required for the "Infrastructure Optimization" include road network, origin-destination travel demand, electricity provision cost, and land cost information. The main outputs of this framework are the bare-bone network of charging stations including the optimum number of chargers and location of charging stations, investment cost, and average users' delay.

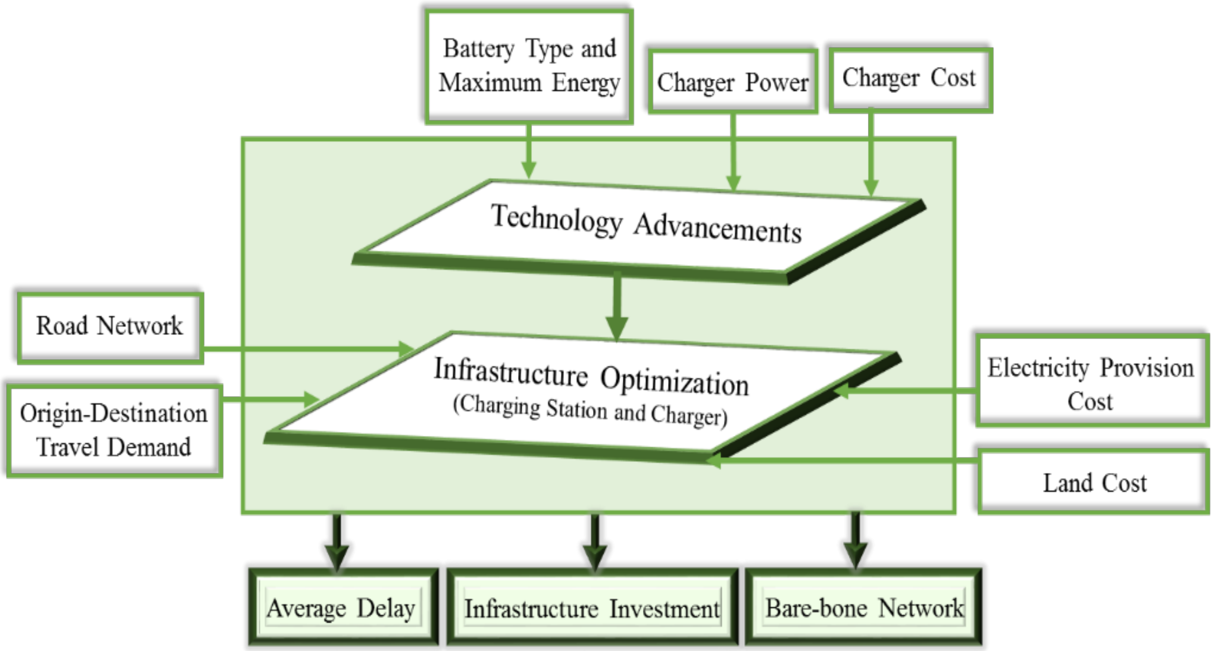

Figure 5-1 Modeling Framework

The infrastructure optimization model implemented in this study is based on chapter 3, which enables

- travel time variation by link/nodes flows along the routes/stations
- tracking the state of fuel for vehicles traveling between different OD pairs
- maintaining an acceptable level of service considering the total delay for all EVs.

5-3- Solution Approach

The optimization model used in this study is a mixed-integer problem with non-linear constraints, which is known to be NP-hard. The commercial solvers, such as Knitro, can solve such problems. However, when the network size increases, solving such problems is computationally challenging for the current commercial solvers. Thus, a metaheuristic approach is developed in this study based on the Simulated Annealing (SA) algorithm. The proposed algorithm can solve NP-hard problems efficiently. It starts with a feasible solution and moves towards neighbor solutions. The neighbor solution is accepted with a certain probability even if it worsens the objective function to avoid getting trapped in a local optimal solution. This algorithm is discussed in detail in chapter 3.

5-3-1- Refining the Discrete Set of Chargers

Chapter 3 incorporate a discrete set of chargers to be built at each charging station. To further improve the solution, a new approach is adopted in this study. In this approach, after solving the problem based on the initial discrete set of chargers, the problem is solved again using the optimal solution of the first step as the initial solution. A new discrete set of chargers for each node is redefined based on the optimal solution in step 1, which supports smaller changes compared to the initial set. This method can further refine the number of chargers to get closer to the global optimal solution and reduces the number of needed chargers by up to twenty percent. The solution framework presented in chapter 3 is updated to make the following flowchart presented in Figure 5-2, which reflects the changes specific to this study. Also, the discrete set is defined and then refined for each combination of charging station power and battery type.

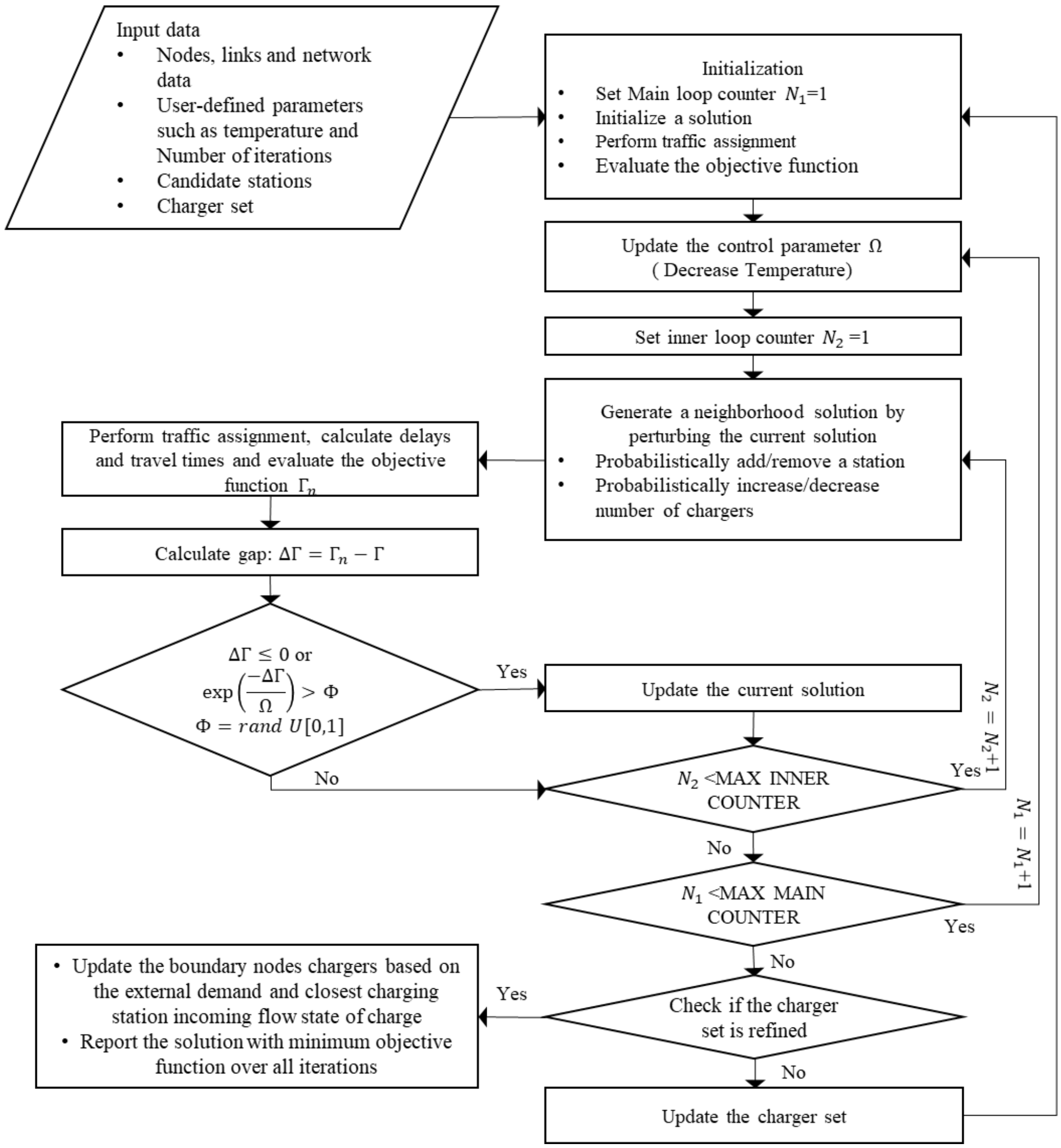

Figure 5-2 SA-based solution framework

5-4- Data Summary

Optimal charging station locations and charger counts per station are not only impacted by vehicle and charger specifications but also heavily depend on the road network characteristics, travel data and costs at each location. Thus, local information is essential. Data acquisition details for the charger placement project of the state of Michigan are presented below, which includes but is not limited to the travel demand information, road network specifications, market share, electricity provision cost, land cost, and the charger and battery cost (Table 5-1).

Table 5-1 Summary of the required data

Data	Stakeholder/Source
Michigan Road Network	Michigan Department of Transportation
Michigan Travel Demand Matrix	Michigan Department of Transportation
Electricity Provision Cost	Utility Companies
Land Cost	Economic Analysis
Vehicle Specifications	Car Companies (Ford Motor Company and General Motors)
Charger Cost and Specifications	Charging Station Companies (ChargePoint and Greenlots)

5-4-1- Michigan Road Network

Michigan road network is provided by the Michigan Department of Transportation (MDOT) (Figure 5-3(a)). As this study focuses on the location of chargers along the highways and major roads in the state of Michigan, the network is simplified to a sketch network (Figure 5-3(b)) which also assists in avoiding the computational challenges and roadway details that are unnecessary for intercity network evaluations.

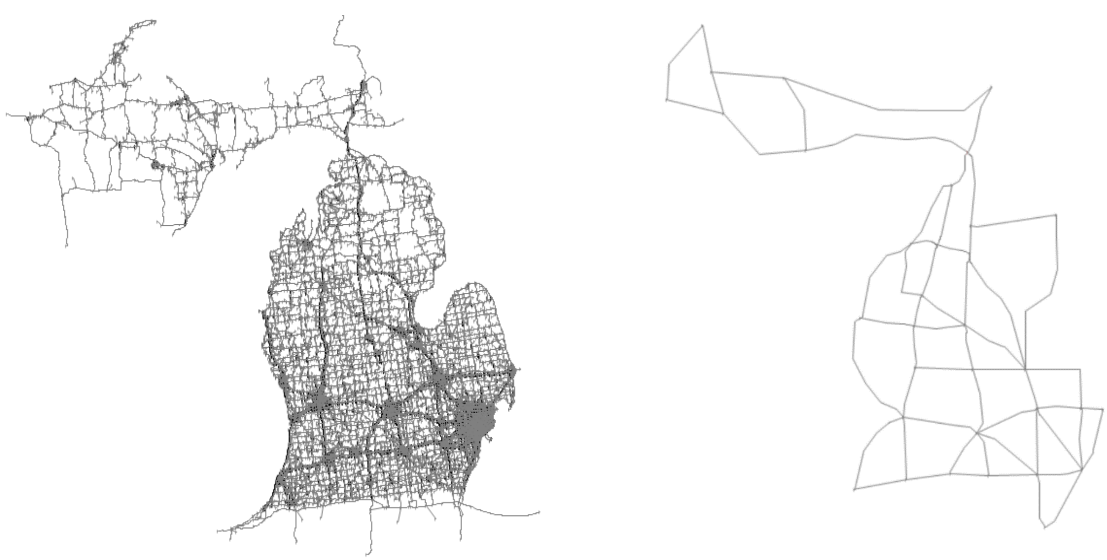

(a) (b)

Figure 5-3 Michigan road network (a) Original Michigan road network from MDOT (b) Simplified intercity road network of the state of Michigan

5-4-2- Origin-Destination Travel Demand

Origin-destination travel demand in Michigan is also provided by MDOT. The OD demand values are obtained from state travel surveys and transferred to the OD demand matrix using the state DOT's planning travel models. This demand table is estimated for about 3,000 traffic analysis zones (TAZs) for a weekday in the fall season with normal weather conditions. The 3,000 TAZs are aggregated to 24 nodes representing large cities throughout the state of Michigan with a population larger than 50,000. The intercity travel demand is aggregated accordingly.

5-4-2-1- External demand estimation

EV trips heading to a neighboring state, or Canada, which are referred to as external demand in this study, and their requisite chargers are also considered in this study. These chargers ensure that the EVs are fully charged before leaving the state and have the opportunity to fully charge as they enter the state at border cities. The border points, which are nodes connecting Michigan to its neighbor states and Canada, are considered as origin/destination nodes for inter-state travels. Then, based on the nationwide origin-destination demand matrix, the external outgoing flows for each border point in the state of Michigan are estimated.

5-4-2-2- Monthly demand variation

Given the fluctuating traffic patterns in different months of a year due to tourism or weather conditions, monthly demands for each OD pair should be estimated, which reflects the existing traffic patterns in the network. The estimation of monthly demand is conducted using the continuous counting stations data provided by MDOT. The fluctuation of total demand in different months shows the least observed travel demand in January and the highest travel demand in July.

5-4-3- EV Specifications

Auto companies present at the various stakeholder meetings throughout the project associated with this study recommended the current EV battery size of 70 kWh, while future battery size is anticipated to be 100kWh. The battery performance in this study is considered to be 3.5 mi/kWh in favorable weather conditions (i.e., in summer and fall); and is supposed to decline by almost 30% in cold temperatures, i.e., winter (Department of Energy, 2020). Furthermore, it is assumed that EVs charge their battery up to the amount that would be enough to reach their destinations; but not more than 80 percent of their battery capacity as charging slows down significantly after this threshold. Furthermore, EV drivers recharge their batteries, when there is at least 20% residual energy in the battery.

5-4-4- Market Share

In terms of EV market share, a recent study in Michigan conducted by Midcontinent Independent System Operator (MISO) suggests the estimated EV market share at 0.14% in 2017 (Lowell et al., 2017). This study also recommends a 6% EV market share in 2030, which means 6% of on-road vehicles in 2030 are anticipated to be EVs. Bloomberg predicts a market share of 11% in 2030, which seemed to be too optimistic based on the feedback from the stakeholder meetings (Lowell et al., 2017).

5-4-5- Charging Station Specifications

The proposed modeling framework for the EV charger placement intends to minimize charging infrastructure investment costs and EV users’ delay. Accordingly, suggested station specifications and set-up costs were requested from different charging station companies, such as ChargePoint® and Greenlots®. In terms of charging power, 50-kW DC fast chargers are currently available, while 150kW and even 350 kW chargers are appearing in the market. The two companies provided costs of site acquisition, project management, equipment, construction, utility upgrade, and maintenance. This study considers detailed site acquisition costs as well as utility costs for the candidate locations. Therefore, these two components are excluded from the costs of charging station companies provided and replaced with more realistic estimates derived from other sources. The details of these cost components are provided in the **Site Acquisition Costs** and **Utility Provision Costs** subsections. Among the above-mentioned costs, site acquisition, utility upgrade, electrical panel and switchgear, engineering, design, permitting and project management costs are incorporated in station costs. On the other hand, DC fast charger, validation and activation costs constitute charger cost. Therefore, stations with higher capacities incur larger charger cost resulting from the cost of each charger, and the activation and validation costs.

5-4-5-1- Site Acquisition Costs

Land acquisition for siting DCFC stations can take many forms from outright purchases to long-term lease contracts with/without site improvements. These facilities may share space with other retail establishments, may be coupled with other transportation fueling stations, or maybe stand-alone establishments to serve the specialty needs of EV drivers. The value of a site hinges on the revenue potential the site promises for an occupant. The existing literature on studies of commercial land values provides some basis for estimating the expected land values for commercial properties (West Technologies, 2015).

In estimating the expected costs of commercial property for siting DCFC stations, the host location population density is the most visible and measurable basis at a macro-level study. One study estimated the elasticity measure as 3.5, which means when the population density increases by one percent, commercial land values increase by 3.5 percent while other elements are held unaltered (Seo et al., 2018). In this study, the land cost is estimated using this elasticity measure, average Michigan commercial property values, average Michigan population density and site-specific population densities (Bigelow, 2017; William Larson, 2015). Table 5-2 shows the minimum, maximum, average, and standard deviation of the estimated land costs.

Table 5-2 Estimated land cost and utility provision cost at candidate points statewide

Type of cost	Minimum	Average	Maximum	Standard Deviation
Land Cost	$162,410	$171,095	$250,175	$16,638
Electricity provision cost	$12,230	$69,539	$275,000	$55,924

5-4-5-2- Electricity Provision Costs

Another important factor in EV charging facility placement is power availability and grid capacity. In this study, the website of the Michigan Public Service Commission ("MPSC - MI Public Service Commission," 2019) was used to pinpoint the utility coverage at each candidate location across the state. Contacting the utility companies, the average electricity provision costs at the locations under their jurisdiction were gathered. These costs include but are not limited to: conduit from the transformer to the meter enclosure, meter enclosure, protective equipment, conduit and conductor from the meter enclosure to the charging station, etc. As this study is performed at a macro level, the provided costs at each location are average values within the considered 5-mile radius. Also, if any candidate location is under the jurisdiction of multiple utility companies, the average cost is considered. The maximum, minimum, average electricity provision costs and standard deviations are as reported in Table 5-2.

5-5- Results and Discussions

The focus of this section is to capture the effects of technology advancements on charger placement in the state of Michigan. The SA based algorithm is applied to the intercity network of Michigan. The SA algorithm parameters are calibrated in (Ghamami et al., 2020a). The number of main and inner iterations are set to 25 and the control parameter is set to 0.85 which is reduced in each main iteration as below.

$$\Omega_{N_1} = 0.05 \times 0.85^{N_1} \tag{5.1}$$

Where Ω_{N_1} is the control parameter of the main iteration N_1. The rest of this chapter first discusses the Robustness and the Impact of Refining the Discrete Set of Chargers followed by a discussion on technology scenarios. Then, charging station configurations and associated delay and costs are presented for each technology scenario, followed by a discussion on the results.

5-5-1- Robustness

This section investigates the impact of stochasticity resulted from different seed numbers on the optimum solution. The SA algorithm uses random numbers to probabilistically choose a neighbor solution and also when it decides to select a solution that increases the objective function value. Therefore, this section seeks to show the robustness of the solution to the different seed numbers. To this end, the impact of 10 different seed numbers, each representing a scenario, are studied considering 1% EV market share, 50 kW charging power, and 70 kWh battery. The optimum objective function value, the charging infrastructure cost, and the cumulative number of chargers for these scenarios are presented in Figure 5-4. Figure 5-4(a) shows that among these scenarios, the optimum objective function value can change up to one percent. The similar objective function values show the availability of almost identical solutions with different representations. Figure 5-4(b) shows the cumulative number of chargers across the scenarios. While there are differences between the scenarios showing different number of chargers in stations, all scenarios have an almost the same total number of chargers. More specifically, the total number of chargers varies almost 2 percent among the scenarios.

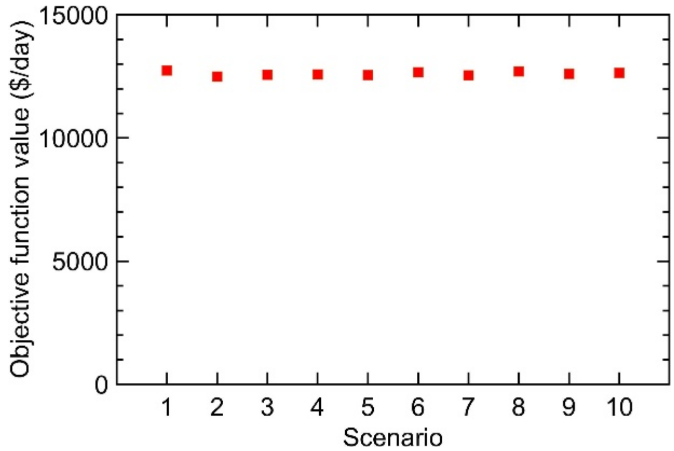

(a)

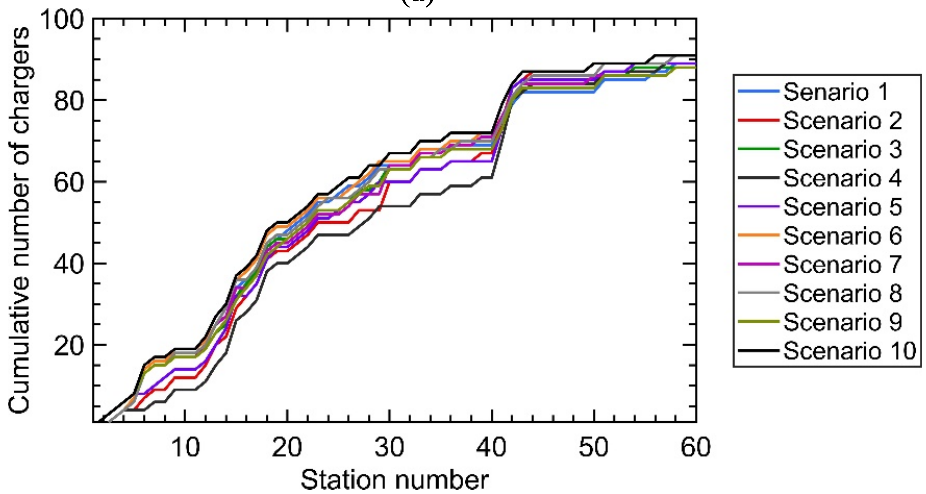

(b)

Figure 5-4 The impact of seed number on the (a) optimum objective function values (b) cumulative number of chargers

5-5-2- Impact of Refining the Discrete Set of Chargers

To account for the exact queuing at charging station, which affect the travel times and the traffic assignment, the number of chargers should be known before the traffic assignment. Therefore, a discrete set of chargers is defined initially and stations can have one of the number of chargers available in the initial set. However, the global optimum number of chargers might be different than the values of the initial set. Therefore, using the solution resulted from the initial set of chargers, a new set of chargers is defined for each location separately. This section investigates the impact of this refinement on the optimal solution. Figure 5-5 shows the initial objective function against the objective function value from the refined set. It shows that the objective function of the refined set always improves the objective function values of the initial set.

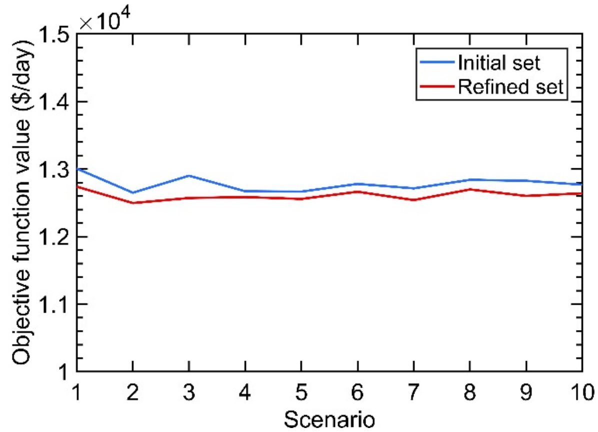

Figure 5-5 The impact of refining the discrete set of chargers on the optimum objective function value

5-5-3- Considered Scenarios

This study seeks to illuminate the DC fast charging planning for the state of Michigan in light of different technologies for battery and DC fast chargers. To this end, a variety of scenarios and demand levels were tested (Fakhrmoosavi et al., 2021). The target year of 2030 with an EV market share of 6% (Lowell et al., 2017) is selected for testing the effects of technology. EV battery performance is expected to drop by 30% due to the impacts of cold weather. Demand analysis revealed that even though the travel demand in Michigan is smaller during winter months, the reduced battery performance calls for a denser network of charging stations during winter months (Fakhrmoosavi et al., 2021).

Table 5-3 Considered scenarios information for the target year of 2030

Scenario	1	2	3	4	5	6
Battery Capacity (kWh)	70	70	70	100	100	100
Charger Power (kW)	50	150	350	50	150	350

Therefore, January demand as the coldest month in Michigan, with 70% of the EV battery performance is considered. In light of these assumptions, the charging station configuration for two battery sizes of 70 kWh and 100 kWh, and three charging powers of 50 kW, 150 kW, and 350 kWh are investigated. Table 5-3 presents the configuration of each considered scenario.

5-5-4- EV Charging Infrastructure Placement

In this chapter, future EV infrastructure requirements in Michigan are investigated under different battery and DCFC technologies in 6 scenarios for the target year of 2030. Figure 5-6 depicts the optimal configuration of charging stations and chargers across Michigan serving all OD demands in each scenario. A solid circle shows a candidate location is selected to be equipped with a charging station, while the radius of the circle indicates the number of chargers required in that area. Comparing the charging configuration of the scenarios with the same battery size, the location and number of charging stations do not vary significantly across the scenarios (also reflected in Table 5-5) as charging stations are required to ensure trip feasibility. However, the number of chargers drops as the charging power increases due to the higher charging speed and throughput, as well as the higher cost of high-tech fast chargers. On the other hand, comparing the scenarios for the same charging power and different battery capacity illuminates the significant impact of battery capacity on charging station locations. The increased battery capacity reduces the charging need and affects the locations where EVs need recharging along their route. Therefore, the configurations resulted from different battery capacities differ significantly in terms of the charging demand of the users.

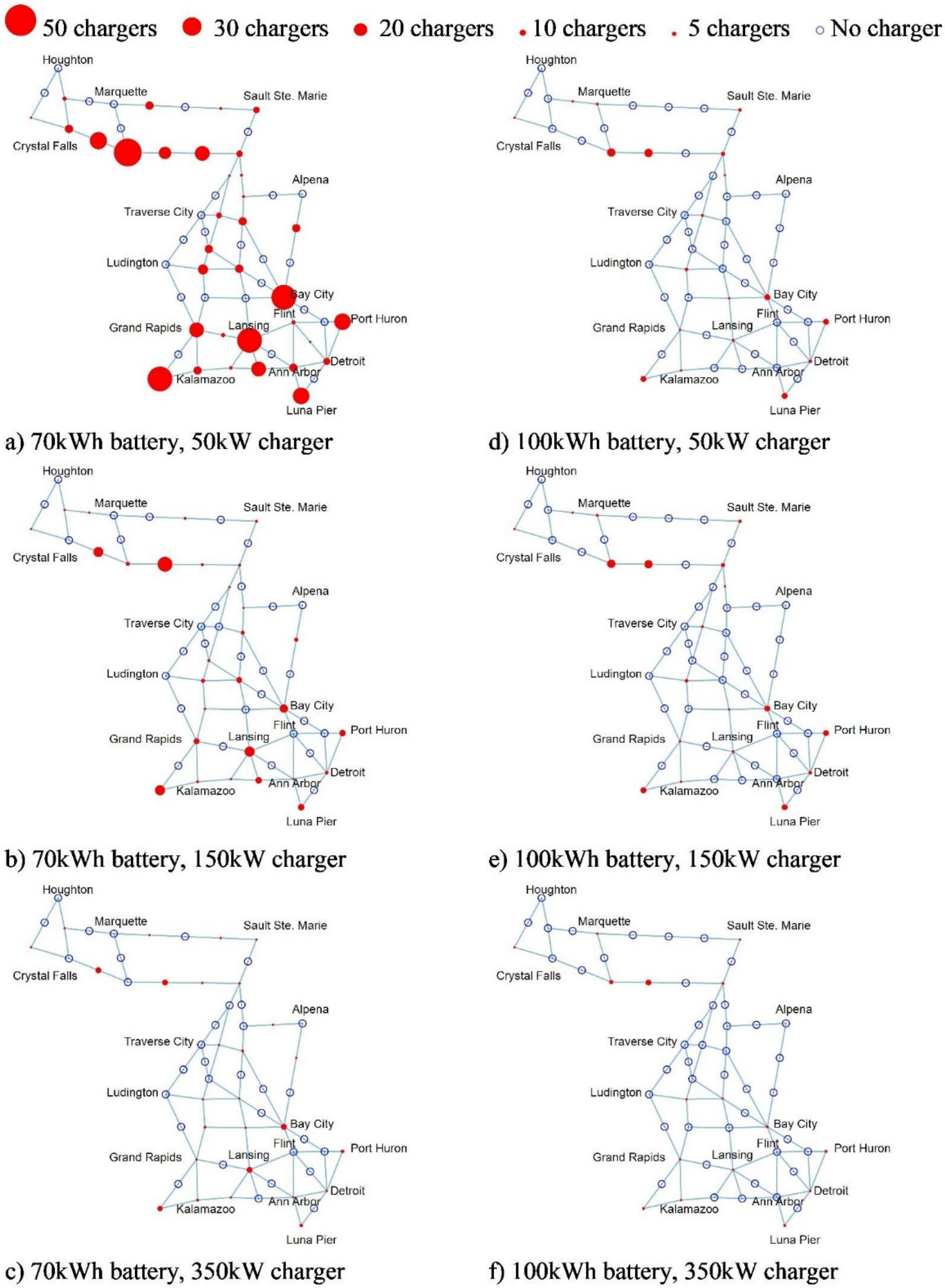

Figure 5-6 Visualized configuration of charging stations under different technologies

Considering all the scenarios, a huge charging infrastructure investment is required to facilitate EV trips in the Upper Peninsula (UP) of Michigan. While this part of Michigan only takes 3% of the state population (U.P. Supply, 2020) and 2% of the state intercity trips, it requires a charging infrastructure investment close to the investment required for the Lower Peninsula (LP) of Michigan. The reason lies behind the trip distances in UP. Due to the long-distance trips in UP, almost all EVs need to recharge their batteries along the route. However, most of the trips in LP are within the EVs' range and do not require any recharging, or they need to recharge just enough to get to their destinations. Table 5-4 presents detailed investment costs and delay time components.

Table 5-4 Scenario results: charging Stations, chargers, required investment, and delay time

	Technology scenarios					
	1	2	3	4	5	6
Battery energy (kWh)	70	70	70	100	100	100
Charging power (kW)	50	150	350	50	150	350
Optimum charger placement						
Number of charging stations	34	29	27	25	19	16
Number of chargers	513	181	90	250	94	46
Investment cost						
Charging station cost (million $)	5.45	5.48	6.14	3.90	3.64	3.76
Land cost (million $)	0.97	0.34	0.17	0.47	0.18	0.09
Charger cost (million $)	17.31	13.80	12.83	8.44	7.17	6.56
Charging infrastructure cost (million $)	25.57	19.62	19.14	12.81	10.98	10.40
Delay time						
Refueling time (hr)	3648	1218	527	1574	524	228
Average delay (min)	30.62	10.60	4.00	39.52	13.49	5.95

According to Table 5-5, when a battery size of 70 kWh is considered for EVs, increasing the charging power reduces the charging infrastructure cost from 25 million dollars to 19 million dollars, which is about a 24% reduction in investment cost. This means that higher throughput leads to a less required number of high-tech fast chargers. It is worth noting that the increase in charging power also decreases the average delay by 87%. Similarly, for 100 kWh batteries, increasing the charging power from 50 kW to 350 kW decreases the infrastructure cost from 12.8 million dollars to 10.4 million dollars, which is about a 19% reduction in investment cost. Furthermore, the average delay decreases from 39 min to 6 min, which is about 85% reduction. All in all, the 100-kWh battery and 350 kW charger can provide the lowest investment cost. However, a 100-kWh battery is 30% more expensive compared to a 70-kWh battery and the battery cost value becomes more significant as the EV market share increases.

Table 5-5 The impact of providing 50 kW chargers for the optimum solution of 150 kW chargers

Optimization Specifications	Charger Power (kW)	150	150	150	150
	Battery Energy (kWh)	70	70	100	100
Installation Specifications	Charger Power (kW)	150	50	150	50
	Battery Energy (kWh)	70	70	100	100
Number of stations		29	29	19	19
Number of chargers		181	181	94	94
Total investment cost (million $)		19.62	11.01	10.98	6.38
Total refueling time (hr)		1218	3756	523	1608
Total queuing delay (hr)		0.99	52469	2.9	20914
Average delay (min)		10.6	525.3	13.5	611
Trip feasibility		Yes	Yes	Yes	Yes

Considering the 50 kW chargers as the currently available technology, further analyses are conducted to investigate how the network would respond if the charging infrastructure configurations are determined for 150kW chargers, but the less costly, easier to access 50kW chargers are installed instead, with the capacity for future upgrade. Table 5-5 provides the results for this strategy for both considered battery sizes. In Table 5-5, columns 3 and 5 represent the results for the scenario of optimum configuration for 150kW chargers and installing 50kW chargers. An important initial observation is that EV trips are feasible even with lower power chargers. On the other hand, replacing 150 kW chargers with 50 kW chargers increases total refueling time by over 200%, causing queuing time and average delay to increase. Thus, the optimal location of charging stations and the allocated chargers for 150kW chargers can serve EV trips with 50kW chargers with smaller investment costs; however, the entire refueling and queuing time in the system, as well as average delay would increase significantly. Therefore, a good strategy is to start building 50kW power chargers with modules that are expandable to 150kW power chargers. It is crucial to monitor the market share growth and expand to 150 kW as the market share increases to avoid significant delays.

5-6- Summary

Infrastructure availability is known to be the key to the adoption of EVs (Nie et al., 2016). In order to make the best investment in the supporting infrastructure to increase market acceptance of EVs, an optimization model is calibrated through series of stakeholder meetings, adjusted through various strategies, and implemented in this study to find the optimum location of charging stations and number of chargers in a real-world application. The target year of 2030 with a market share of 6% is selected to anticipate the upcoming EV demand and provide the requisite charging infrastructure accordingly. The intercity travel demand reduces during winter in Michigan. However, the battery performance also reduces in cold weather by about 30%. Former studies have revealed that reduced battery performance has a larger impact on infrastructure requirements compared to that of the demand. Thus, January demand is selected, being the coldest month in Michigan, with 70% battery performance. The aim of this study is to investigate the trade-off between the charging infrastructure cost and the delay experienced by users including detouring delay, charging delay, and queuing delay. At another level, this study investigates the impact of different technologies on the configuration of charging infrastructure, experienced delays, and total system cost. Three different charging technologies with charger powers of 50 kW, 150 kW, and 350 kW, as well as two different battery types with capacities of 70 kWh and 100 kWh, are considered (based on the discussion with stakeholders of the project). The combinations of these technologies are investigated to provide information regarding future planning. The analyses lead to the following findings:

- The size of the battery determines the location of charging stations.
- The number of chargers is a function of the charging power.
- Charging stations with higher power have a higher cost, but they decrease the total required infrastructure cost and users' delay considering the higher rate of return.
- The configuration of high-power charging stations can be applied for the same battery size with a lower-power charger; the network would be feasible for EVs. However, EV users experience high delays due to queuing at charging stations.
- The level of investment is a function of trips' length and frequency rather than the population or population density.

Chapter 6 - Electric Vehicle Fast Charging Infrastructure Planning in Urban Networks

6-1- Overview

Distances of single urban trips are generally much shorter than the range of typical EVs in the market, but vehicles are supposed to serve a daily chain of trips instead of a single trip. Also, not all urban trips can begin with fully charged batteries due to various reasons such as unavailability of level 2 (L2, with 6.2 kW power) chargers (Wood et al., 2017), lack of charging time, or owners simply forgetting to fully recharge over the night. To address the range anxiety issue, this chapter introduces an integrated framework for urban fast charging infrastructure. It develops an integrated modeling framework for urban charging infrastructure planning, considering DC fast chargers with 50 kW to 150 kW charging powers.

To estimate the EVs charging demand, a comprehensive data set that includes daily chains of trips for all travelers and availability of level 2 chargers at each intermediate destination is required. However, most of the urban planning agencies rely on static zone-to-zone demand tables with aggregate data on trip purposes and land use characteristics at zone levels. Thus, an innovative approach is developed in this study to: (i) generate required dynamic travel demand information from available aggregate data, (ii) build a charging behavior simulation tool to assign the stochastic initial state of charge for each vehicle trajectory according to the departure time, trip purpose, and land use characteristics at the origin, (iii) feed this spatial and temporal distribution of charging demand into a novel agent-based charging infrastructure optimization framework, which captures travelers' charging behavior for a given market share of EVs, and ensures the feasibility of all EV trips. The mathematical model is decomposed into two subproblems that find the optimal location of stations and the number of chargers at each location separately.

The state-wide roadway network in Michigan provided by the Michigan Department of Transportation (MDOT) is considered as the main network of interest. Real-time traffic volume observations from loop detectors are used together with daily static demand data to estimate time-dependent demand tables. Then, a simulation-based dynamic traffic assignment tool, DYNASMART-P, is used to provide trip trajectories, and zone-to-zone time-dependent travel time and distance skims. Time-dependent trip purposes are also available from a travel survey in Michigan (Wilaby and Casas, 2016). Finally, land-use attributes at origin and destination zones are used to determine trip purposes and to simulate charging behavior for any city of interest in the state-wide network. Regional networks for three cities with various sizes, namely Marquette, Lansing, and Detroit, are used to demonstrate the successful implementation of the proposed optimization framework for various charging technological advancement.

The remainder of this chapter is organized as follows. The next section provides a literature review on charging station optimization and lists the key contributions of this study. Next, the research framework section presents the traffic simulation model, the charging behavior simulation model, the optimization model, as well as a solution methodology. The next section demonstrates numerical experiments including setup of the case studies, data, and results. Finally, the last section provides summary concluding remarks.

6-2- Research Framework

This section first presents the proposed research framework (Figure 6-1) by demonstrating the connections between traffic simulation, charging behavior simulation, and a mathematical optimization model. The traffic simulation component uses the Origin-Destination (OD) demand table and road network properties as inputs, incorporating a simulation-based dynamic traffic assignment tool (DYNASMART-P), to analyze the travelers' route choice behavior. Trip trajectories and skim tables are the main output of this component. The former includes traveled paths and travel time stamps along each path for each vehicle, and the latter are the average zone-to-zone travel distances and times. The next component, charging behavior simulation, utilizes temporal distribution of trip purposes, land use data, and trip trajectories from the first component to simulate travelers' charging behavior based on a random distribution of the initial state of charge and the required energy to complete their trips. The vehicles unable to fulfill their trips need to be recharged, forming the charging demand. This charging demand along with travel skims will be fed into an agent-based urban charging infrastructure planning model. This model, which is formulated as a nonlinear mixed-integer program, is decomposed into two subproblems; one locates the charging stations in the network, and the other finds the number of chargers at each station.

This section also presents a decomposition approach to solve the mathematical optimization model. Once the charging station location is determined based on station costs, refueling times, and travel detours for those in need of recharging, the time-dependent incoming flow and required energy in each station can be used to determine the number of charges needed to minimize the deterministic or stochastic queuing delay. The first subproblem is a linear mixed-integer mathematical model. While commercial solvers, e.g. CPLEX and Gurobi, can solve it for small-scale networks, a metaheuristic algorithm is developed for larger-scale networks in this study. The second subproblem is a non-linear mixed-integer mathematical model whose objective function is proven to be convex, and hence the golden section method is proposed to solve this subproblem.

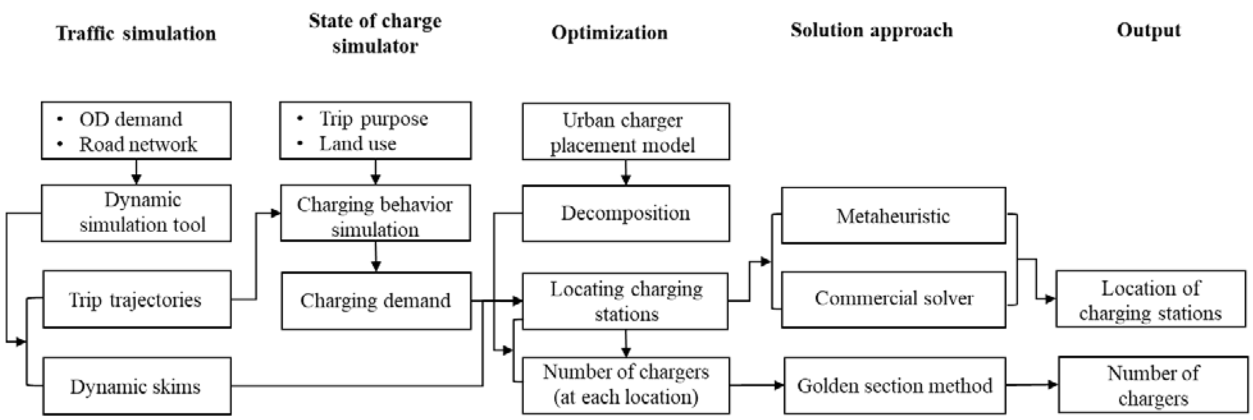

Figure 6-1 Components in the proposed research framework

6-2-1- Traffic and Charging Behavior Simulation

The statewide road network of Michigan consists of 37,125 links, 16,976 nodes, and 2,330 traffic analysis zones. The static demand matrix for different OD pairs is provided on the daily basis by Michigan Department of Transportation (MDOT). Hourly factors are multiplied into the static demands to convert them into a time-dependent OD demand matrix. Hourly factors are estimated based on the information of 122 loop detectors installed across Michigan highways. These loop detectors are mostly located inside the city boundaries, which are the focus of the current study. For example, Detroit, Lansing, and Marquette networks contain 46, 20, and 2 loop detectors on their links, respectively. To consider the directionality of traffic during different hours of a day, the closest loop detector counting the traffic of the same direction as the OD pair direction is found. Based on the traffic counts of the selected loop detector for the OD pair of interest, the hourly demand factors are then defined for the OD pair.

Travelers' route choice is a collective decision-making process that results in a certain traffic state and congestion level at the network level. Traffic simulation provides trip trajectories that can be used to predict the time-dependent charging demand. Each trajectory provides information regarding the chosen path, timestamps of travel along the path, origin zone, destination zone, departure time interval, vehicle type (randomly assigned based on the given market share), total travel time, and total travel distance. In this study, a mesoscopic traffic simulation tool, DYNASMART-P (Jayakrishnan et al., 1994), is incorporated to provide agent-based information applicable to the state-wide network of Michigan, and then the required trip trajectories for the cities of interest are extracted. The trajectories of all vehicles, along with the dynamic skims including travel times and distances for every OD-pair are reported as the outputs of this research component.

Intercity trips are often considered as stand-alone trips, in which EVs are highly likely to have fully charged batteries due to their preplanned nature. Urban trip, however, is part of a chain of trips, in which EVs might have any state of charge (depending on the availability of chargers and dwell time for recharging at the trip origin). Therefore, the charging incidence in one trip may depend on its sequential trip as well, i.e., the vehicle might recharge during a feasible trip to prevent charging in a subsequent infeasible one (Usman et al., 2020). However, the availability of trip chain information is still limited and transportation agencies still rely on zone-to-zone OD demand tables. Therefore, developing a framework to capture the EVs charging demand based on zone-to-zone OD demands is crucial. In this study, a simulation tool is developed to estimate the charging behavior of EVs based on their departure time, trip purpose, and land use characteristics of their origin and destination zones. The simulation tool estimates the initial state of charge at the origin, and the desired state of charge that the EV drivers prefer to have upon arrival at the destination.

The proposed simulation tool distinguishes the trips that begin from certain origins; e.g. it considers a higher initial state of charge for single-family residential areas than multi-family ones, as well as workplaces since some workplaces provide level 2 charging facilities for their employees. To this end, the simulation tool incorporates a survey conducted by MDOT in 2016

(Wilaby and Casas, 2016) that presents the time-dependent trip purpose distribution in the state of Michigan. Seven groups of activities are considered in the survey, including home-based work (HBWork), non-home-based work (NHBWork), home-based school (HBSchool), home-based shop (HBShop), home-based social (HBSocial), home-based other (HBOther), and non-home-based other (NHBOther). HBWork shows a trip directly from home to work or from work to home. NHBWork shows trips with one end at work while the other end is not home. HBSchool shows a trip from home to school or from school to home. HBShop shows a trip from home to shop or shop to home. HBSocial shows a trip from home to a recreational place or vice versa. HBOther shows a trip which has one end at home while the other end is not in the previous groups. NHBWork shows a trip that has an end at work, but its other end is not home. NHBOther shows the trips that has no end at home or work. Assuming users might have access to chargers at home or workplace, the charging behavior is affected by four groups of activities: HBWork, NHBWork, NHBOther, and the home-based non-work (HBNWork). Note that HBSchool, HBShop, HBSocial, and HBOther are combined in the latter group (HBNWork), since they all provide similar charging opportunity for users. Based on the time-dependent trip purpose distribution in Michigan, the probability of each trip belonging to one of these four groups at each time interval can be calculated.

The other input to the simulation tool is the land use characteristics at the origin and destination of trips. The simulation tool focuses on three land use characteristics due to their impacts on charging behavior, namely residential (R), commercial (C), and other (O) and their area ratio (the ratio of the land use characteristic area over the total TAZ area) in zone $\mathcal{k}$ is denoted by $\mathcal{S}_{\mathcal{k}}^1$, $\mathcal{S}_{\mathcal{k}}^2$, and $\mathcal{S}_{\mathcal{k}}^3$, respectively ($\mathcal{S}_{\mathcal{k}}^1 + \mathcal{S}_{\mathcal{k}}^2 + \mathcal{S}_{\mathcal{k}}^3 = 1$). Note that the last category, O, includes recreational, transport, and agricultural land uses. Thus, there are nine possible combinations of origin and destination zone types for each trip. The unadjusted static probability of origin (o)-destination (d) paired land use characteristics, p_{od}^{ij}, is defined as below:

$$p_{od}^{ij} = S_o^i . S_d^j \qquad (6.1)$$

Where i and j represents the land use characteristics. Assuming the purpose of each trip can be captured stochastically through its origin and destination land use, the nine possible combinations are crossed with the four sets of activities discussed earlier. Therefore, HBWork includes R-C and C-R, HBOther includes R-R, O-R, and R-O, NHBWork includes C-C, C-O, and O-C, and NHBOther includes O-O. Since the time-dependent distribution of each trip purpose (activity) is known, the origin-destination paired land use probabilities need to be adjusted according to their trip departure time intervals, using a temporal factor defined as follows:

$$T_{od,m}^t = \frac{A_m^t}{\sum_{ij} x_m^{ij} S_o^i . S_d^j}. \qquad (6.2)$$

Where $T_{od,m}^t$ is the temporal factor for activity m at time t for od and A_m^t is the time dependent share of activity. x_m^{ij} is a binary parameter indicating if land use combination ij is a subset of m. The probability associated with each OD pair land use can be adjusted for each time interval by multiplying the defined temporal factor. The probability associated with each OD pair land use can be adjusted for each time interval by multiplying the defined temporal factor. Then, the origin-destination pair land use (thus associated trip purpose group) can be probabilistically assigned for each EV trajectory. To clarify this point, assume a hypothetical example as follows: Assume that HBWork share for a trip departure time interval is 0.55, shares of R and C land uses at the trip origin zone are 0.7 and 0.2, and shares of R and C land uses at the trip destination zone are 0.3 and 0.5. Then, the unadjusted probability associated with R-C and C-R would be $0.7 \times 0.5 = 0.35$, and $0.2 \times 0.3 = 0.06$, respectively. The temporal factor would be $(0.55/\,(0.35 + 0.06))$ and the adjusted probability for the trip to have R-C as the origin-destination paired land use would be $0.35 \times (0.55/\ (0.35 + 0.06))$.

Once the trip purpose, origin-destination paired land use characteristics, and residential type (if applicable) are assigned for each EV trajectory, using associated truncated random normal distributions, the initial and desired state of charge would be determined for the trajectory. The difference between the desired state of charge and the initial state of charge plus the charge spent en-route to reach the destination is the total charge required for each EV trajectory. If this value is positive, the EV would need to recharge along its path to the destination and its charging demand should be provided to the optimization model as an input; otherwise, the EV trajectory would not need recharging and would not be considered in the optimization model.

6-2-3- The Mathematical Optimization Model

This section aims to present the developed modeling framework that minimizes the cost for providing the charging infrastructure, as well as the users' charging, queuing, and detour delays. The notations presented in Table 6-1is used in this chapter:

Table 6-1 Nomenclature

Sets	
$i \in I$	Set of zones
$\tau \in T$	Set of time intervals that vehicles get to charging stations
$\theta \in T$	Set of time intervals that vehicles leave charging stations
$j \in J$	Set of electric vehicles that need recharging
Decision variables	
x_i	Binary decision variable for availability of a charging station at zone i which equals 1 if there is a charging station at zone i and zero otherwise
z_i	Integer decision variable for number of chargers to be provided at the charging station in zone i
State Variables	
$Q_{ij}^{\tau\theta}$	Charging incidence matrix, which is one if EV j arrives to charging station in zone i at time interval τ and depart from it towards its destination at time interval θ
π_i^{τ}	Total charging and queuing delay experienced by EVs reaching to the charging station of zone i at time τ
TTd_j	Detour travel time required to reach the assigned charging station for EV j refueling

Table 6-1 (cont'd)

y_i^τ	Total number of EVs visiting the charging station at zone i at time τ
v_i^τ	Total energy demand of EVs visiting charging station in zone i at time τ
$\tilde{t}_i^\tau$	Average remaining charging time for users at zone i at time τ
μ_i^τ	Service rate of the charging station in zone i at time τ
λ_i^τ	Arrival rate to the charging station in zone i at time τ
q_i^τ	Queuing time for the last vehicle joining the queue of the charging station in zone i at time τ
χ_i^τ	Incidence matrix of observing queuing for the entire period of τ at the charging station of zone i
δ_i^τ	Portion of time that queue length is greater than zero in charging station of zone i during time interval τ
$\bar{W}_i^\tau$	Average waiting time in charging station of zone i for EVs arriving at time τ
R_{ij}	Refueling time for EV j recharging at the charging station of zone i
ρ_i^τ	Utilization rate of charging station zone i at time τ
P_{i0}^τ	Probability of not having any vehicles using any chargers at charging station of zone i at time τ
l_i^τ	Number of customers in the queue at charging station of zone i at time τ
Parameters	
C_i^s	Cost of building and maintaining a charging station at zone i, converted to the depreciation cost per day (the assumed analysis period in the model formulation)
C_i^p	Cost of one charger installation and maintenance at zone i, converted to the depreciation cost per day
γ	Value of time
M	An arbitrary big number
E_{ij}^θ	Required energy for EV j to reach the charging station at zone i and depart from it toward its destination at time interval θ
ζ_j	Desired state of charge for EV j at the destination
F	Maximum amount of charge that EVs can store
s_j	Initial state of charge for EV j
β	Battery performance
$d_{(a,b)}^c$	Distance between the centroid of zones a and b for vehicles departing at time c
s_{max}	State of charge that the charging speed drops beyond it
s_{min}	Minimum state of charge that drivers let their batteries drop to
$t_{(a,b)}^c$	Average travel time of vehicles departing zone a to destination zone b departing at time c
t_j'	Departure time for EV j from its origin
t_j	Departure time interval for EV j from its origin
$O(j)$	Origin zone of EV j
$D(j)$	Destination zone of EV j
T_0	Duration of each time interval
α	Charging efficiency of batteries
P	Charging power
ε	An arbitrary small number

Three main assumptions are made to formulate the problem of interest in this study:

i. Users select the path, and a charging station if needed, that minimizes their total travel time (including detour, queueing, and recharging time).

ii. Detour of EVs for recharging does not affect network link travel times, i.e. EVs are not congestion makers, but congestion takers (Sheppard et al., 2017).

iii. Travel distances in urban networks are within the full range of EVs. Therefore, EVs that need recharging only recharge one time per route.

The network considered in this study consists of a set of zones ($i \in I$). A set of time intervals ($\tau \in T$) at which EVs can arrive at charging stations. This discrete set allows the model to capture the visiting flow to stations over time. Another set of time intervals ($\theta \in T$) shows the time intervals at which vehicles depart the charging stations. This set enables the model to differentiate between the congestion levels in the arrival and departing time intervals. We assume T_0 is the duration of each time interval. Each electric vehicle ($j \in J$) has a trajectory that is known as a priori, with origin $O(j)$, destination $D(j)$, exact departure time t_j', departure time interval t_j, trip length $d_{(O(j),D(j))}^{t_j}$, travel time $t_{(O(j),D(j))}^{t_j}$, initial state of charge s_j, and desired state of charge at destination ζ_j. The solid line in Figure 6-2 shows the shortest direct path from origin to destination.

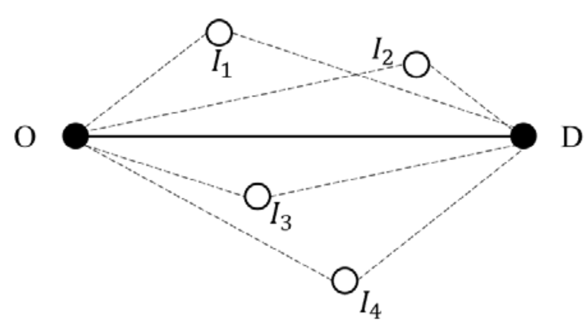

Figure 6-2 An electric vehicle's route choices

If a lack of energy is an issue, the EV must recharge at one of the available charging station options ($I_n, n = 1 \dots 4$). The EV will charge enough to reach its destination with its desired state of charge at destination (ζ_j). The energy required for EV j to reach to its destination, while visiting a charging station along its route and leaving it at time θ can be calculated as:

$$E_{ij}^{\theta} = \zeta_j F - s_j F + \frac{1}{\beta}[d_{(O(j),i)}^{t_j} + d_{(i,D(j))}^{\theta}], \qquad \forall\, j \in J, i \in I. \tag{6.3}$$

In the above formulation, F is the battery capacity and β is the battery performance in ($\frac{mile}{kWh}$), which converts the distance to energy. While EVs battery performances might differ based on the vehicle type and model, an average battery performance is considered for all EVs in the urban network. The required energy is calculated using the desired state of charge at destination, the initial state of charge and the distances from the origin zone to the charging zone, and from the charging zone to the destination zone. Having the charging demand, an agent-based model can be formulated as follows:

$$\min \sum_{i \in I}(C_i^s x_i + C_i^p z_i) + \gamma(\sum_{i \in I}\sum_{\tau \in T}\pi_i^{\tau} + \sum_{j \in J} TTd_j)\ . \tag{6.4}$$

The objective function (6.4) consists of two main terms. The first term calculates the total infrastructure investment cost including the costs associated with the availability of charging stations, x_i, and the integer variable z_i that represents the number of chargers at each location i. The next term provides the monetary value of the total delay of all EV travelers that need recharging, including those related to the total queueing and charging delays, π_i^{τ}, at all charging stations for different arrival time intervals, as well as those related to the total detour time, TTd_j, experienced by EV users to access a charging station. These delays are multiplied by the value of time factor, γ, to calculate their monetary values. Please note that just an average value of time is considered for simplicity. This assumption can be easily updated and the research framework can be adjusted to capture the variations of value of time due to different classes of users, activities, and trip purposes. The objective function (6.4) is subject to constraints (5-18) and (21-27).

$$x_i \in \{0,1\}, \text{and } z_i \in \{0,1,2,\dots\}, \qquad \forall\, i \in I \tag{6.5}$$

$$z_i \leq x_i M, \qquad \forall\, i \in I \tag{6.6}$$

$$\sum_{\tau \in T} \sum_{\theta \in T} Q_{ij}^{\tau\theta} E_{ij}^{\theta} \leq s_{max} F - s_j F + \frac{d_{(O(j),i)}^{t_j}}{\beta}, \qquad \forall\, j \in J, i \in I \tag{6.7}$$

$$\sum_{i \in I} \sum_{\tau \in T} \sum_{\theta \in T} Q_{ij}^{\tau\theta} d_{(O(j),i)}^{t_j} \leq \beta(s_j - s_{min}) F, \qquad \forall\, j \in J \tag{6.8}$$

$$\sum_{\tau \in T} \sum_{\theta \in T} Q_{ij}^{\tau\theta} \leq x_i, \qquad \forall\, i \in I, \forall j \in J \tag{6.9}$$

$$\sum_{\tau \in T} \sum_{\theta \in T} \sum_{i \in I} Q_{ij}^{\tau\theta} = 1, \qquad \forall j \in J \tag{6.10}$$

$$TTd_j = \sum_{\tau \in T} \sum_{\theta \in T} \sum_{i \in I} Q_{ij}^{\tau\theta} \left(t_{(O(j),i)}^{t_j} + t_{(i,D(j))}^{\theta} - t_{(O(j),D(j))}^{t_j} \right), \qquad \forall\; j \in J \tag{6.11}$$

$$t'_j + t_{(O(j),i)}^{t_j} - T_0 \tau \leq \left(1 - Q_{ij}^{\tau\theta}\right) M, \qquad \forall\, \tau \in T, \theta \in T, i \in I, j \in J \tag{6.12}$$

$$t'_j + t_{(O(j),i)}^{t_j} - T_0(\tau - 1) \geq \left(Q_{ij}^{\tau\theta} - 1\right) M, \qquad \forall\, \tau \in T, \theta \in T, i \in I, j \in J \tag{6.13}$$

Constraint (6.5) states the binary decision variable to determine if a zone is equipped with a charging station ($x = 1$) or not ($x = 0$). Constraint (4) is a logic constraint ensuring that there is no charger in zone i if the zone does not have a charging station. Constraint (6.7) accounts for the maximum charge intake. It limits the charging incidence matrix by not letting the required charge exceeds the available fast charging capacity in the battery at the time of arrival to the station. Constraint (6.8) ensures that each EV can only be charged in zones within its viable range. Constraint (6.9) ensures that charging can only happen when there is a charging station at zone i. Constraint (6.10) ensures that each EV charges exactly one time (note that the trajectories are filtered to the EVs requiring recharging). Constraint (6.11) calculates the detour travel time for each EV to get to the charging station. The detoured path travel time includes the average time-dependent travel time from the origin to the charging station and then to the destination. The original path travel time is the average travel time of vehicles with the origin of *O*(*j*) and destination of *D*(*j*). Constraints (6.12) and (6.13) are feasibility constraints that ensure vehicles can be allocated to a charging station upon arrival at the station.

$$y_i^\tau = \sum_{j\in J}\sum_{\theta\in T} Q_{ij}^{\tau\theta}, \qquad \forall\, \tau \in T, i \in I, \tag{6.14}$$

$$v_i^\tau = \sum_{j\in J}\sum_{\theta\in T} Q_{ij}^{\tau\theta} E_{ij}^{\theta}, \qquad \forall\, \tau \in T, i \in I\,. \tag{6.15}$$

Constraints (6.14) and (6.15) find the temporal charging demand for each station. Constraint (6.14) calculates the total number of EVs visiting the charging station of zone i at time τ, y_i^τ. Constraint (6.15) finds the required energy for all EVs visiting the charging station of zone i during time interval τ, v_i^τ. The arrival rate, λ_i^τ, which is the average number of EV users per charger visiting the station of zone i at time interval τ, is defined as:

$$\lambda_\mathrm{i}^\tau = \frac{y_i^\tau}{T_0 z_i}, \qquad \forall\, \tau \in T, i \in I\;\;. \tag{6.16}$$

Similarly, the average charging time for a group of EVs visiting the charging station of zone i is denoted by $\tilde{t}_i^\tau$ and defined as:

$$\tilde{t}_i^\tau = \alpha\,\frac{v_i^\tau}{P y_i^\tau}, \qquad \forall\, \tau \in T, i \in I. \tag{6.17}$$

Where P represents the charging power. The service rate, μ_i^τ, is defined as the number of EVs that can be charged in one hour and is calculated as follows:

$$\mu_i^\tau = \frac{1}{\tilde{t}_i^\tau}, \qquad \forall\, \tau \in T, i \in I. \tag{6.18}$$

The queueing delay at the end of time interval τ can be calculated as follows:

$$q_i^\tau = \frac{(\lambda_i^\tau - \mu_i^\tau)T_0}{\mu_i^\tau} + q_i^{\tau-1}, \qquad \forall\, \tau \in T, i \in I. \tag{6.19}$$

Here, q_i^τ shows the longest waiting time experienced in station i at time interval τ. When EVs reach charging stations, four scenarios might occur depending on the remaining queue from the previous time interval, the arrival rate, and the service rate. These scenarios are illustrated in Figure 6-3. If there is no remaining queue and the service rate is greater than the arrival rate, $(\mu_i^\tau > \lambda_i^\tau)$, EVs experience no queue (Figure 6-3(a)). If there is no remaining queue, $(q_i^{\tau-1} = 0)$, but the arrival rate is greater than the service rate, $(\mu_i^\tau < \lambda_i^\tau)$, EVs experience queuing during the entire time interval (Figure 6-3(b)). If there is a remaining queue form the previous time interval, $(q_i^{\tau-1} > 0)$, and the service rate cannot dissipate the queue by the end of the time interval, EVs experience queue during the entire time interval (Figure 6-3(c)). In this case, charging access cannot be provided to any incoming flow. Therefore, all vehicles will experience the queue and wait in line to get access to an available charger at a later time. In the last scenario (Figure 6-3(d)), there is a remaining queue from the previous time interval but it dissipates before the end of the current time interval. Therefore, after a time, δ_i^τ, the incoming EVs can be charged upon their arrival. The value of δ_i^τ can be calculated based on Figure 6-3(d) as follows.

$$y_i^* = \delta_i^\tau \lambda_i^\tau \tag{6.20}$$

$$y_i^* = (\delta_i^\tau - q_i^{\tau-1})\mu_i^\tau \tag{6.21}$$

$$\delta_i^\tau \lambda_i^\tau = (\delta_i^\tau - q_i^{\tau-1})\mu_i^\tau \rightarrow \delta_i^\tau \lambda_i^\tau - \delta_i^\tau \mu_i^\tau = -q_i^{\tau-1}\mu_i^\tau \tag{6.22}$$

$$\rightarrow \delta_i^\tau(\mu_i^\tau - \lambda_i^\tau) = \mu_i^\tau q_i^{\tau-1} \rightarrow \delta_i^\tau = \frac{\mu_i^\tau q_i^{\tau-1}}{\mu_i^\tau - \lambda_i^\tau} \tag{6.23}$$

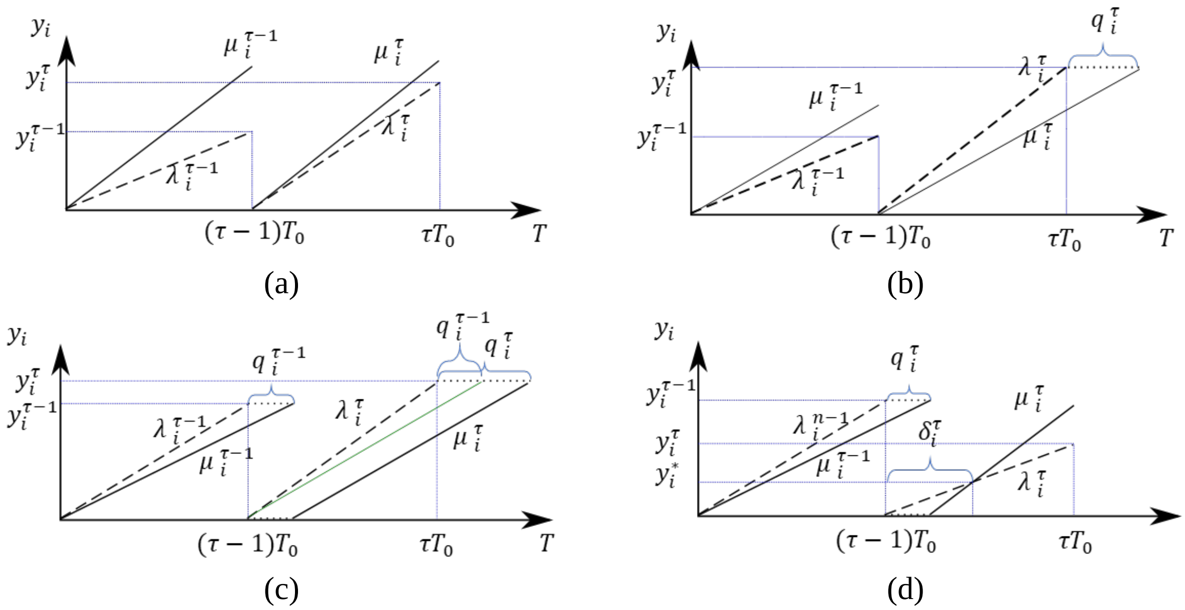

Figure 6-3 Four queuing scenarios upon the arrival of EVs at charging stations

The above-mentioned deterministic queuing formulations can be summarized as follows:

$$q_i^\tau \geq \frac{(\lambda_i^\tau - \mu_i^\tau)T_0}{\mu_i^\tau} + q_i^{\tau-1} \tag{6.24}$$

$$q_i^\tau \geq 0, \qquad \forall\, i \in I \tag{6.25}$$

$$q_i^0 = 0, \qquad \forall\, i \in I \tag{6.26}$$

$$\frac{(\lambda_i^\tau - \mu_i^\tau)T_0}{\mu_i^\tau} + q_i^{\tau-1} \leq \chi_i^\tau M, \qquad \forall\, \tau \in T, i \in I \tag{6.27}$$

$$\frac{(\lambda_i^\tau - \mu_i^\tau)T_0}{\mu_i^\tau} + q_i^{\tau-1} \geq (\chi_i^\tau - 1)M, \qquad \forall\, \tau \in T, i \in I \tag{6.28}$$

$$\delta_i^\tau = T_0\chi_i^\tau + \frac{\mu_i^\tau q_i^{\tau-1}}{\mu_i^\tau - \lambda_i^\tau}(1 - \chi_i^\tau), \qquad \forall\, \tau \in T, i \in I \tag{6.29}$$

$$\bar{W}_i^\tau = \frac{\delta_i^\tau}{T_0}\left(\frac{q_i^\tau + q_i^{\tau-1}}{2}\right), \qquad \forall\, \tau \in T, i \in I. \tag{6.30}$$

Constraints (6.24-26) calculate the queuing delay at the end of each time interval. Constraint (6.24) sets a lower bound for the queuing delay by summing the queuing delay of the previous time interval and the additional queuing delay for the current interval. Constraint (6.25) ensures that the estimated queue is always non-negative. Constraint (6.26) is a boundary condition assuming that the system starts with no initial queue. Constraints (6.27) and (6.28) determine the type of queuing for time interval τ using the fully queued incidence matrix χ_i^τ. If the left-hand side of equation (6.27) is positive, resulting in a positive queue at the end of the time interval, the fully queued incidence matrix would be equal to one ($\chi_i^\tau = 1$). In this case, constraint (6.28) would not be binding. If the left-hand side of the constraint (6.28) becomes negative, the fully queued incidence matrix would be set to zero ($\chi_i^\tau = 0$). In this case, constraint (6.27) would not be binding. Constraint (6.29) calculates the portion of time interval with a queue. If the fully queued incidence matrix is equal to one, the second term of this constraint is zero and $\delta_i^\tau = T_0$. If the queue dissipates within the time interval, the first term will be zero and the second term calculates the δ_i^τ. Constraint (6.30) calculates the average queuing time for EVs visiting the charging station in zone i at time interval τ.

Finally, the following constraints provides the relationships among various time variables.

$$R_{ij}^\theta = \alpha \frac{E_{ij}^\theta}{P}, \qquad \forall\, i \in I, j \in J \tag{6.31}$$

$$\pi_i^\tau = y_i^\tau \bar{W}_i^\tau + \sum_{\theta \in T} \sum_{j \in J} Q_{ij}^{\tau\theta} R_{ij}^\theta, \qquad \forall\, \tau \in T, i \in I \tag{6.32}$$

$$t_j' + t_{(o(j),i)}^{t_j} + R_{ij}^\theta + \bar{W}_i^\tau - T_0\theta \le \left(1 - Q_{ij}^{\tau\theta}\right)M, \qquad \forall\, \tau \in T, \theta \in T, i \in I, j \in J \tag{6.33}$$

$$t_j' + t_{(o(j),i)}^{t_j} + R_{ij}^\theta + \bar{W}_i^\tau - T_0(\theta - 1) \ge \left(Q_{ij}^{\tau\theta} - 1\right)M, \qquad \forall\, \tau \in T, \theta \in T, i \in I, j \in J \tag{6.34}$$

Constraint (6.31) calculates the required time to recharge each EV at each charging station considering the loss of electricity factor and the charging power. Constraint (6.32) calculates the total delay in each charging station by summing up the total queuing delay for all EVs visiting the charging station at that time interval and the total refueling time of EVs for all departure time intervals from that station. Constraints (6.33) and (6.34) determine the departure time interval in which a vehicle would be able to leave the station. They ensure that the summation of the EV departure time, average travel time from origin to the charging station, the refueling time and waiting time in the queue matches the departure time interval from the station.

Note in this mathematical modeling, only deterministic queuing is considered. In the next section the presented mathematical model is decomposed to two-subproblems. In the second subproblem the proposed solution approach accounts for both deterministic and stochastic queueing delays.

6-2-3- Solution Methodology

The proposed Mixed-Integer Non-Linear Programming (MINLP) model in the previous section has multiple nonlinear constraints. The impact of queuing on the assignment of charging demands to charging stations, makes the problem highly nonlinear and challenging. In the literature, queuing time is usually considered only to determine the number of required chargers via a bi-level formulation or as a separate problem (Jung et al., 2014; Wang et al., 2019; Xie et al., 2018). Therefore, the proposed problem is decomposed into two subproblems assuming the queuing does not affect the assignment of charging demands to charging stations. Since the decomposition approach is a heuristic approach, an implicit enumeration approach is compared with this approach for a small case study in the numerical experiments section to show its efficiency and accuracy. Note that the formulated problem is highly non-linear with mixed-integer variables. Thus, there is no exact solution methodology, and common commercial solvers cannot be implemented even for small case studies. Even in the decomposed approach, the first subproblem requires a heuristic approach for large scale applications.

6-2-3-1- Optimal Locating of Charging Stations

In the first subproblem, a minimization problem is solved that considers the monetary value of detour and refueling times and the cost of charging stations, ignoring the charging queue. In this study, the number of chargers in each station is not limited, thus enough chargers would be provided at each station to provide a consistent level of service at each location, proportional to the charging demand. The mathematical model for the first subproblem, including the objective function and constraints, is as follows:

$$\min \sum_{i \in I} (C_i^s x_i) + \gamma \Big(\sum_{\tau \in T} \sum_{\theta \in T} \sum_{i \in I} \sum_{j \in J} Q_{ij}^{\tau\theta} R_{ij}^{\theta} + \sum_{j \in J} TTd_j \Big) \qquad (6.35)$$

Subject to:

Constraints (6.5), (6.7-13), (6.31), and

$$t_j' + t_{(O(j),i)}^{t_j} + R_{ij}^{\theta} - T_0\theta \leq \left(1 - Q_{ij}^{\tau\theta}\right)M, \qquad \forall\, \tau \in T, \theta \in T, i \in I, j \in J \qquad (6.36)$$

$$t_j' + t_{(O(j),i)}^{t_j} + R_{ij}^{\theta} - T_0(\theta + 1) \geq \left(Q_{ij}^{\tau\theta} - 1\right)M, \qquad \forall\, \tau \in T, \theta \in T, i \in I, j \in J \qquad (6.37)$$

In this subproblem, the departure time confines the charging incidence matrix through constraints (6.36-37). In this model, the queuing delay in charging stations is ignored, unlike the primary optimization model. Therefore, per assumption, vehicles can be charged once they get to charging stations.

The objective function (6.35) along with its constraints form a mixed-integer linear model. Commercial solvers such as CPLEX and Gurobi, solve moderate sized instances effectively. However, as the size of the problem grows, the computational requirements increase exponentially. Therefore, a metaheuristic approach is also provided for large-scale case studies based on

Simulated Annealing (SA) approach. For more details please refer to (Ghamami et al., 2020a, 2016b; Kavianipour et al., 2019; Zockaie et al., 2016) for similar applications of the SA algorithm. To improve the efficiency of the algorithm, the following strategies are shown to be effective in generating neighboring solutions. More details of the algorithm can be found in Figure 6-4.

1. To add a station randomly to a traffic analysis zone, each zone is weighted based on the number of crossing EV trajectories. Accordingly, the zones visited by a higher number of crossing trajectories, have a higher chance of being added to the current solution.
2. To remove a station randomly from traffic analysis zones equipped with one in the current solution, the zones are weighted based on the inverse of their number of incoming EV flows. Accordingly, stations with a lower incoming flow, have a higher chance to be removed from the current solution.

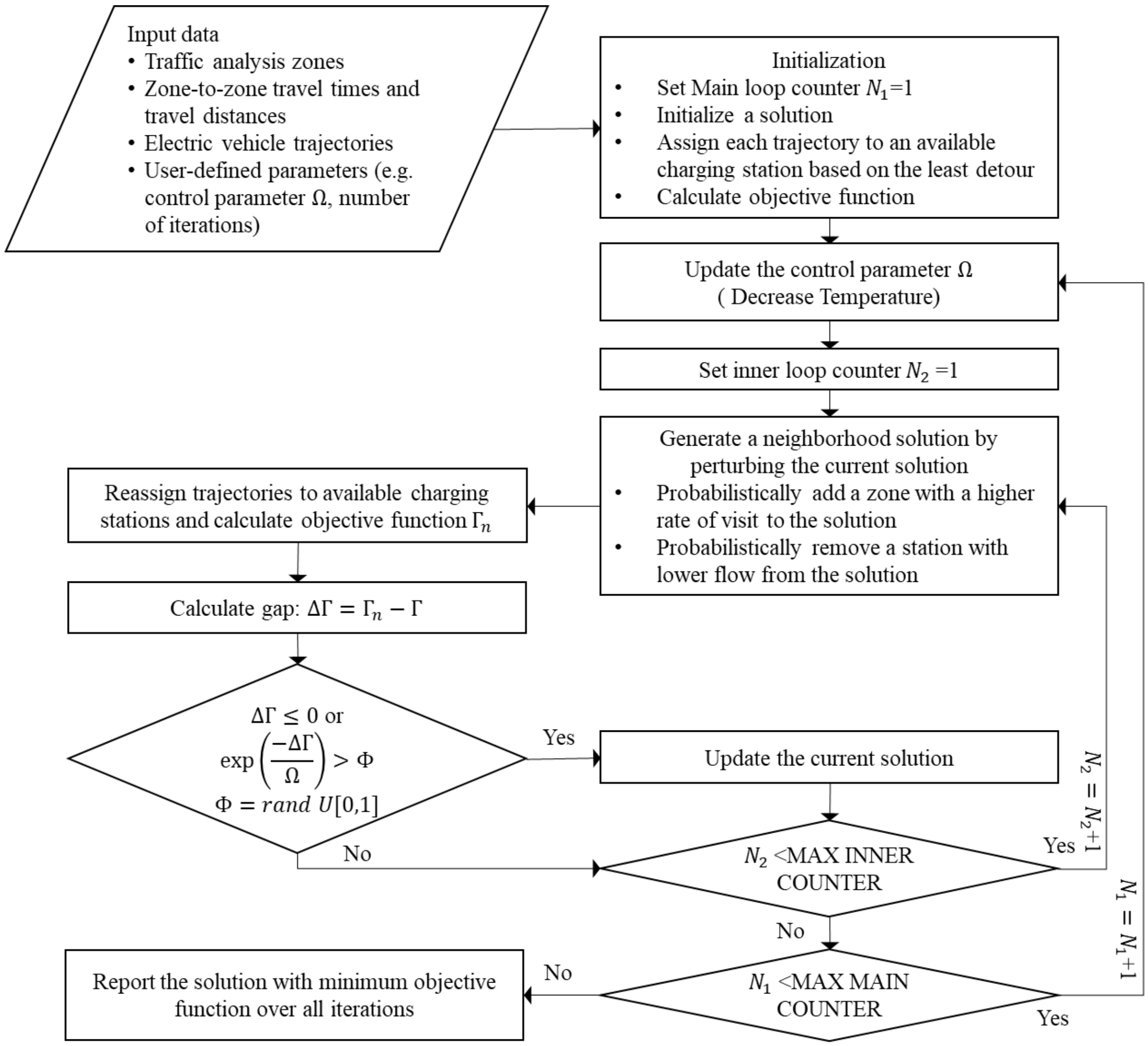

Figure 6-4 The SA-based solution algorithm to find the optimal location of charging stations

6-2-3-2- Optimal Number of Chargers at Each Charging Station

To find the number of chargers in each charging station, the second subproblem is formulated as follows for each selected station in the first subproblem such as i:

$$\min C_i^p z_i + \gamma \sum_{\tau \in T} y_i^\tau \bar{W}_i^\tau \qquad (6.38)$$

Subject to

(6.14-18) and (6.24-30)

The objective function (6.38) includes the total installation and maintenance costs of chargers, and the monetary value of total travelers' queuing delay at each station, which depends on the number of chargers allocated to the station. The objective function needs to be minimized for each charging station selected in the first subproblem, to find the optimum number of chargers, as the main decision variable. This problem is a MINLP.

In the first subproblem, EV trajectories requiring recharging are assigned to each charging station, forming a temporal arrival distribution for each charging station. Based on the availability of chargers at the station, they either charge upon their arrival or wait in the queue for an available charger. This subproblem makes a trade-off between providing more chargers or letting users wait in the queue for an available charger.

Assuming a uniform arrival and service rates for each time interval, the queuing behavior can be modeled based on a deterministic queue modeling approach (Zukerman, 2013), as presented in (6.24-30). The objective function (6.38) along with its constraints forms a mixed-integer problem with nonlinear constraints and is convex as shown below.

First, we examine the objective function:

$$\Gamma = C_i^p z_i + \gamma \sum_{\tau \in T} y_i^\tau \bar{W}_i^\tau = C_i^p z_i + \sum_{\tau \in T} y_i^\tau \frac{\delta_i^\tau}{T_0}\left(\frac{q_i^\tau + q_i^{\tau-1}}{2}\right) \tag{6-39}$$

In the above formulation, C^p and γ are parameters and y_i^τ is known as it is the output of the location subproblem. Based on the (6.29), δ_i^τ is a function of χ_i^τ and z_i. q_i^τ is also a function of χ_i^τ, z_i, and $q_i^{\tau-1}$.

Inductive reasoning can be used to show the convexity of q_i^τ as follows:

Step 1: The convexity of q_i^τ should be checked for $\tau = 1$.

$$q_i^\tau = \frac{(\lambda_i^\tau - \mu_i^\tau)T_0}{\mu_i^\tau}\chi_i^\tau \tag{6.40}$$

$$\text{If } \chi_i^1 = 0 \rightarrow q_i^1 = 0 \rightarrow Convex \tag{6.41}$$

$$\text{If } \chi_i^1 = 1 \rightarrow q_i^\tau = \frac{\left(\frac{y_i^\tau}{T_0 z_i} - \mu_i^\tau\right)T_0}{\mu_i^\tau} \rightarrow \frac{d(q_i^\tau)}{dz} = -\frac{y_i^\tau}{\mu_i^\tau {z_i}^2} \rightarrow \frac{d^2(q_i^\tau)}{dz^2} = 2\frac{y_i^\tau}{\mu_i^\tau {z_i}^3} = 2\frac{y_i^1}{\mu_i^1 {z_i}^3} \tag{6.42}$$

(6.41) and (6.42) are both convex, which shows the convexity of the q_i^τ for $\tau = 1$.

Step 2: It is assumed that q_i^τ is convex for $\tau = n - 1 \longrightarrow q_i^{n-1}$ is convex.

Step 3: The convexity of q_i^τ should be checked for $\tau = n$

$$q_i^n = \chi_i^n(\frac{T_0}{\mu_i^n}\left(\frac{y_i^n}{T_0 z_i} - \mu_i^n\right) + q_i^{n-1}) \tag{6.43}$$

$$\text{If } \chi_i^n = 0 \rightarrow q_i^n = 0 \tag{6.44}$$

$$\text{If } \chi_i^n = 1 \rightarrow q_i^n = \frac{T_0}{\mu_i^n}\left(\frac{y_i^n}{T_0 z_i} - \mu_i^n\right) + q_i^{n-1} \tag{6.45}$$

(6.44) is convex. (6.45) consists two terms: the first is convex similar to (6.42) and the second term is convex per assumption in step 2. Therefore, the convexity of q_i^τ can be concluded based on inductive reasoning.

The next step is to prove the convexity of the objective function. The objective function is a function of z_i and $\chi_i^n, n = 1, \dots \tau$. The first part of the objective function is convex. Therefore, the second part is evaluated for convexity as follows:

$$\Gamma' = \gamma \sum_{\tau \in T} y_i^\tau \overline{W}_i^\tau \tag{6.46}$$

The convexity of $y_i^\tau \overline{W}_i^\tau$ is similar to the convexity of Γ'(Boyd and Vandenberghe, 2009).

$$\Gamma'' = y_i^\tau \overline{W}_i^\tau = y_i^\tau \frac{\delta_i^\tau}{T_0}(\frac{q_i^\tau + q_i^{\tau-1}}{2}) = \frac{y_i^\tau}{2T_0}\delta_i^\tau(q_i^\tau + q_i^{\tau-1}) \tag{6.47}$$

The convexity of $\delta_i^\tau(q_i^\tau + q_i^{\tau-1})$ is similar to the convexity of Γ"(Boyd and Vandenberghe, 2009).

$$\delta_i^\tau = T_0\chi_i^\tau + \frac{\mu_i^\tau q_i^{\tau-1}}{\mu_i^\tau - \lambda_i^\tau}(1-\chi_i^\tau) \tag{6.48}$$

$$q_i^\tau = \chi_i^\tau(\frac{T_0}{\mu_i^n}(\lambda_i^\tau - \mu_i^n) + q_i^{\tau-1}) \tag{6.49}$$

$$\delta_i^\tau(q_i^\tau + q_i^{\tau-1}) = \left[T_0\chi_i^\tau + \frac{\mu_i^\tau q_i^{\tau-1}}{\mu_i^\tau - \lambda_i^\tau}(1-\chi_i^\tau)\right]\left[\chi_i^\tau(\frac{T_0}{\mu_i^n}(\lambda_i^\tau - \mu_i^n) + q_i^{\tau-1}) + q_i^{\tau-1}\right] \tag{6.50}$$

χ_i^τ is a binary variable indicating if there is a queue in the time interval ($\chi_i^\tau = 1$) or not ($\chi_i^\tau = 0$). Therefore, the convexity of the function is evaluated for different values of χ_i^τ.

Case 1: $\chi_i^\tau = 1$

$$\Gamma^3 = \delta_i^\tau(q_i^\tau + q_i^{\tau-1}) = T_0\left(\frac{T_0}{\mu_i^\tau}(\lambda_i^\tau - \mu_i^\tau) + 2q_i^{\tau-1}\right) = \frac{{T_0}^2}{\mu_i^\tau}(\lambda_i^\tau - \mu_i^\tau) + 2T_0 q_i^{\tau-1} \tag{6.51}$$

(6.51) is convex as it is the summation of two convex terms, as proved in the above section, and this indicates the convexity of the objective function when $\chi_i^\tau = 1$.

Case 2: $\chi_i^\tau = 0$

$$\Gamma^4 = \delta_i^\tau(q_i^\tau + q_i^{\tau-1}) = \frac{\mu_i^\tau q_i^{\tau-1}}{\mu_i^\tau - \lambda_i^\tau} q_i^{\tau-1} = \frac{\mu_i^\tau (q_i^{\tau-1})^2}{\mu_i^\tau - \lambda_i^\tau} \tag{6.52}$$

μ_i^τ does not affect the convexity of (6.52). Therefore, considering $\lambda_{\mathrm{i}}^\tau = \frac{y_i^\tau}{T_0 z_i}$, the convexity of this phrase can be evaluated as follows:

$$\Gamma^5 = \frac{(q_i^{\tau-1})^2}{\mu_i^\tau - \lambda_i^\tau} \tag{6.53}$$

$$\frac{d(\Gamma^5)}{dz} = \frac{2q_i^{\tau-1}\frac{dq_i^{\tau-1}}{dz}\left(\mu_i^\tau - \frac{y_i^\tau}{T_0 z_i}\right) - \frac{y_i^\tau}{T_0 {z_i}^2}(q_i^{\tau-1})^2}{(\mu_i^\tau - \frac{y_i^\tau}{T_0 z_i})^2} \tag{6.54}$$

$$\frac{d(\Gamma^5)}{dz} = \frac{2q_i^{\tau-1}\frac{dq_i^{\tau-1}}{dz}}{\mu_i^\tau - \frac{y_i^\tau}{T_0 z_i}} - \frac{\frac{y_i^\tau}{T_0 {z_i}^2}(q_i^{\tau-1})^2}{(\mu_i^\tau - \frac{y_i^\tau}{T_0 z_i})^2} \tag{6.55}$$

$$\frac{d^2(\Gamma^5)}{dz^2} = \frac{\left[2\left(\frac{dq_i^{\tau-1}}{dz}\right)^2 + 2q_i^{\tau-1}\frac{d^2 q_i^{\tau-1}}{dz^2}\right]\left(\mu_i^\tau - \frac{y_i^\tau}{T_0 z_i}\right) - \frac{y_i^\tau}{T_0 {z_i}^2} 2q_i^{\tau-1}\frac{dq_i^{\tau-1}}{dz}}{(\mu_i^\tau - \frac{y_i^\tau}{T_0 z_i})^2}$$

$$- \frac{\left[-\frac{2y_i^\tau}{T_0 {z_i}^3}(q_i^{\tau-1})^2 + 2\frac{y_i^\tau}{T_0 {z_i}^2} q_i^{\tau-1}\frac{dq_i^{\tau-1}}{dz}\right]\left(\mu_i^\tau - \frac{y_i^\tau}{T_0 z_i}\right)^2}{\left(\mu_i^\tau - \frac{y_i^\tau}{T_0 z_i}\right)^4} \tag{6.56}$$

$$+ \frac{2\frac{y_i^\tau}{T_0 {z_i}^2}\left(\mu_i^\tau - \frac{y_i^\tau}{T_0 z_i}\right)\frac{y_i^\tau}{T_0 {z_i}^2}(q_i^{\tau-1})^2}{(\mu_i^\tau - \frac{y_i^\tau}{T_0 z_i})^4}$$

As $\chi_i^\tau = 0 \longrightarrow \mu_i^\tau > \lambda_i^\tau \longrightarrow \mu_i^\tau > \frac{y_i^\tau}{T_0 z_i} \longrightarrow \mu_i^\tau - \frac{y_i^\tau}{T_0 z_i} > 0$ Further, as proved in (6.45), the first derivative of q_i^τ is negative. Therefore, the second derivative is always positive since all terms in (6.56) are positive. As the objective function is convex for both of the cases, we can conclude that it is always convex.

Since the objective function is strictly convex and the constraints are convex, the proposed problem can be solved using numerical solution approaches such as the Golden-section search technique. This technique is designed to find the extreme value of a function in a pre-defined interval as its domain (Kiefer, 1953). The deterministic queuing assumption provides the minimum number of chargers required to support the charging demand.

The deterministic queueing model assumes zero queueing delay when the service rate is greater than the arrival rate. Thus, if the model provides enough chargers to avoid the deterministic queue, then the service rate would be greater than the arrival rate. Assuming a Poisson distribution for the arrival process and an exponential distribution for the service rates, a stochastic queuing model can be implemented (Zukerman, 2013) for the cases that the average service rate exceeds the average arrival rate. It should be noted that if the arrival rate is greater than the service rate, only the deterministic approach is applicable. If a steady-state condition is assumed in each time interval, the M/M/k (M stands for Markovian, which is a Poisson distribution for arrival rates and an exponential distribution for service time distribution and k represents multiple number of chargers) queuing model can be used to model the stochastic queuing delay. The formulation is as follows:

$$\rho_i^\tau = \frac{\lambda_i^\tau}{z_i \mu_i^\tau}, \qquad \forall\, \tau \in T, i \in I \tag{6.57}$$

$$P_{i0}^\tau = \left(\sum_{m=0}^{z_i - 1} \frac{(z_i \rho_i^\tau)^m}{m!} + \frac{(z_i \rho_i^\tau)^{z_i}}{z_i!\,(1-\rho_i^\tau)}\right)^{-1}, \qquad \forall\, \tau \in T, i \in I \tag{6.58}$$

$$l_i^\tau = \frac{P_{i0}^\tau (\frac{\lambda_i^\tau}{\mu_i^\tau})^{z_i} \rho_i^\tau}{z_i!\,(1-\rho_i^\tau)^2}, \qquad \forall\, \tau \in T, i \in I \tag{6.59}$$

$$\bar{W}_i^\tau = \frac{l_i^\tau}{\lambda_i^\tau}, \qquad \forall\, \tau \in T, i \in I \tag{6.60}$$

In these formulations, equation (6.57) finds the utilization, ρ_i^τ, at each charging station in each time interval. Equation (6.58) finds the probability that there is no queue in the system. Equation (6.59) finds the number of customers in the queue. Finally, equation (6-60) calculates the average waiting time in the queue. These equations are based on queuing theory for M/M/k queues. For more information on queuing theory, please refer to (Zukerman, 2013). The average queue size of the M/M/k system is convex respect to the traffic flow (Grassmann, 1983). Therefore, the optimum value of the objective function can be calculated using the Golden-section search technique similar to the deterministic approach. The two-stage framework for finding the optimal number of chargers considering both deterministic and stochastic approaches is presented in Figure 6-5. Note that the deterministic model provides a lower bound for the stochastic model, without which the Golden-section method cannot be applied to the stochastic model. Furthermore, in case of a non-zero deterministic queue in the first stage, the stochastic queueing model would be irrelevant.

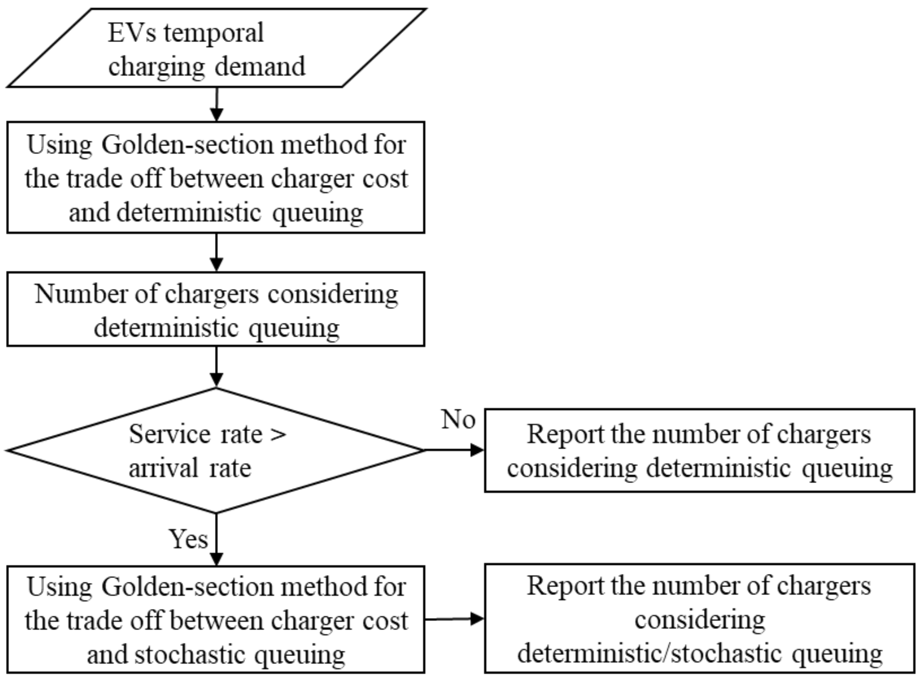

Figure 6-5 Two-stage framework for finding the optimal number of chargers considering deterministic and stochastic queuing delays

6-3- Numerical Experiments

This section first introduces the case studies and their network specifications. Then, it provides the input data used in the charging behavior simulator. Next, it briefly discusses the considered parameter values in the optimization model. It is worth noting that these values are derived based on the provided feedback in stakeholder meetings in Michigan and can be calibrated for each region. based on the input from various stakeholders' meeting as part of the EV charger placement project in Michigan. Finally, some scenarios are introduced to be accompanied by sensitivity analyses to provide applied insights for the EV fast-charging infrastructure deployment in urban areas.

6-3-1- Case Studies

The road network and OD travel demand information in the State of Michigan are provided by MDOT. The regional road networks for the cities of Marquette, Lansing and Detroit are extracted, as shown in Figure 6-6, beyond the actual city borders. The city of Marquette is considered as a small sized network which has 62 nodes, 21 zones, 336 lane-miles in length. The city of Lansing is considered as a medium-sized network with 896 nodes, 91 zones, 2,030 lane-miles in length. The city of Detroit is the large-scale network used in this study, which has 5,461 nodes, 301 zones, and 8,776 lane-miles in length.

The land use information is provided by MDOT for each traffic analysis zone in the state-wide network. The land acquisition costs are provided for each traffic analysis zone by city municipalities. Utility provision costs are provided through utility companies serving these three cities (DTE Energy and Consumers Energy). Two levels of powers are considered for charging stations: 1) 50 kW with a station cost of $48,437 and a charger cost of $33,750, 2) 150 kW with a station cost of $80,125 and a charger cost of $76,250. Two battery sizes of 70 kWh and 100 kWh are considered for EVs. The battery performance is assumed to be 3.5 mi/kWh during the summer, with a 30% reduction for winter weather conditions (the latter is considered as the critical case for Michigan). An EV adoption rate of 6% is considered, which means that 6% of total trajectories are by EVs, based on the projected 2030 EV market share in Michigan by MISO Energy (MISO Energy, 2018). A value of time of $18/hour is used to monetarize traveler delay. The combination of the two battery capacities and charger powers leads to four scenarios, which are investigated for each city in the next section.

Figure 6-6 (a) Michigan state-wide network (b) City of Marquette case study network (c) City of Lansing case study network (d) City of Detroit case study network

In this study, the initial state of charge (as a fraction of the EV battery capacity) before noon is assumed to follow a normal distribution with the average and standard deviation values presented in Table 6-2. It is worth noting that these values are based on the current circumstances in Michigan. For the trips departing between noon and 5:00 PM, the mean values are assumed to be reduced by 0.1. For trajectories departing after the 5:00 PM, another 0.1 reduction is implemented. Moreover, a normal distribution with a mean of 0.15 and a standard deviation of 0.1 is considered for the desired state of charge for EVs at their destination.

Table 6-2 Parameters of normal distributions for the initial state of charge

	Initial state of charge (% battery)			
Battery (kWh)	70		100	
	Mean	SD	Mean	SD
Home- single family	0.75	0.05	0.7	0.05
Home- multi family	0.5	0.2	0.6	0.2
Work	0.6	0.2	0.65	0.3
Other	0.55	0.3	0.6	0.3

6-3-2- Results

In this section, we first explore various aspects of the solution methodology to demonstrate the performance of the proposed approach (i.e. validation of the decomposition approach for the main problem, comparison of the metaheuristic approach with the commercial solver for the first subproblem, and comparison of the deterministic and stochastic queuing models in the second subproblem). Then, the results are provided for the four defined scenarios in two large case studies.

6-3-2-1- Enumeration versus Decomposition

To test the performance of the decomposition approach, i.e., its solution quality and convergence speed, we compare it with a simple enumeration approach which exhaust all facility combinations. Since such a simple approach cannot be applied even to small-sized networks, two subsets of zones are selected as candidate locations for the charging stations in the smallest case study, Marquette network. We test two applications, respectively with 5 and 7 randomly selected zones (out of 21 zones) to be candidates for charging stations. Based on the charging behavior simulation and for a scenario with 70 kW battery, 197 EV trajectories need recharging. The maximum number of required chargers at each station should not be bounded in theory, but failure to set a cap on the maximum number of chargers prevents exhausting all combinations. Therefore, a subset of scenarios needs be considered. The solution from the decomposition approach uses a maximum of three chargers per stations. Hence, we set the maximum number of chargers per station to be four in our enumerations, which makes the total number of possible charge installation combinations equal to 5^5 and 5^7 for the two applications. If the enumeration technique has the option to build 4 chargers and selects to build less at all stations, the resulted solution by the enumeration technique is the optimal solution. In another word, it suggests that the cap on the maximum number of chargers has not affected the optimum solution in the enumeration process, otherwise it would have required at least 4 chargers. For each of these combinations, the assignment of charging demand to available charging stations is solved using Knitro, and then the objective function is evaluated. The combination with the minimum objective function value is compared with that from the decomposition approach. The results are presented in Table 6-3 for both applications.

Table 6-3 Comparing the enumeration and decomposition technique for a small network

Scenario	5 Candidate Stations			7 Candidate Stations		
Technique	Enumeration	Decomposition	Percent Difference	Enumeration	Decomposition	Percent Difference
Number of Stations	4	4	0.0%	4	4	0.0%
Number of Chargers	8	9	12.5%	9	9	0.0%
Average Charging delay (min)	15.73	15.82	0.6%	15.31	15.31	0.0%
Average detour delay (min)	5.84	5.75	-1.5%	4.51	4.51	0.0%
Station Cost (m$)	0.56	0.56	0.0%	0.56	0.56	0.0%
Chargers Cost (m$)	0.29	0.32	12.5%	0.32	0.32	0.0%
Infrastructure Cost (m$)	0.84	0.88	4.2%	0.88	0.88	0.0%
Total objective function value ($/day)	1,511	1,520	0.6%	1,417	1,417	0.0%
Solution time (s)	12,600	4	-100.0%	241,200	4	-100.0%

The results show that the decomposition technique provides a solution that is very close to, or identical to, the optimal solution (within zero or one percent difference). However, the solution time is much faster. Since the number of facility combinations grows exponentially with the network size (e.g., number of candidate zones), it is impossible to solve the full-scale problem even for small case studies via the enumeration approach. In contrast, the decomposition approach can provide a near-optimum solution instantaneously for this small case study.

6-3-2-2- Robustness

This section studies the impact of seed numbers on the optimum solution. Seed numbers determine the random number generation, which can affect the simulated users' charging behavior since the initial/desired SOC are determined based on random numbers. Thus, the impact of 10 different seed numbers, i.e., scenarios, are studied in the medium sized network, city of Lansing, as presented in Figure 6-7.

The objective function, number of stations, and number of chargers are compared in these scenarios. Figure 6-7(a) shows that the objective function values variation is almost 3 percent in these scenarios, which shows the availability of almost identical solutions with different representations. Figure 6-7(b) shows that most of the scenarios have 16 charging stations, while the highest number of charging station is 18. Lastly, Figure 6-7(c) shows the cumulative number of chargers for each scenario. Based on this figure, the scenarios have similar locations for charging. Further, the number of chargers is almost the same in each charging station which shows the similarity of the results. While the differences in scenarios are small, the solution robustness can be improved by considering multiple random seeds for random number generation and applying the proposed framework for each scenario. Since the focus of the study is to develop the framework, the numerical experiments are performed for one seed number.

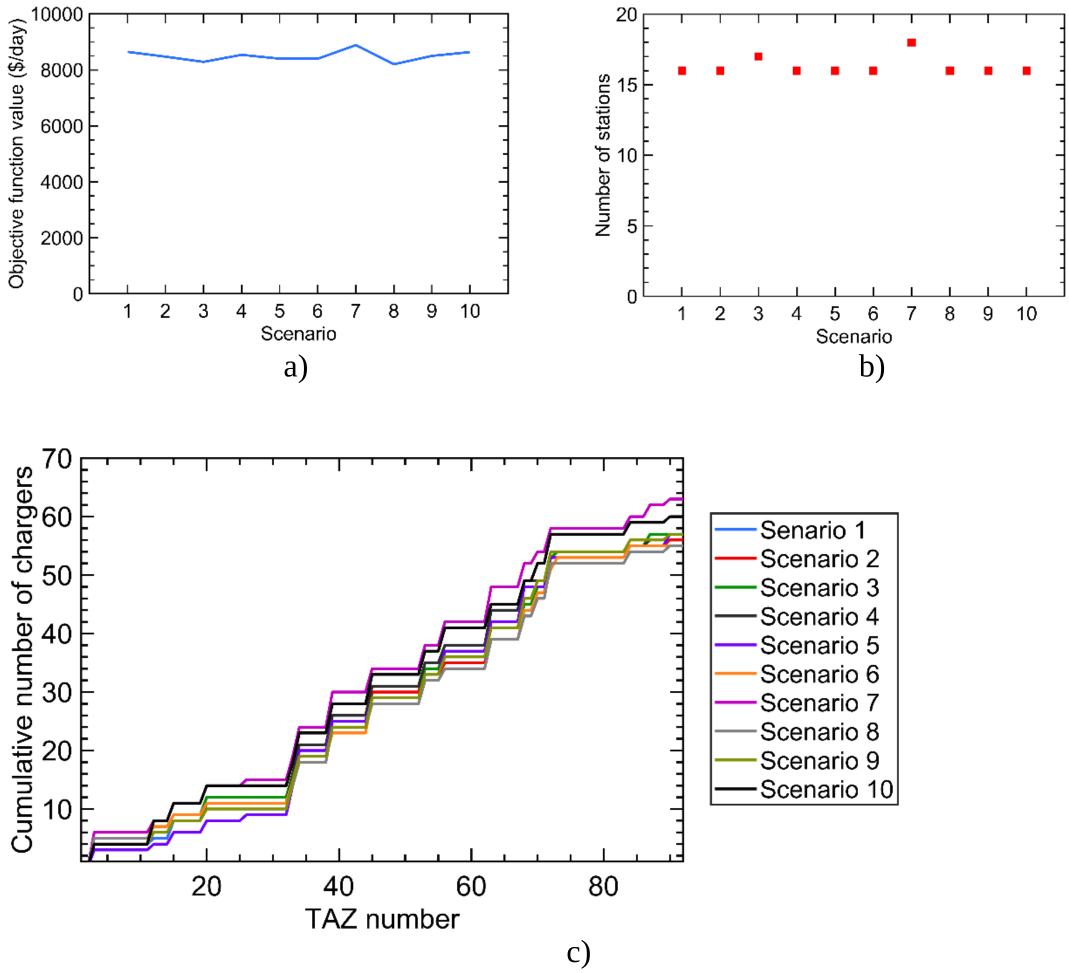

Figure 6-7 The impact of seed number on the (a) optimum objective function value (b) number of stations (c) cumulative number of chargers for city of Lansing

6-3-2-3- CPLEX versus Simulated Annealing

We further test the SA approach for the first subproblem (i.e., locating charging stations). Figure 6-8 shows the convergence of the metaheuristic approach for the city of Lansing toward the optimal value provided by CPLEX. It shows that the objective function of the metaheuristic approach can get very close to the optimal solution.

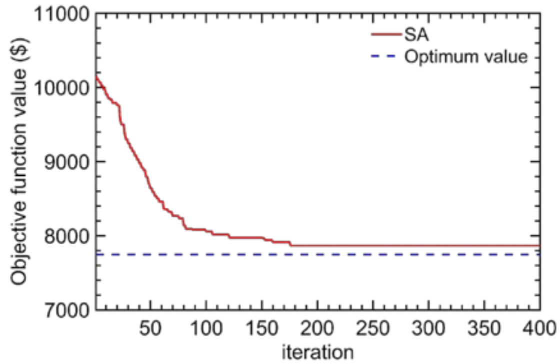

Figure 6-8 The convergence of the metaheuristic method toward the optimal objective function provided by CPLEX for the city of Lansing

The solution quality of the metaheuristic approach is evaluated for the city of Lansing and Detroit in Table 6-4.

Table 6-4 Comparing CPLEX and SA performance in solving station location subproblem

City	Lansing			Detroit		
Technique	CPLEX	SA	Percent difference	CPLEX	SA	Percent difference
Battery size (kWh)	70	70	-	70	70	-
Charging station (kW)	50	50	-	50	50	-
Number of zones	92	92	-	301	301	-
EV Trajectories	28,574	28,574	-	212,299	212,299	-
Number of Stations	16	16	0.0%	62	62	0.0%
Number of Chargers	87	92	5.7%	641	639	-0.3%
Average delay (min)	10.75	10.93	1.7%	11.19	11.37	1.6%
Station Cost (m$)	2.52	2.66	5.3%	15.37	15.37	0.0%
Chargers Cost (m$)	3.48	3.30	-5.2%	23.22	23.15	-0.3%
Infrastructure Cost (m$)	6.00	5.95	-0.8%	38.59	38.52	-0.2%
Charging station location subproblem objective function value ($/day)	7,747	7,860	1.5%	67,543	69,193	2.4%
Total objective function value ($/day)	8,803	8,858	0.6%	74,507	76,118	2.2%
Required memory (GB)	5.20	0.82	-84.2%	107	4.2	-96.1%
Solution time (s)	323	238	-26.3%	16,717	8311	-50.3%

Although the optimum objective function value for the first subproblem increases by 1.5% and 2.4% for the two cities, the computational efficiency in terms of the required memory is decreased significantly by 84% and 96%, respectively. Furthermore, the solution time of the metaheuristic approach is reduced by a 30% margin for the medium-size case study, and over 50% for the large-scale case study. One should note that the problem size is only almost tripled in terms of the number of zones from Lansing case study to Detroit case study. However, the memory requirement is increased by a factor of 20. This shows the importance of the metaheuristic approach for even larger case studies. Furthermore, the charging station configurations at the network level are provided in Figure 6-9.

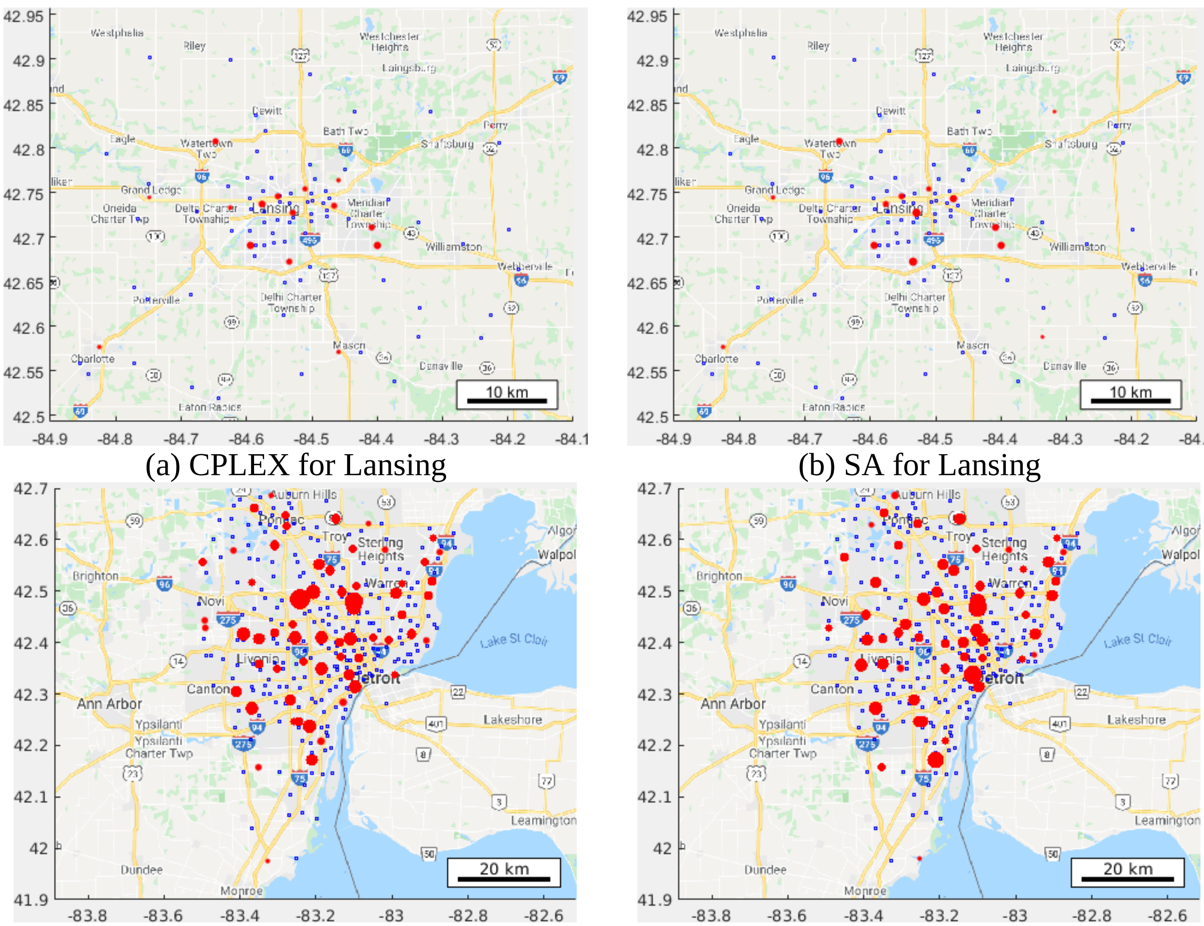

(a) CPLEX for Lansing

(b) SA for Lansing

(c) CPLEX for Detroit

(d) SA for Detroit

Figure 6-9 Charging station configurations for the cities of Lansing and Detroit with CPLEX and SA algorithm

The red dots represent installed charging stations, while the blue dots show candidate locations that have not been selected. The size of each red dot represents the recommended number of chargers. The size of the traffic analysis zones increases as the population density decreases. Figure 6-9 shows that the locations of charging stations are almost the same in both approaches.

6-3-2-4- Deterministic versus Stochastic Queueing Models

Deterministic queuing provides a zero-queuing time when the service rate exceeds the arrival rate. In this case, a steady state stochastic queuing, which does not exist when the service rate is smaller than arrival rate, can be applied. Figure 6-10 compares the deterministic queueing model with an M/M/k model for a sample charging station, and provides the values of the two-stage model.

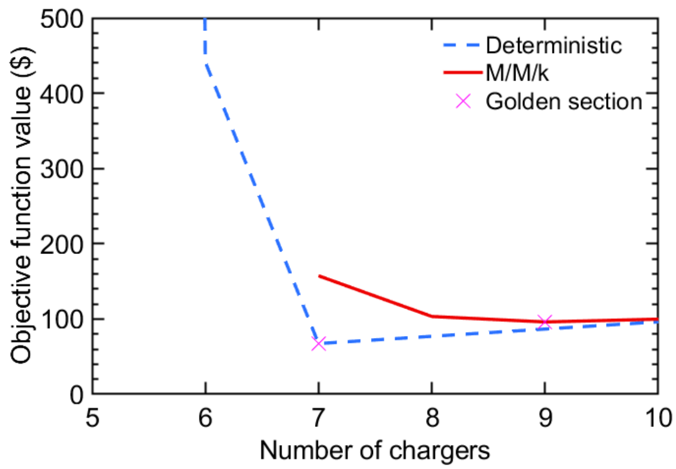

Figure 6-10 The optimum number of chargers for a sample charging stations considering deterministic and stochastic queuing models

Note that the deterministic model provides a left bound (minimum number of chargers that certify higher service rate relative to the arrival rate) for the stochastic model, without which the Golden-section method cannot be applied to the stochastic model. The figure plots the objective function value relative to the number of chargers for each stage. The objective function of the stochastic queuing can be determined when the service rate is higher than the arrival rate, as reflected in

Figure 6-10. As it is shown, a greater number of chargers is required to count for the stochastic queueing delay, in addition to the deterministic queueing delay.

6-3-2-5- Scenario results

For Lansing and Detroit, four scenarios are investigated based on battery capacity and charging power. Table 6-5 summarizes the model outputs.

Table 6-5 Comparing the optimum solutions under various battery capacity and charger power for the cities of Lansing and Detroit

City	Lansing				Detroit			
Battery size (kWh)	70	100	70	100	70	100	70	100
Charging power (kW)	50	50	150	150	50	50	150	150
Number of zones	92	92	92	92	301	301	301	301
# EV trajectories	28,574	28,574	28,574	28,574	212,299	212,299	212,299	212,299
# of stations	16	14	13	10	62	51	52	40
# of chargers	85	89	36	33	639	618	239	228
Station cost (Million dollar)	2.52	2.21	2.47	1.88	15.37	12.64	14.54	11.18
Charger cost (Million dollar)	3.39	3.56	2.96	2.73	23.15	22.39	18.82	17.95
Total infrastructure cost (Million dollar)	5.91	5.78	5.43	4.62	38.52	35.03	33.35	29.13
Average charging and queuing delay (min)	10.8	14.74	3.83	5.26	11.37	15.29	3.98	5.30

Consideration of 150 kW chargers provides a lower total investment cost despite a higher unit cost for these chargers. Furthermore, they provide lower charging and queuing times for travelers. Meanwhile, the 70 kWh vs. 100 kWh battery scenarios demonstrate a slight reduction in the number of charging stations under the larger battery size, as expected. However, the total number of chargers remains almost the same. The main reason for this observation may be caused by the fact that the charging behavior simulation tool uses various distributions for the initial and desired states of charge as a fraction of the battery size. This is a different pattern relative to a recent study (Ghamami et al., 2020a) for intercity networks (which is different in nature to urban areas).

6-4- Summary

This study develops a methodological framework to find the optimum investment plan for building a network of charging stations for urban areas considering queueing delays and feasibility of EV trips. This study finds the locations for charging stations and the number of chargers at each location, with an approximate cost of building such networks. A charging behavior simulator tool is developed and used along with a traffic simulation tool to provide an agent-based charging demand as the main input. No study in the literature captures all of these features for urban areas. The optimization model is decomposed into two subproblems. The first subproblem finds the location of the charging stations, and the second subproblem finds the required number of chargers at those stations. The former is solved using two approaches, a metaheuristic algorithm and using commercial solvers. The latter is solved using the Golden-section method via a two-stage algorithm that captures both deterministic and stochastic queueing delays. The methodology is first validated for a small case study in the city of Marquette. Then, the research approach and results are presented for two urban areas in Michigan, namely the cities of Lansing and Detroit, to ensure the feasibility of the urban trips of EV users in those regions by 2030 under a predicted market share. The winter scenario with 70 percent battery performance is tested under battery energy levels of 70 kWh and 100 kWh, and charger power levels of 50 kW and 150 kW.

The results of the tested scenarios provide the key findings as follows:

- The decomposition approach provides near-optimum solution to the main problem (within one percent of the optimal solution provided by the enumeration approach) in the small case study.

- 150 kW chargers reduce the charging and waiting time for travelers, as compared to that of 50 kW chargers.
- Due to the higher throughput of 150kW charger, the number of 150 kW chargers needed to support the EV trips in urban areas is much smaller than that of 50 kW chargers. Therefore, implementing a network of 150 kW chargers is less costly despite the higher per unit cost of these chargers.
- The battery size does not affect the number of chargers in urban areas, unlike the intercity network, as the length of the urban trips is significantly lower than the range of EVs.

Chapter 7 - Macro Analysis to Estimate Electric Vehicles Fast-Charging Infrastructure Requirements in Small Urban Areas

7-1- Overview

The current EV charging infrastructure planning studies and tools require detailed information, extensive resources, and skills that can be a significant barrier to urban areas for finding the required charging infrastructure to support a targeted EV market share. This chapter develops a set of regression models to estimate the number of required public DCFC charging stations and chargers to meet the charging demand of EV trips in urban areas. These models require basic information and are easier to implement than other charging infrastructure planning techniques, e.g., optimization-based frameworks, which are computationally challenging and require detailed information and extensive resources and skills to be implemented. The policy-makers and city planners can easily implement these regression models to estimate macro-level charging infrastructure in each urban area for different technological advancements, and EV market share.

In this study, the regression models are calibrated based on four groups of input data, including network-specific data, travel data, technology-specific data, and charging infrastructure data. Network-specific data includes information regarding the number of TAZs, and lane length of the road network. Travel data provides information on travel demand and VMT. Technology-specific data provides information on battery size, charging power, and EV market share. The charging infrastructure data is provided using a recent simulation-optimization study by Kavianipour et al. (Kavianipour et al., 2021). The models are calibrated and validated using the data of eight major cities in Michigan. 70% of available data are used for calibration, and the remaining 30% are incorporated for validation purposes. As the data set is an over-dispersed count data, the NB regression model is used, and RMSE and MAE metrics were implemented to validate the model.

7-2- Research Framework

This section first presents the research framework (Figure 7-1) to show the connections among the different steps involved in calibrating the macro charging planning model, its validation, and application. The modeling starts by feeding the inputs, i.e., OD dynamic travel demand and network configurations including nodes and links, to a dynamic traffic assignment (DTA) tool, i.e., DYNASMART-P. The DTA generates two key outputs: vehicle trajectories and dynamic skims. These data and other inputs such as land use characteristics, market share of EVs, and battery capacity are fed to the charging behavior simulation module, which assesses the feasibility of each trajectory. The infeasible trajectories are the input to a micro charging optimization model determining the location of level 3 public direct current fast charging (DCFC) stations and the number of chargers within each station as its outputs. This information is aggregated and incorporated with other aggregate data to calibrate macro models. Note that the difference between the state of the charge at the origin and the destination of the trajectory determines the feasibility of a trajectory. The infeasible trajectories are the trajectories that cannot fulfill their trips based on these states of charge and the required charge to reach the destination.

The macro charging infrastructure framework illustrates the connection between the input data, micro charging infrastructure model, and calibration of regression models. The calibration of macro models is coupled with a validation process incorporating additional data obtained from the micro model for scenarios other than that used for the calibration process. The macro charging infrastructure framework considers aggregate network information, aggregate travel demand, i.e., vehicle miles traveled (VMT), technology information, and aggregate charging infrastructure data.

Note that the latter is the output of the micro charging infrastructure model. The generated scenarios are stored and divided into calibration and validation data sets. Note that the macro charging infrastructure framework requires a variety of scenarios as data inputs for calibration and validation. These scenarios are generated in the scenario generator, which includes all the information stored in each scenario as shown in Figure 7-1. Then these scenarios are fed into the micro charging infrastructure framework to generate aggregate charging infrastructure information, which is then used as inputs for developing the macro models. It is also worth noting that the micro charging infrastructure model consists of an optimization model used to plan for the EV charging infrastructure for future EV trips. In the absence of actual data for the future EV trips and very low current EV penetration rate, the model relies on realistic assumptions for travel pattern and charging behavior verified by various stakeholders, including transportation engineers, planners, charging station companies, OEMs, utility companies, and the EV users. Further, the macro model is an aggregate model developed using the outputs of the micro model. Thus, the macro model is validated using a random sample of the output of the micro model. It is based on the aggregate travel data that is often available for the smaller cities. The macro models are developed to overcome the challenges associated with the data limitations in smaller urban areas.

The macro model usage diagram presented in Figure 7-1 shows the required data to use the specified regression models to be developed in this study. It shows that the required charging infrastructure in urban areas can be estimated based on the VMT, target technology, and aggregated network information. The rest of this section discusses both micro and macro charging infrastructure frameworks in detail.

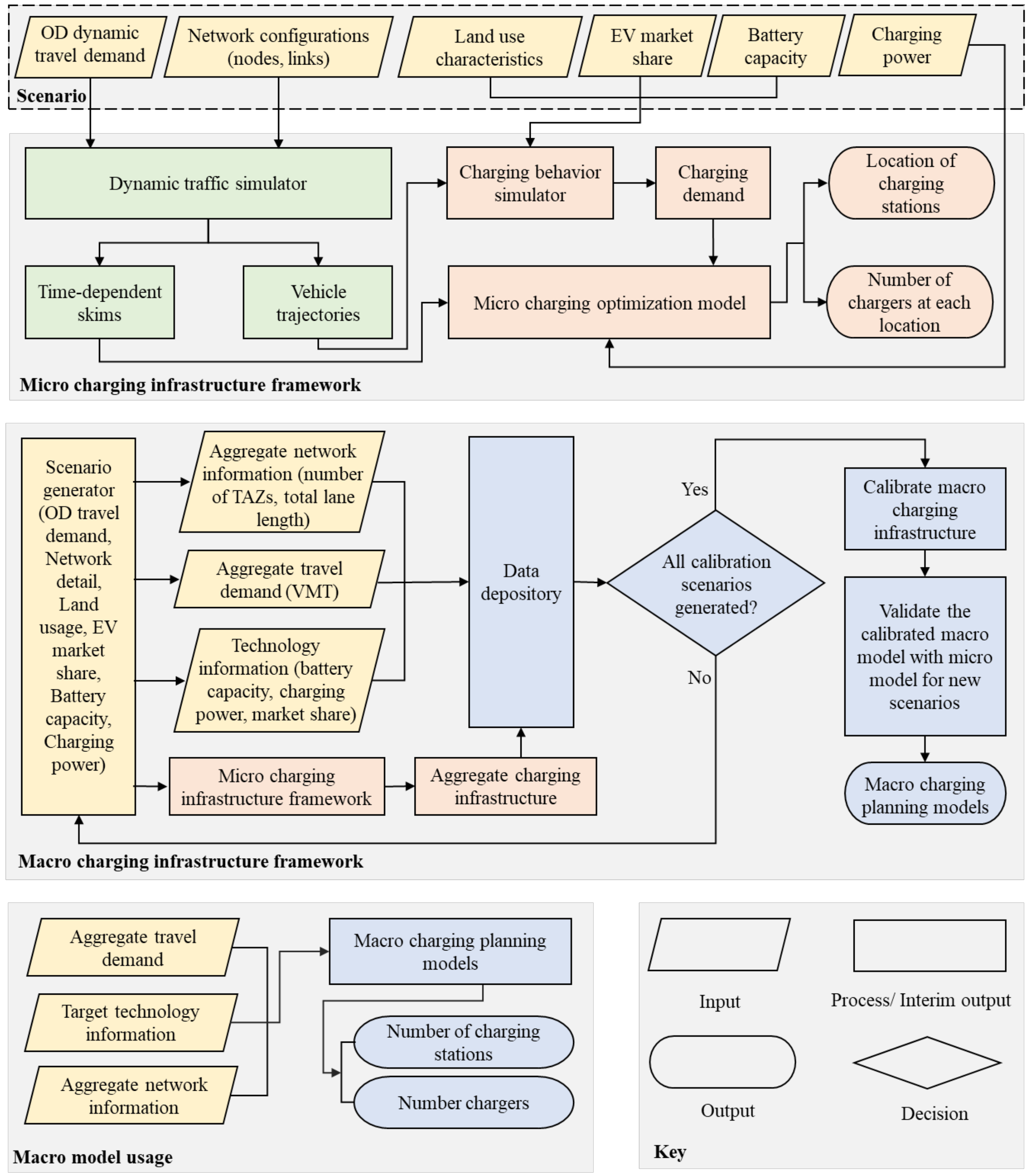

Figure 7-1 Research framework components to develop macro charging planning models

7-2-1- Micro charging infrastructure framework

To optimize the EV charging infrastructure investment, this study uses the micro-scaled simulation-optimization framework developed in chapter 6 to simulate the travel and charging behavior of EV drivers and find the optimum charging configuration addressing the EV charging demand in urban areas. This chapter implements the modeling framework for different urban areas in Michigan to develop macro-scale models that can estimate the required charging infrastructure for other urban areas (in Michigan and elsewhere). Incorporating future EV adoption rates and possible technological advancements are the key inputs to these models.

The objective function of the developed model in chapter 6 is as follows:

$$\min \sum_{k \in K} (C_k^s x_k + C_k^p z_k) + \gamma (\sum_{k \in K} \pi_k + \sum_{r \in R} \tau_r) \tag{7.1}$$

The objective function consists of two main terms. The first one calculates the charging infrastructure investment cost, including the cost of charging station, C_k^s, and charger cost, C_k^p, at each location $k \in K$. The availability of charging stations and the number of chargers in each location is specified by x_k and z_k, respectively. The second term calculates the monetary cost of users' experienced delay using the value of time factor, γ. It considers the charging and waiting in queue delay at each charging station π_k and detour delay, τ_r, for every trajectory $r \in R$. The objective function of the micro model is subjected to a set of constraints which consider:

- Charging within the available battery capacity: this constraint prevents EVs to charge more than their battery capacity
- Maintaining a minimum level of charge: this constraint makes the vehicles choose a charging station that is within their range in order to not drop below a minimum level of charge
- Charging vehicles where charging stations exist: this constraint enforces that the number of vehicles that recharge at any location, other than stations, is equal to zero.
- Providing feasibility for all EV trips: this constraint enforces that all vehicles with charging demand must be recharged.

- Calculating dynamic detours and waiting times: the study considers dynamic travel times and travel distances changing throughout the day. Further, it considers the waiting and detour time to select the optimum location to charge for each vehicle.

The results of the optimization problem, which includes the number of public DCFC charging stations and chargers for each scenario and the associated battery sizes and charging powers, are the inputs to the macro models for their calibration and validation.

7-2-2- Macro charging infrastructure framework

In this section, a set of macro models are specified to estimate the number of public DCFC charging stations and chargers required to support EV trips in urban areas (regardless of their spatial distribution). To this end, the macro models are calibrated based on Negative Binomial (NB) regression to examine how the number of charging stations and chargers vary with respect to input variables, including network size, travel demand, technological information (i.e., EV battery size and charging power), and EV market shares. Note that the NB regression is preferred to the linear regression model due to the nature of the dependent variables, which are count data (Washington et al., 2011). The calibration of macro-scale models is coupled with the validation process to assess the difference between the estimated and observed values in the validation data set.

7-2-2-1- Negative Binomial Regression

The dependent variables in charging planning studies, namely the number of charging stations and chargers, are count data consisting of non-negative integer values. The most common statistical methods used to model count data are Poisson and NB regression models (Washington et al., 2011). The Poisson model assumes the mean of the count data is equal to its variance. However, the variance can be significantly larger than the mean, which is called over-dispersion (Washington et al., 2011). The Poisson model may yield inaccurate results when overdispersion is present. This problem can be solved by implementing a generalized form of the Poisson model, referred to as the NB regression model. The data summary indicates that the variance is significantly larger than the mean of dependent variables (Table 7-5**)**. Hence, the NB model is implemented, which is expressed as follows:

$$y_i = \exp(\beta_1 x_{1i} + \beta_2 x_{2i} + \cdots \beta_q x_{qi} + \epsilon_i) \quad (7.2)$$

Where y_i is the observed value of the dependent variable for i^{th} observation and q represents the total number of independent variables. $x_{1i}, x_{2i}, \dots, x_{qi}$ are the observed values of independent variables for the observation i and $\beta_1, \beta_2, \dots, \beta_q$ are the coefficients of the independent variables. $\exp(\epsilon_i)$ is a Gamma distributed disturbance term with a mean equal to one and a variance equal to α, the over-dispersion parameter. The over-dispersion parameter captures the effect of variance not equal to the mean as shown below (Washington et al., 2011) Where $E(\lambda_i)$ is the expected value of the dependent variable λ_i:

$$Var(\lambda_i) = E(\lambda_i) + \alpha E(\lambda_i)^2 \quad (7.3)$$

7-2-2-2- Calibration and Validation

The maximum likelihood method is adopted to calibrate the NB model and estimate the coefficients, using the statistical software SPSS. In an iterative procedure, the model Goodness-of-fit test is considered based on (Cameron and Trivedi, 2013; Naderan and Shahi, 2010; Washington et al., 2011): correlation between the variables, the *p-value* less than 5%, the ratio of deviance and degrees of freedom around 0.8-1.2, and the Akaike's Information Criterion (AIC). The model having the lowest value of AIC is the optimum model. The AIC is defined as follows:

$$AIC = -2LL(\beta) + 2(p + 1) \quad (7.4)$$

Where p is the number of predictors in the model, and $LL(\beta)$ is the log-likelihood value at the convergence of the model. The model is validated by considering the two widely used metrics

(Wang and Lu, 2018; Washington et al., 2011), Root Mean Square Error (RMSE) and Mean Absolute Error (MAE), as follows:

$$RMSE = \sqrt{\frac{\sum_{i=1}^{n}(\hat{y}_i - y_i)^2}{n}} \tag{7.5}$$

$$MAE = \frac{\sum_{i=1}^{n}|\hat{y}_i - y_i|}{n} \tag{7.6}$$

Where y_i and $\hat{y}_i$ are the i^{th} observed and predicted values of the dependent variable, respectively. The term n denotes the total number of observations.

7-3- Numerical Analysis

This section first discusses the case study, including the study network and its specifications, technology scenarios, and market shares. Then, the results of the micro charging planning model, along with their statistics, are discussed. This information is used as the input to the macro charging planning model. Next, the calibrated regression models are introduced, and finally, the model validation results are provided.

7-3-1- Case Study

This study uses the Michigan road network presented in Figure 7-2 provided by the Michigan Department of Transportation (MDOT). This network consists of 37,125 links, including 11,516 freeways or highways, 20,742 arterials, and 4,867 ramps. The daily demand of this network provided by MDOT is 28,859,401 trips for a weekday in the Fall. The static OD demand table of Michigan is converted to a time-dependent OD demand table using a set of time factors. These time factors are calculated by matching the observed traffic flow captured by loop detectors installed on Michigan highways and the estimated traffic in DYNASMART-P (Kavianipour et al., 2021). The time-dependent OD demand and the road network are the inputs to the DYNASMART-P. This tool simulates travelers' route choices and finds the network equilibrium dynamically. The outputs of this simulation are vehicle trajectories and network zone-to-zone skims, which are inputs to the micro charging planning model. Initially, the models were obtained considering the data set of Detroit. However, the data set of Detroit does not represent a good fit for small urban areas. Hence, it was excluded from the analysis (see Figure 7-3 and Figure 7-4**)**.

Figure 7-2 Michigan state-wide transportation network and selected cities for macro-scale model calibration and validation

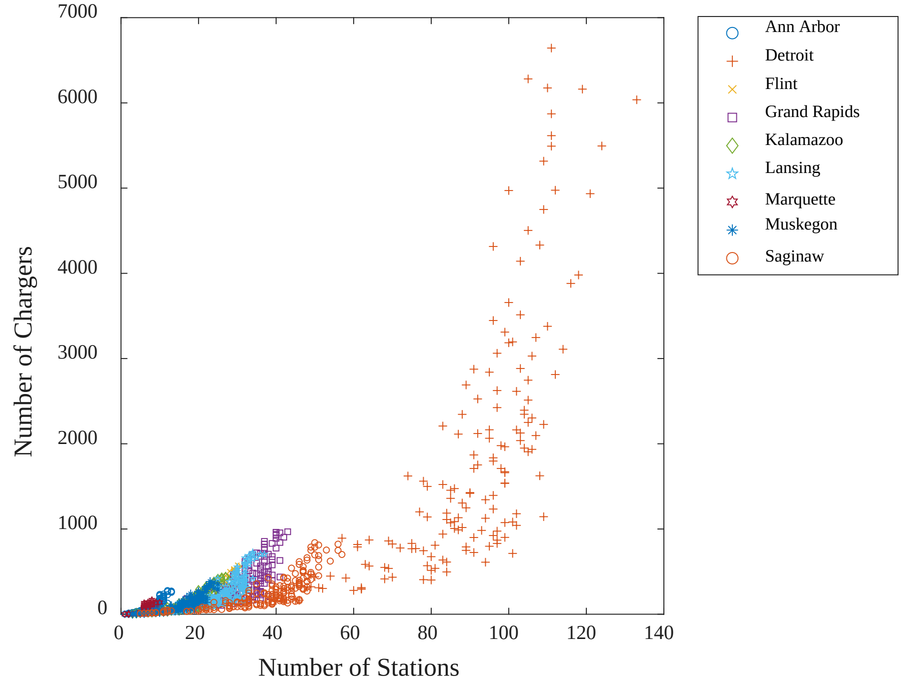

Figure 7-3 Number of chargers vs number of stations for different scenarios of all the cities in Michigan

Since the urban charging planning addresses the charging demand of unfulfilled trips within the city boundaries, the vehicle trajectories of each urban area must be extracted to be used in the micro charging planning approach. Therefore, this study extracts trajectories for eight cities (excluding Detroit) highlighted in Figure 7-2. These cities are selected based on their network size and population. The network characteristics and travel demand of these cities are provided in Table 7-1. In this table, the number of Traffic Analysis Zones (TAZs) and lane length represent the size of the network, while the travel demand and vehicle miles traveled represent the traffic in the network.

This study considers different scenarios for each city based on EV battery sizes including 70 kWh, 85 kWh, 100 kWh, and 115 kWh with an energy consumption rate of 0.3 kWh/mile (Ghamami et al., 2020b, 2019a). The charging powers range from 50 kW to 300 kW and their associated costs provided by charging station companies (ChargePoint and Greenlots), are presented in Table 7-2 (Ghamami et al., 2020b, 2019a). The land use acquisition costs and electricity provision costs required for estimating the location-specific station costs are provided by the city municipalities and utility companies, respectively (Ghamami et al., 2020b, 2019a).

Table 7-1 Network characteristics and travel demand for considered cities

Cities /Parameter	Number of TAZs	Network Lane Length (mi)	Travel Demand (# of daily trips)	Vehicle Miles Traveled (per day)
Muskegon	52	916	535,443	3,161,057
Ann Arbor	36	789	624,618	3,894,950
Kalamazoo	55	1128	712,796	4,085,052
Flint	84	1557	985,411	6,760,436
Saginaw	116	2726	1,054,842	7,122,931
Lansing	91	2030	1,086,242	7,183,037
Grand Rapids	82	2045	1,726,732	10,447,668
Marquette	21	336	178,741	931,957

Table 7-2 Charging infrastructure cost for different charging power (Ghamami et al., 2020b, 2019a)

Power (kW)	Charger Cost ($)	Charging Station Cost ($)
50	33,750	48,438
100	62,083	69,563
150	76,250	80,125
300	142,500	124,000

Table 7-3 Descriptive Statistics for the land cost and utility cost across different DCFC locations in Michigan (Ghamami et al., 2020b, 2019a).

Type of cost	Mean	Standard Deviation	Minimum	Maximum
Land acquisition cost ($/acre)	181,305	31,709	68,197	314,756
Electricity provision cost ($)	96,987	46,417	50,000	231,585

The summary of these costs is presented in Table 7-3. The land use characteristic information at the zone level is provided by the Michigan Department of Transportation (MDOT) (Ghamami et al., 2020b, 2019a). Further, each of the technology scenarios is tested for EV market shares, ranging from 1 to 50 in 5 percent incremental steps. The market share assumptions are based on the forecasted EV market share in the target year of 2050 (*Electric Vehicle Cost-Benefit Analysis Plug-in Electric Vehicle Cost-Benefit Analysis: Michigan*, 2017). Hence, the 50% EV market share in 2050 is considered as an upper bound for the statistical analysis and developing the micro and macro models. Note that market share is defined as the percent of total vehicles traveling in each city that are electrified. The number of vehicles is directly correlated with the number of trips used as input to the micro-scale model. Thus, a higher EV market share represents a higher share of randomly assigned trajectories as EVs. In total, there are 1,405 different scenarios considering all eight cities. The charging infrastructure requirements in all of these scenarios are obtained using the micro-level optimization model. In the micro-level optimization model, the value of drivers' time is considered to be $18/hr.

7-3-2- Micro Charging Planning Results

The micro charging infrastructure data is generated using the simulation-optimization approach developed in chapter 6. Table 7-4 summarizes the infrastructure requirements for the listed urban areas considering the different technology and EV market share scenarios. This table shows the range of number of stations, number of chargers, total infrastructure cost, and average charging and queuing delay for the different scenarios of each urban area considered in this study.

Table 7-4 Summary of Infrastructure Requirements for Different Scenarios (EV battery sizes of 70-115 kWh, charging powers of 50-300 kW, and market shares of 1-50%)

Urban Area	Number of Stations	Number of Chargers	Infrastructure Cost (million Dollars)	Average Charging & Queuing Delay (min)
Ann Arbor	1-13	2-278	0.64-14.40	0.21-19.06
Flint	3-32	6-581	1.51-28.75	0.14-21.59
Grand Rapids	6-43	12-969	2.50-52.09	1.10-18.44
Kalamazoo	3-28	6-446	0.89-21.49	0.98-21.65
Lansing	3-37	6-728	1.59-39.04	0.78-20.33
Marquette	1-10	2-170	0.50-7.18	1.52-20.02
Muskegon	3-25	6-387	1.04-17.14	0.97-19.09
Saginaw	5-57	10-843	1.94-38.65	1.06-19.47

7-3-3- Regression Models

7-3-3-1- Data Descriptions

This study calibrates a set of regression models using the data set generated by implementing the micro-model for the above-mentioned eight cities in Michigan for different EV market shares and technology scenarios.

The dependent variable in this study are:

- EVs market share (%) (ρ)
- Urban VMT (million miles/day) (V)
- Road network lane length (1000 mi) (L)
- Number of TAZs (T)
- Number of nodes (I)
- EVs battery size (kWh) (E)
- Charging power at charging stations (kW) (P)
- Generated travel demand (1000 trips/day) (D)

The independent variables are:

- Number of chargers (ψ)
- Number of charging stations (χ)

The descriptive statistics of the input data set are presented in Table 7-5. There are a total of 1,405 observations. The study generates data points for each city considering variations of the EV market share (1-50%), EV battery size (70-115 kWh), and charging power (50-300 kW). 70% (1,012 observations) of the data are randomly selected to calibrate the regression models, and the remaining 30% of the data (393 observations) are used for the model validation following the common approach in the literature (Gholamy et al., 2018). For the calibration data set, the number of TAZs ranges from 21 to 116. The average lane length of the network is 1,438 miles. The VMT ranges from 931,957 to 10,447,668. The market share of EVs varies from 1% to 50%. The dependent variables are the number of charging stations and the number of chargers in the urban area. The number of charging stations has an average of 19, a standard deviation of 12, ranging from 1 to 57. The number of chargers has an average of 170, a standard deviation of 176, and varies from 2 to 969. It was also observed that the variables presenting the city characteristics (number of TAZs, number of nodes, travel demand, road network lane length, and VMT) are strongly correlated to each other (Table 7-5**)** as their correlation coefficients are greater than 0.7 (Clark, 2018).

Table 7-5 Descriptive Statistics for Dependent and Independent Variables

	Variable	Mean	Std. Deviation	Minimum	Maximum
Calibration group (N=1,012)	Battery size (kWh)	93	17	70	115
	Charging Power (kW)	151	95	50	300
	Number of TAZs	67	30	21	116
	Market share (%)	25	16	1	50
	Number of nodes	575	302	62	1,031
	Travel demand (1,000 trips/day)	853	426	179	1,727
	Lane length (miles)	1,438	749	336	2,726
	VMT (1000 miles/day)	5,389	2,760	932	10,448
	Dependent Variables				
	Number of Stations	19	12	1	57
	Number of Chargers	170	176	2	969
	Total observations (N)	1012			
	Variable	Mean	Std. Deviation	Minimum	Maximum
Validation group (N=393)	Battery size (kWh)	92	16	70	115
	Charging Power (kW)	148	89	50	300
	Number of TAZs	67	29	21	116
	Market share (%)	25	16	1	50
	Number of nodes	588	307	62	1,031
	Travel demand (1,000 trips/day)	885	449	179	1,727
	Lane length (miles)	1,441	723	336	2,726

Table 7-5 (cont’d)

	VMT (1000 miles/day)	5,571	2,867	932	10,448
	Dependent Variables				
	Number of Stations	19	12	2	56
	Number of Chargers	173	184	4	956
	Total observations (N)	393			

		Battery size	Charging Power	Market share	# of TAZs	# of nodes	Travel demand	Lane length	VMT
Correlation	Battery size	1.00	0.02	0.02	0.01	0.00	0.00	0.01	0.00
	Charging Power	0.02	1.00	-0.01	0.00	-0.01	-0.01	0.00	-0.01
	Market share	0.02	-0.01	1.00	-0.01	-0.01	0.00	-0.01	0.00
	# of TAZs	0.01	0.00	-0.01	1.00	0.85	0.74	0.98	0.81
	# of nodes	0.00	-0.01	-0.01	0.85	1.00	0.95	0.88	0.98
	Travel demand	0.00	-0.01	0.00	0.74	0.95	1.00	0.80	0.99
	Lane length	0.01	0.00	-0.01	0.98	0.88	0.80	1.00	0.84
	VMT	0.00	-0.01	0.00	0.81	0.98	0.99	0.84	1.00

7-4- Results

The NB regression analysis is done for the calibration group to obtain models estimating the number of charging stations/chargers. Including the data of Detroit in the data set results in regression models that cannot accurately estimate the required charging infrastructure of Detroit and adversely affect the predicted charging infrastructure for other cities as well, especially the number of charging stations (Figure 7-4**)**. Hence, Detroit is excluded from the data set. It is important to note that these regression models are macro-models that are developed to estimate charging infrastructure in small or mid-sized urban areas to be easily implemented by stakeholders.

However, large-scale networks entail detailed micro-level optimization models to estimate optimized charging infrastructure and locations.

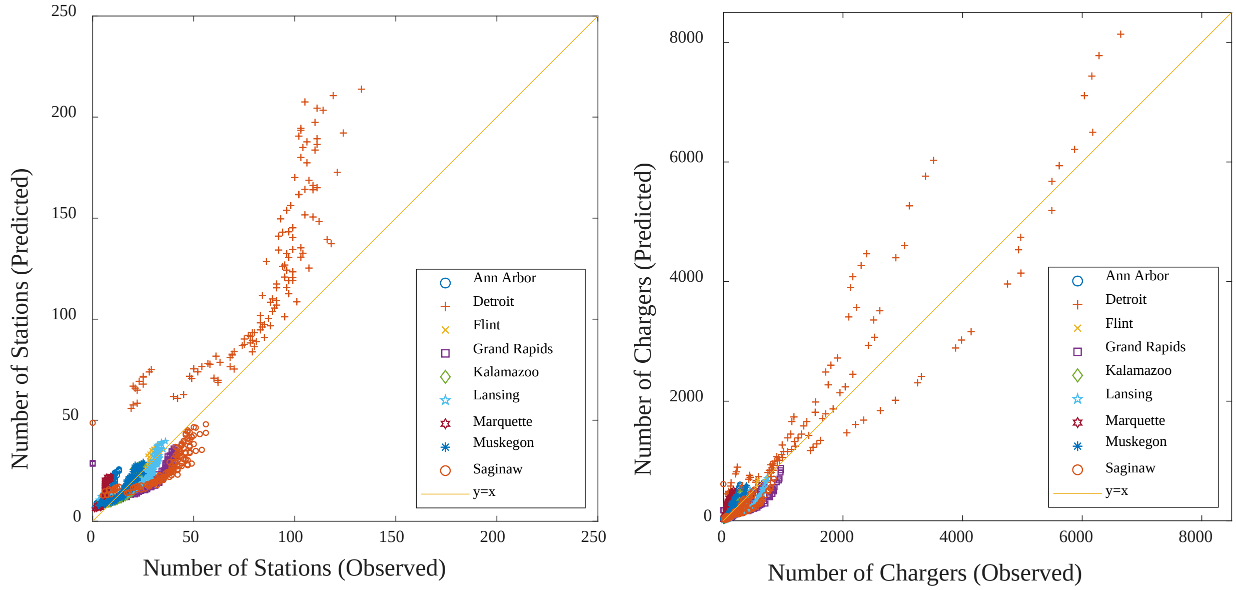

a) Number of stations   b) Number of chargers

Figure 7-4 Predicted versus observed values of the dependent variable (including Detroit) for the calibration data set

The optimum regression models for the number of charging stations/chargers are presented in Table 7-6. All the variables in the NB regression model have a p-value of less than 0.01. The models presented are the best models based on the lowest AIC, RMSE, MAE values, and the practical relation of the independent and dependent variables. The calibrated model for charging stations has battery size, charging power, EV market share, and road network lane length, as independent variables. The model suggests that the required number of charging stations decreases for larger battery sizes and higher charging power. The larger battery size means more energy can be stored in the battery. Hence, the number of EV trajectories that require recharging decreases, reducing the required number of charging stations in the process. The higher charging power increases the throughput at each charger and reduces the users' delays. Therefore, each charging station with the same number of chargers can serve more vehicles, which decreases the required total number of charging stations. Since a higher EV market share means more EV trips, more charging stations are required to serve these increased trips, which justifies the positive sign of EV market share. The larger road network lane length would also mean more routes which would result in more and longer detours even for a similar charging demand. Thus, the number of charging stations increases to ensure trip feasibility, and reduce detours of the EV trips.

Table 7-6 Calibrated Negative Binomial Models to Estimate the Number of Charging stations/Chargers

	Parameter	Coefficients	Standard Error	p-value
Number of Stations (N=1,012)	Intercept	1.6536	0.04848	<0.01
	Battery size (kWh)	-0.0017	0.00043	<0.01
	Charging power (kW)	-0.0009	0.00008	<0.01
	Market share (%)	0.0199	0.00051	<0.01
	Road network lane length (1,000 mi)	0.6510	0.01037	<0.01
	Dispersion parameter	0.0019		
	Deviance/df	1.193		
	Log-Likelihood	-2929.658		
	Akaike's Information Criterion (AIC)	5871.316		
Number of Chargers (N=1,012)	Parameter	Coefficients	Standard Error	p-value
	Intercept	3.0306	0.08383	<0.01
	Battery size (kWh)	0.0030	0.00077	<0.01
	Charging power (kW)	-0.0058	0.00013	<0.01
	Market share (%)	0.0436	0.00095	<0.01
	VMT (million miles)	0.2111	0.00513	<0.01
	Dispersion parameter	0.1608		
	Deviance/df	1.060		
	Log-Likelihood	-5227.156		
	Akaike's Information Criterion (AIC)	10466.312		

	Dependent Variable	Equations	Calibration RMSE	Calibration MAE	Validation RMSE	Validation MAE
Calibration & Validation	Number of Stations	$\chi = e^{1.654-0.002(E)-0.001(P)+0.020(\rho)+0.651(L}$	4.48	3.58	4.78	3.78
	Number of Chargers	$\psi = e^{3.031+0.003(E)-0.006(P)+0.044(\rho)+0.211(V}$	87.78	49.77	101.97	54.65

The best-calibrated model predicting the number of chargers is a function of battery size, charging power, EV market share, and the total VMT (Table 7-6). The larger battery size indicates the less frequent but longer charging time for each user. Hence, the number of chargers increases with the size of the battery to reduce the user delay and the queue at each charging station. Note that even though the total charging demand remains the same, the vehicles with larger batteries charge for a longer duration and less frequently. But these less frequent long-duration charging can still cause a queue formation at the charging stations, especially during peak hours, thereby increasing the delay. Thus, to avoid the queue formation and delay, more chargers are required for larger battery sizes. The higher charging power increases the throughput at each charger. Hence, each charger can serve a greater number of users, which reduces the overall number of chargers in the system. The higher EV market share indicates more EV trips; thus, a larger number of chargers are required to meet the energy demand of increased EV trips. Further, if the VMT in the system increases, more energy is required to travel more miles. Thus, more chargers are required to serve the increased energy demand in the system.

The calibrated models are applied to the remaining 30% of the data set for its validation. The RMSE and MAE values for the calibration and validation (predicted) groups are shown in Table 7-6**.** Considering the descriptive statistics (Table 7-5), the RMSE and MAE values for the validation group are comparable to that of the RMSE and MAE of the calibration data set. Further, the plot of predicted values versus the observed values for the validation group indicates that the errors are within acceptable range (Figure 7-5**)**. Hence, the developed regression models can satisfactorily predict the number of charging stations/chargers for the different scenarios/regions.

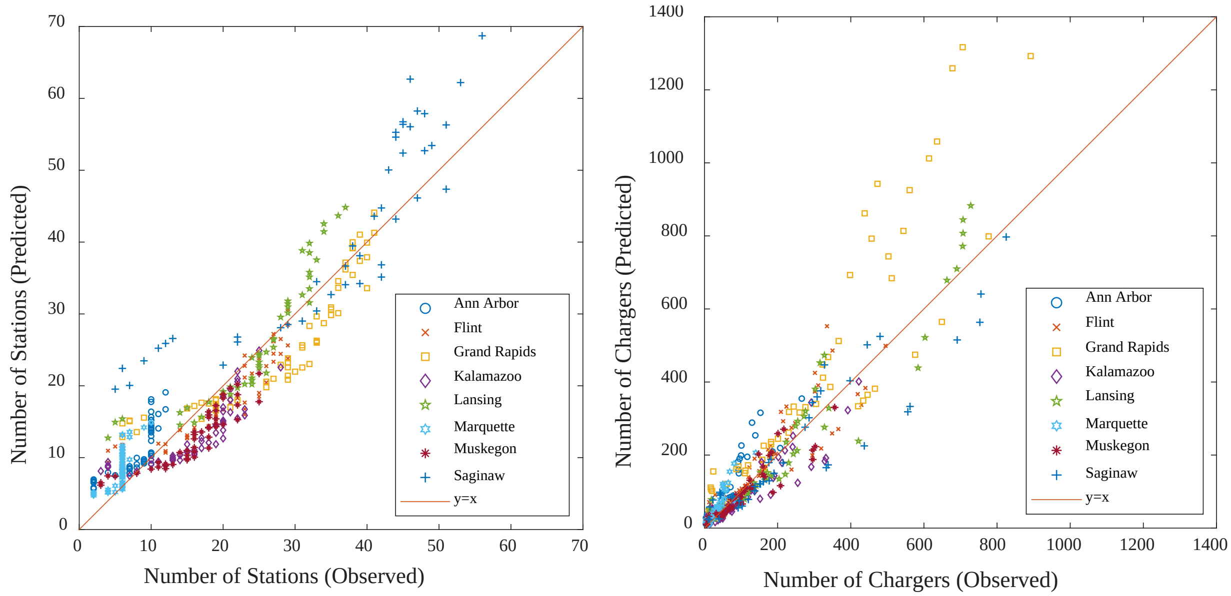

a) Number of charging stations b) Number of chargers

Figure 7-5 Predicted versus observed values of the dependent variable (excluding Detroit) for the validation data set

7-5- Summary

Electric vehicles are proposed to substitute conventional vehicles due to their high energy efficiency and potential to reduce carbon footprint. However, the limited range and lack of charging infrastructure are the major challenges in adopting these vehicles. One of the key factors in the EV market growth is the availability of adequate charging infrastructure. This study develops a set of regression models to estimate the number of required public DCFC charging stations and chargers to meet the charging demand of EV trips in urban areas. These models require basic information and are easier to implement than other charging infrastructure planning techniques, e.g., optimization-based frameworks, which are computationally challenging and require detailed information and extensive resources and skills to be implemented. The policy-makers and city planners can easily implement these regression models to estimate macro-level charging infrastructure in each urban area for different technological advancements, and EV market share.

In this study, the regression models are calibrated based on four groups of input data, including network-specific data, travel data, technology-specific data, and charging infrastructure data. Network-specific data includes information regarding the number of TAZs, and lane length of the road network. Travel data provides information on travel demand and VMT. Technology-specific data provides information on battery size, charging power, and EV market share. The charging infrastructure data is provided using a recent simulation-optimization study by Kavianipour et al. (Kavianipour et al., 2021). The models are calibrated and validated using the data of eight major cities in Michigan. 70% of available data are used for calibration, and the remaining 30% are incorporated for validation purposes. As the data set is an over-dispersed count data, the NB regression model is used, and RMSE and MAE metrics were implemented to validate the model. The numerical results show a successful model validation, and the key findings of the study are as follows:

- The negative binomial regression model can be calibrated and be implemented to predict the required number of charging stations and chargers in urban areas.
- The number of charging stations reduces with an increase in charging power and EV battery size, while it increases with an increase in market share of EVs, and the road network lane length
- The number of chargers reduces with an increase in charging power, while it increases with EVs market share, battery size, and VMT in the system.

The developed models represent the most impactful factors for planning EV charging infrastructure. The main factors impacting the number of required charging stations are the vehicles' battery size, charging stations' power, EV market share, and road network lane length, while the factors to predict the number of chargers are the vehicles' battery size, charging stations' power, EV market share, and the total VMT. Hence, it is observed that while vehicles' battery size, charging stations' power, and EV market share impact both chargers and charging stations, VMT defines energy demand and thus impacts the number of chargers and road network lane length impacts detour and thus the number of charging stations.

Chapter 8 - Concluding Remarks and Future Research

8-1- Concluding Remarks

EVs are considered a sustainable alternative to CVs to decrease the GHGs and dependence on fossil fuel. However, their adoption is hindered due to some obstacles, including limited range, long charging time, and lack of supporting charging infrastructure. Providing a dense network of fast-charging stations can facilitate the travel of EVs and also promote their adoption. On the other hand, advancing the battery and charging technologies can increase the range of EVs and reduce their charging time, respectively. This study presents a mathematical framework to find the optimum configuration of charging infrastructure to support long-distance trips in intercity and urban networks considering various operational conditions. It realistically captures the travel patterns for a mixed fleet of electric and conventional vehicles in intercity networks and considers flow-dependent recharging/queuing delays at charging stations. This framework is then extended to capture the monthly traffic demand and battery performance variations, which are two main contributing factors in defining the infrastructure needs of EV users, particularly in states with adverse weather conditions. For the case study of Michigan, it is shown that the decreased battery performance in months with adverse weather dictates the optimal charging infrastructure, overshadowing the increased demand in favorable weather conditions. Afterward, this study investigates the impacts of different battery and charger technologies on the optimal configuration of charging infrastructure for the intercity networks. It is shown that the location of charging stations merely depends on the battery capacity while the charging power dictates the number of required chargers.

Finally, this study introduces an integrated framework for urban fast-charging infrastructure to optimize the configuration of charging facilities. Unlike intercity trips that OD trips are considered, urban trips need to be individually considered since they might start with any state of charge. After generating trip trajectories, a state-of-the-art tool is developed to simulate charging behavior, resulting in the temporal charging demand. This demand is addressed by providing a network of charging stations. It is shown that the problem can be decomposed into two subproblems, where the location of charging stations and the number of chargers are found separately. The key findings of this study are as follows.

- Building an enabling charging infrastructure network to support EVs intercity trips is less expensive compared to increasing the battery capacity.
- The assumed values for charger cost and value of time calls for providing as many chargers as needed to avoid deterministic queuing.
- The battery size determines the location of charging stations in intercity networks, while the EV market share affects the number of chargers within charging stations.
- The numerical results establish the sensitivity of optimal configuration and numbers of charging stations and chargers to monthly OD demand variations and battery performance reduction in winter months.
- The optimum charging infrastructure for OD demand and battery performance of January is closer to the optimum results for the entire year rather than OD demand and battery performance of other months.
- Charging stations with higher power have a higher cost, but they decrease the total required infrastructure cost and users' delay considering the higher rate of return.
- The decomposition approach for urban networks provides a near-optimum solution to the main problem in the small case study.

- The battery size does not affect the number of chargers in urban areas, unlike the intercity network, as the length of the urban trips is significantly lower than the range of EVs.
- The negative binomial regression model can be calibrated and be implemented to predict the required number of charging stations and chargers in urban areas.

8-2- Future Research Directions

The proposed methodologies and models in this study to find the optimal charging infrastructure configurations benefit from realistic capturing of user behavior and near-global-optimum solutions. However, there are still some limitations to consider for future studies. For instance, the urban model in Chapter 6 assumes that EVs only recharge during their infeasible trip. However, they might recharge in a feasible trip to prevent future recharging. This behavior must be captured to provide a solution that can better address the EVs charging demand. This requires a more in-depth study of users' behavior, a possible future research direction. In this regard, various strategies for spatial and temporal pricing of electricity can be studied to explore their impacts on congestion and the required number of chargers. Further, incorporating trip chain data and adjusting the model accordingly is an important future research direction. Another future path to consider is the impact of vehicle type and model on the battery performance and capacity.

Finally, the proposed regression models in Chapter 7 are easy to apply and do not require detailed information. Including additional information such as the population and demographics of the cities can make the model more robust. Another scope for future research would be to consider a more extensive data set to build more profound regression models. Further, this model considers realistic assumptions on travel patterns and charging behavior verified through various stakeholder meetings; However, there is no actual data available for the high level of adoption to validate the micro model. As a future research direction, it is vital to gather data for EV market share propagation and charging infrastructure throughout the time and validate the proposed micro models. Further, the current study focuses on developing models to predict level 3 public DCFC chargers by considering homogeneous users with vehicles of identical battery sizes. In future, the modeling framework can be extended to consider heterogeneous users and mix of level 2 and level 3 public chargers. Also, these models consider the urban characteristics of the cities in Michigan and account for the impact of cold weather on the optimum charging infrastructure; hence they can be easily applied to any city with similar conditions to Michigan. However, cities with different weather conditions and urban characteristics would require macro models calibrated using unadjusted battery size and the associated urban characteristics.

REFERENCES

REFERENCES

Bai, Y., Hwang, T., Kang, S., Ouyang, Y., 2011. Biofuel refinery location and supply chain planning under traffic congestion. Transp. Res. Part B Methodol. 45, 162–175. https://doi.org/10.1016/J.TRB.2010.04.006

Berman, O., Larson, R.C., Fouska, N., 1992. Optimal Location of Discretionary Service Facilities. Transp. Sci. 26, 201–211.

Bigelow, D., 2017. USDA ERS - Farmland Value [WWW Document]. URL https://www.ers.usda.gov/topics/farm-economy/land-use-land-value-tenure/farmland-value (accessed 10.15.18).

Bikcora, C., Verheijen, L., Weiland, S., 2015. Semiparametric density forecasting of electricity load for smart charging of electric vehicles, in: 2015 IEEE Conference on Control Applications (CCA). pp. 1564–1570.

Boyd, S., Vandenberghe, L., 2009. Convex Optimization, 7th ed, Communication Networking. Cambridge University Press, Cambridge. https://doi.org/10.1016/B978-012428751-8/50019-7

Cai, H., Jia, X., Chiu, A.S.F., Hu, X., Xu, M., 2014. Siting public electric vehicle charging stations in Beijing using big-data informed travel patterns of the taxi fleet. Transp. Res. Part D Transp. Environ. 33, 39–46. https://doi.org/10.1016/j.trd.2014.09.003

Cameron, A.C., Trivedi, P.K., 2013. Regression Analysis of Count Data, Second Edi. ed, Regression Analysis of Count Data, Second Edition. Cambridge University Press. https://doi.org/10.1017/CBO9781139013567

Chen, R., Qian, X., Miao, L., Ukkusuri, S. V., 2020. Optimal charging facility location and capacity for electric vehicles considering route choice and charging time equilibrium. Comput. Oper. Res. 113, 104776. https://doi.org/10.1016/j.cor.2019.104776

Chen, T.D., Kockelman, K.M., Khan, M., 2013. Locating Electric Vehicle Charging Stations Parking-Based Assignment Method for Seattle, Washington. Transp. Res. Rec. J. Transp. Res. Board 2385, 28–36. https://doi.org/10.3141/2385-04

Clark, J., 2018. Pearson Correlation Coefficient [WWW Document]. Magoosh.

Dashora, Y., Barnes, J.W., Pillai, R.S., Combs, T.E., Hilliard, M., Chinthavali, M.S., 2010. The PHEV Charging Infrastructure Planning (PCIP) Problem. Int. J. Emerg. Electr. Power Syst. 11, 7. https://doi.org/10.2202/1553-779X.2482

Daskin, M.S., 1995. Network and Discrete Location, Network and Discrete Location. https://doi.org/10.1002/9781118032343

Deb, S., Tammi, K., Kalita, K., Mahanta, P., 2018. Review of recent trends in charging infrastructure planning for electric vehicles. Wiley Interdiscip. Rev. Energy Environ. 7, e306. https://doi.org/10.1002/wene.306

Department of Energy, 2020. Maximizing Electric Cars' Range in Extreme Temperatures [WWW Document]. Dep. Energy. URL https://www.energy.gov/eere/electricvehicles/maximizing-electric-cars-range-extreme-temperatures

Donadee, J., Ilic, M., Karabasoglu, O., 2014. Optimal autonomous charging of electric vehicles with stochastic driver behavior, in: 2014 IEEE Vehicle Power and Propulsion Conference (VPPC). pp. 1–6.

Dong, J., Lin, Z., 2012. Within-day recharge of plug-in hybrid electric vehicles: Energy impact of public charging infrastructure. Transp. Res. Part D Transp. Environ. 17, 405–412. https://doi.org/10.1016/J.TRD.2012.04.003

Dong, J., Liu, C., Lin, Z., 2014. Charging infrastructure planning for promoting battery electric vehicles: An activity-based approach using multiday travel data. Transp. Res. Part C Emerg. Technol. 38, 44–55. https://doi.org/10.1016/J.TRC.2013.11.001

Eberhard, M., Tarpenning, M., 2006. The 21 st Century Electric Car.

Eisenman, S.M., List, G.F., 2004. Using probe data to estimate OD matrices, in: Proceedings. The 7th International IEEE Conference on Intelligent Transportation Systems (IEEE Cat. No. 04TH8749). pp. 291–296.

Electric Vehicle Cost-Benefit Analysis Plug-in Electric Vehicle Cost-Benefit Analysis: Michigan, 2017.

Electrify America, 2017. Our Plan | Electrify America [WWW Document].

Erdoğan, S., Miller-Hooks, E., 2012. A Green Vehicle Routing Problem. Transp. Res. Part E Logist. Transp. Rev. 48, 100–114. https://doi.org/10.1016/J.TRE.2011.08.001

Fakhrmoosavi, F., Kavianipour, M., Shojaei, M. (Sam), Zockaie, A., Ghamami, M., Wang, J., Jackson, R., 2021. Electric Vehicle Charger Placement Optimization in Michigan Considering Monthly Traffic Demand and Battery Performance Variations. Transp. Res. Rec. J. Transp. Res. Board. https://doi.org/10.1177/0361198120981958

Frade, I., Ribeiro, A., Gonçalves, G., Antunes, A.P., 2011. Optimal Location of Charging Stations for Electric Vehicles in a Neighborhood in Lisbon, Portugal. Transp. Res. Rec. J. Transp. Res. Board 2252, 91–98. https://doi.org/10.3141/2252-12

Ghamami, M., Kavianipour, M., Zockaie, A., Hohnstadt, L.R., Ouyang, Y., 2020a. Refueling infrastructure planning in intercity networks considering route choice and travel time delay for mixed fleet of electric and conventional vehicles. Transp. Res. Part C Emerg. Technol. 120, 102802. https://doi.org/10.1016/j.trc.2020.102802

Ghamami, M., Nie, Y. (Marco), Zockaie, A., 2016a. Planning charging infrastructure for plug-in electric vehicles in city centers. Int. J. Sustain. Transp. 10, 343–353. https://doi.org/10.1080/15568318.2014.937840

Ghamami, M., Zockaie, A., Miller, S., Kavianipour, M., Fakhrmoosavi, F., Singh, H., Jazlan, F., Shojaie, M., 2020b. Electric Vehicle Charger Placement Optimization in Michigan: Phase II - Urban.

Ghamami, M., Zockaie, A., Miller, S., Kavianipour, M., Shojaie, M., Fakhrmoosavi, F., Hohnstadt, L., Singh, H., 2019a. Electric Vehicle Charger Placement Optimization in Michigan: Phase I-Highways (Supplement I: Full Tourism Analysis).

Ghamami, M., Zockaie, A., Nie, Y.M., 2016b. A general corridor model for designing plug-in electric vehicle charging infrastructure to support intercity travel. Transp. Res. Part C Emerg. Technol. 68, 389–402. https://doi.org/10.1016/j.trc.2016.04.016

Ghamami, M., Zockaie, A., Wang, J., Miller, S., Kavianipour, M., Shojaie, M., Fakhrmoosavi, F., Hohnstadt, L., Singh, H., 2019b. Electric Vehicle Charger Placement Optimization in Michigan: Phase I – Highways.

Gholamy, A., Kreinovich, V., Kosheleva, O., 2018. Why 70/30 or 80/20 Relation Between Training and Testing Sets: A Pedagogical Explanation. Dep. Tech. Reports 1209.

Gnann, T., Funke, S., Jakobsson, N., Plötz, P., Sprei, F., Bennehag, A., 2018. Fast charging infrastructure for electric vehicles: Today's situation and future needs. Transp. Res. Part D Transp. Environ. https://doi.org/10.1016/j.trd.2018.03.004

Grassmann, W., 1983. The Convexity of the Mean Queue Size of the M/M/c Queue with Respect to the Traffic, Source: Journal of Applied Probability.

Green Car Reports, 2017. Volkswagen diesel scandal : Breaking News, Photos, & Videos - Green Car Reports [WWW Document].

Hajibabai, L., Bai, Y., Ouyang, Y., 2014. Joint optimization of freight facility location and pavement infrastructure rehabilitation under network traffic equilibrium. Transp. Res. Part B Methodol. 63, 38–52. https://doi.org/10.1016/J.TRB.2014.02.003

Hao, X., Wang, H., Lin, Z., Ouyang, M., 2020. Seasonal effects on electric vehicle energy consumption and driving range: A case study on personal, taxi, and ridesharing vehicles. J. Clean. Prod. 249, 119403.

He, F., Wu, D., Yin, Y., Guan, Y., 2013. Optimal deployment of public charging stations for plug-in hybrid electric vehicles. Transp. Res. Part B Methodol. 47, 87–101. https://doi.org/10.1016/J.TRB.2012.09.007

He, F., Yin, Y., Lawphongpanich, S., 2014. Network equilibrium models with battery electric vehicles. Transp. Res. Part B Methodol. 67, 306–319. https://doi.org/10.1016/J.TRB.2014.05.010

He, F., Yin, Y., Zhou, J., 2015. Deploying public charging stations for electric vehicles on urban road networks. Transp. Res. Part C Emerg. Technol. 60, 227–240. https://doi.org/10.1016/j.trc.2015.08.018

He, J., Yang, H., Tang, T.-Q., Huang, H.-J., 2018. An optimal charging station location model with the consideration of electric vehicle's driving range. Transp. Res. Part C Emerg. Technol. 86, 641–654. https://doi.org/10.1016/J.TRC.2017.11.026

He, Y., Kockelman, K.M., Perrine, K.A., 2019. Optimal locations of U.S. fast charging stations for long-distance trip completion by battery electric vehicles. J. Clean. Prod. 214, 452–461. https://doi.org/10.1016/j.jclepro.2018.12.188

Hodgson, M.J., 1990. A Flow-Capturing Location-Allocation Model. Geogr. Anal. 22, 270–279. https://doi.org/10.1111/j.1538-4632.1990.tb00210.x

Jayakrishnan, R., Mahmassani, H.S., Hu, T.-Y., 1994. An evaluation tool for advanced traffic information and management systems in urban networks. Transp. Res. Part C Emerg. Technol. 2, 129–147.

Jing, W., Kim, I., Ramezani, M., Liu, Z., 2017. Stochastic traffic assignment of mixed electric vehicle and gasoline vehicle flow with path distance constraints. Transp. Res. Procedia 21, 65–78. https://doi.org/10.1016/J.TRPRO.2017.03.078

Jung, J., Chow, J.Y.J., Jayakrishnan, R., Park, J.Y., 2014. Stochastic dynamic itinerary interception refueling location problem with queue delay for electric taxi charging stations. Transp. Res. Part C Emerg. Technol. 40, 123–142. https://doi.org/10.1016/j.trc.2014.01.008

Kavianipour, M., Fakhrmoosavi, F., Singh, H., Ghamami, M., Zockaie, A., Ouyang, Y., Jackson, R., 2021. Electric vehicle fast charging infrastructure planning in urban networks considering daily travel and charging behavior. Transp. Res. Part D Transp. Environ. 93, 102769. https://doi.org/10.1016/j.trd.2021.102769

Kavianipour, M., Saedi, R., Zockaie, A., Saberi, M., 2019. Traffic State Estimation in Heterogeneous Networks with Stochastic Demand and Supply: Mixed Lagrangian–Eulerian Approach. Transp. Res. Rec. 2673, 114–126. https://doi.org/10.1177/0361198119850472

Kiefer, J., 1953. Sequential Minimax Search for a Maximum. Proc. Am. Math. Soc. 4, 502. https://doi.org/10.2307/2032161

Krisher, T., 2019. AAA: Cold weather can cut electric car range over 40 percent [WWW Document]. URL https://apnews.com/04029bd1e0a94cd59ff9540a398c12d1 (accessed 11.4.19).

Kuby, M., Lim, S., 2007. Location of Alternative-Fuel Stations Using the Flow-Refueling Location Model and Dispersion of Candidate Sites on Arcs. Networks Spat. Econ. 7, 129–152. https://doi.org/10.1007/s11067-006-9003-6

Kuby, M., Lim, S., 2005. The flow-refueling location problem for alternative-fuel vehicles.

Socioecon. Plann. Sci. 39, 125–145. https://doi.org/10.1016/J.SEPS.2004.03.001

Li, M., Jia, Y., Shen, Z., He, F., 2017. Improving the electrification rate of the vehicle miles traveled in Beijing: A data-driven approach. Transp. Res. Part A Policy Pract. https://doi.org/10.1016/j.tra.2017.01.005

Lim, S., Kuby, M., 2010. Heuristic algorithms for siting alternative-fuel stations using the Flow-Refueling Location Model. Eur. J. Oper. Res. 204, 51–61. https://doi.org/10.1016/J.EJOR.2009.09.032

Lowell, D., Jones, B., Seamonds, D., 2017. Electric Vehicle Cost-Benefit Analysis Plug-in Electric Vehicle Cost-Benefit Analysis: Michigan.

Lu, C.-C., Mahmassani, H.S., Zhou, X., 2009. Equivalent gap function-based reformulation and solution algorithm for the dynamic user equilibrium problem. Transp. Res. Part B Methodol. 43, 345–364. https://doi.org/10.1016/J.TRB.2008.07.005

M.J. Bradley & Associates [WWW Document], 2021. URL https://mjbradley.com/sites/default/files/ILIT_User_Guide_v4.0.pdf (accessed 7.6.20).

Mc Donald, J.F., 1993. Local property tax differences and business real estate values. J. Real Estate Financ. Econ. 6, 277–287. https://doi.org/10.1007/BF01096962

Metropolis, N., Rosenbluth, A.W., Rosenbluth, M.N., Teller, A.H., Teller, E., 1953. Equation of State Calculations by Fast Computing Machines. Cit. J. Chem. Phys 21, 1087. https://doi.org/10.1063/1.1699114

Mirchandani, P., Adler, J., Madsen, O.B.G., 2014. New Logistical Issues in Using Electric Vehicle Fleets with Battery Exchange Infrastructure. Procedia - Soc. Behav. Sci. 108, 3–14. https://doi.org/10.1016/J.SBSPRO.2013.12.815

Mirchandani, P., Francis, R.L., 1990. Discrete location theory. Wiley, New York.

Mirhassani, S.A., Ebrazi, R., 2013. A Flexible Reformulation of the Refueling Station Location Problem. Transp. Sci. 47, 617–628. https://doi.org/10.1287/trsc.1120.0430

MISO Energy, 2018. Real-Time Displays [WWW Document]. URL https://www.misoenergy.org/markets-and-operations/real-time-displays/ (accessed 10.15.18).

MPSC - MI Public Service Commission [WWW Document], 2019. URL https://www.michigan.gov/mpsc/ (accessed 10.15.18).

Murakami, Y., Takabayashi, Y., Noro, Y., 2014. Photovoltaic power prediction and its application to smart grid, in: 2014 IEEE Innovative Smart Grid Technologies-Asia (ISGT ASIA). pp. 47–50.

Naderan, A., Shahi, J., 2010. Aggregate crash prediction models: Introducing crash generation concept. Accid. Anal. Prev. 42, 339–346. https://doi.org/10.1016/J.AAP.2009.08.020

Nie, Y. (Marco), Ghamami, M., 2013. A corridor-centric approach to planning electric vehicle charging infrastructure. Transp. Res. Part B Methodol. 57, 172–190. https://doi.org/10.1016/J.TRB.2013.08.010

Nie, Y., Ghamami, M., Zockaie, A., Xiao, F., 2016. Optimization of incentive polices for plug-in electric vehicles. Transp. Res. Part B Methodol. 84, 103–123. https://doi.org/10.1016/j.trb.2015.12.011

Nourbakhsh, S.M., Ouyang, Y., 2010. Optimal fueling strategies for locomotive fleets in railroad networks. Transp. Res. Part B Methodol. https://doi.org/10.1016/j.trb.2010.03.003

Peeta, S., Mahmassani, H.S., 1995. System optimal and user equilibrium time-dependent traffic assignment in congested networks. Ann. Oper. Res. 60, 81–113. https://doi.org/10.1007/BF02031941

Riemann, R., Wang, D.Z.W., Busch, F., 2015. Optimal location of wireless charging facilities for electric vehicles: Flow capturing location model with stochastic user equilibrium. Transp. Res. Part C Emerg. Technol. https://doi.org/10.1016/j.trc.2015.06.022

Seo, K., Salon, D., Kuby, M., Golub, A., 2018. Hedonic modeling of commercial property values: distance decay from the links and nodes of rail and highway infrastructure. Transportation (Amst). 1–24. https://doi.org/10.1007/s11116-018-9861-z

Shahraki, N., Cai, H., Turkay, M., Xu, M., 2015. Optimal locations of electric public charging stations using real world vehicle travel patterns. Transp. Res. Part D Transp. Environ. 41, 165–176. https://doi.org/10.1016/j.trd.2015.09.011

Sheppard, G., Waraich, R., Campbell, A., Pzdnukhov, A., R. Gopal, A., 2017. Lawrence Berkeley National Laboratory Recent Work Title Modeling plug-in electric vehicle charging demand with BEAM, the framework for behavior energy autonomy mobility.

Shortt, A., O'Malley, M., 2014. Quantifying the long-term impact of electric vehicles on the generation portfolio. IEEE Trans. Smart Grid 5, 71–83.

Shukla, A., Pekny, J., Venkatasubramanian, V., 2011. An optimization framework for cost effective design of refueling station infrastructure for alternative fuel vehicles. Comput. Chem. Eng. 35, 1431–1438. https://doi.org/10.1016/j.compchemeng.2011.03.018

Singh, H., Kavianipour, M., Soltanpour, A., Fakhrmoosavi, F., Ghamami, M., Zockaie, A., Jackson, R., 2022. Macro Analysis to Estimate Electric Vehicles Fast-Charging Infrastructure Requirements in Small Urban Areas: Transp. Res. Rec. https://doi.org/10.1177/03611981221093625

Sweda, T., Klabjan, D., 2011. An Agent-Based Decision Support System for Electric Vehicle Charging Infrastructure Deployment.

Tate, E.D., Harpster, M.O., Savagian, P.J., 2008. The electrification of the automobile: From conventional hybrid, to plug-in hybrids, to extended-range electric vehicles. SAE Tech. Pap. https://doi.org/10.4271/2008-01-0458

U.P. Supply, 2020. Population and Geography of the Upper Peninsula [WWW Document]. URL https://upsupply.co/upper-peninsula-population-and-geography (accessed 11.18.19).

U.S. Census Bureau, 2010. Census 2010 [WWW Document].

U.S. Department of Transportation, 2017. Alternative Fuel Corridors - Environment - FHWA [WWW Document].

U.S. Energy Information Administration, 2019. U.S. energy consumption by source and sector, 2019 [WWW Document]. URL https://www.eia.gov/totalenergy/data/monthly/pdf/flow/css_2019_energy.pdf (accessed 11.19.20).

U.S Department of Energy, 2017. Alternative Fuels Data Center: Alternative Fueling Station Locator [WWW Document].

Union of Concerned Scientists, 2018. Electric Vehicle Battery: Materials, Cost, Lifespan | Union of Concerned Scientists [WWW Document]. URL https://www.ucsusa.org/clean-vehicles/electric-vehicles/electric-cars-battery-life-materials-cost#.W2E2mZ9Kh9O (accessed 8.1.18).

United States Environmental Protection Agency, 2018. Fast Facts on Transportation Greenhouse Gas Emissions [WWW Document]. United States Environ. Prot. Agency. URL https://www.epa.gov/greenvehicles/fast-facts-transportation-greenhouse-gas-emissions (accessed 12.23.18).

Upchurch, C., Kuby, M., Lim, S., 2009. A model for location of capacitated alternative-fuel stations. Geogr. Anal. 41, 127–148. https://doi.org/10.1111/j.1538-4632.2009.00744.x

Usman, M., Knapen, L., Yasar, A.U.H., Bellemans, T., Janssens, D., Wets, G., 2020. Optimal recharging framework and simulation for electric vehicle fleet. Futur. Gener. Comput. Syst. 107, 745–757. https://doi.org/10.1016/j.future.2017.04.037

Wang, C., He, F., Lin, X., Shen, Z.J.M., Li, M., 2019. Designing locations and capacities for charging stations to support intercity travel of electric vehicles: An expanded network approach. Transp. Res. Part C Emerg. Technol. 102, 210–232. https://doi.org/10.1016/j.trc.2019.03.013

Wang, W., Lu, Y., 2018. Analysis of the Mean Absolute Error (MAE) and the Root Mean Square Error (RMSE) in Assessing Rounding Model. IOP Conf. Ser. Mater. Sci. Eng. 324. https://doi.org/10.1088/1757-899X/324/1/012049

Wardrop, J.G., 1952. Some Theoritical Aspects of ROad Traffic Research. Proc. Inst. Civ. Eng. 1, 325–362. https://doi.org/10.1680/ipeds.1952.11259

Washington, S.P., Karlaftis, M.G., Mannering, F.L., 2011. Statistical and econometric methods for transportation data analysis.

West Technologies, N., 2015. Costs Associated With Non-Residential Electric Vehicle Supply Equipment Factors to consider in the implementation of electric vehicle charging stations.

Wilaby, M., Casas, J., 2016. MI Travel Counts III.

William Larson, 2015. New Estimates of Value of Land of the United States | U.S. Bureau of Economic Analysis (BEA) [WWW Document]. Bur. Econ. Anal. URL https://www.bea.gov/research/papers/2015/new-estimates-value-land-united-states (accessed 10.15.18).

Wood, E., Rames, C., Muratori, M., Raghavan, S., Melaina, M., 2017. National Plug-In Electric Vehicle Infrastructure Analysis, NREL. https://doi.org/10.13140/RG.2.2.25881.93280

Xi, X., Sioshansi, R., Marano, V., 2013. Simulation – optimization model for location of a public electric vehicle charging infrastructure. Transp. Res. PART D 22, 60–69. https://doi.org/10.1016/j.trd.2013.02.014

Xie, F., Liu, C., Li, S., Lin, Z., Huang, Y., 2018. Long-term strategic planning of inter-city fast charging infrastructure for battery electric vehicles. Transp. Res. Part E Logist. Transp. Rev. 109, 261–176. https://doi.org/10.1016/j.tre.2017.11.014

Xie, S., Chen, X., Wang, Z., Ouyang, Y., Somani, K., Huang, J., 2016. Integrated Planning for Multiple Types of Locomotive Work Facilities Under Location, Routing, and Inventory Considerations. INFORMS J. Appl. Anal. 46, 391. https://doi.org/10.1287/inte.2016.0857

Yang, J., Dong, J., Hu, L., 2017. A data-driven optimization-based approach for siting and sizing of electric taxi charging stations. Transp. Res. Part C Emerg. Technol. 77, 462–477. https://doi.org/10.1016/j.trc.2017.02.014

Zhang, K., Lu, L., Lei, C., Zhu, H., Ouyang, Y., 2018. Dynamic operations and pricing of electric unmanned aerial vehicle systems and power networks. Transp. Res. Part C 92, 472–485. https://doi.org/10.1016/j.trc.2018.05.011

Zockaie, A., Aashtiani, H.Z., Ghamami, M., Marco Nie, Y., 2016. Solving Detour-Based Fuel Stations Location Problems. Comput. Civ. Infrastruct. Eng. 31, 132–144. https://doi.org/10.1111/mice.12170

Zockaie, A., Saberi, M., Saedi, R., 2018. A resource allocation problem to estimate network fundamental diagram in heterogeneous networks: Optimal locating of fixed measurement points and sampling of probe trajectories. Transp. Res. Part C Emerg. Technol. 86, 245–262. https://doi.org/10.1016/J.TRC.2017.11.017

Zukerman, M., 2013. Introduction to Queueing Theory and Stochastic Teletraffic Models.